

## 6.2 Degassing History of Earth

Youxue Zhang, University of Michigan, Ann Arbor, MI, USA

© 2014 Elsevier Ltd. All rights reserved.

---

<b>6.2.1</b>	<b>Introduction</b>	37
6.2.1.1	Mantle Degassing Processes	38
6.2.1.2	Definition of Reservoirs	38
6.2.1.3	Closed-System Degassing Versus Open-System Behavior	39
6.2.1.4	Brief Literature Overview	40
<b>6.2.2</b>	<b>Partitioning and Solubility of Volatile Components</b>	41
6.2.2.1	Partition Coefficients	41
6.2.2.2	Solubilities	42
<b>6.2.3</b>	<b>Volatile Data</b>	42
6.2.3.1	Beginning Comments About Noble Gases	42
6.2.3.2	He	43
6.2.3.3	Ne	45
6.2.3.4	Ar	49
6.2.3.5	Kr	52
6.2.3.6	Xe	52
6.2.3.7	N <sub>2</sub>	54
6.2.3.8	CO <sub>2</sub>	55
6.2.3.9	H <sub>2</sub> O	56
6.2.3.10	Summary of Various Paradoxes and Uncertainties	57
<b>6.2.4</b>	<b>Modeling Degassing, Recycling, and Atmosphere Evolution</b>	58
6.2.4.1	Various Mantle Degassing Models in the Literature	58
6.2.4.1.1	General model features	58
6.2.4.1.2	Bulk degassing models	59
6.2.4.1.3	Solubility-controlled degassing model	59
6.2.4.1.4	Steady-state degassing model	60
6.2.4.2	Evaluation of Some Assumptions in Degassing Models	60
6.2.4.2.1	Closed-system assumption	60
6.2.4.2.2	Testing the degassing models	60
6.2.4.2.3	Does the least-radiogenic OIB represent UPM?	61
6.2.4.3	Other Sources of Gases for the Atmosphere	61
6.2.4.3.1	Impact degassing	61
6.2.4.3.2	Cometary injection	62
<b>6.2.5</b>	<b>Discussion</b>	62
6.2.5.1	Where Is the Primitive Undegassed Mantle?	62
6.2.5.2	Paradigm Shift from the Assumption of Closed-System Degassing to Open-System Degassing	63
6.2.5.3	Recycling from Surface to the Mantle and Volatile Fluxes from the Core	63
6.2.5.4	Updating Models on Mantle Degassing, Recycling, and Atmosphere Evolution	64
<b>6.2.6</b>	<b>Conclusions and Outlook</b>	64
6.2.6.1	What Are Known About Earth Degassing?	64
6.2.6.2	Uncertainties and Paradoxes	64
6.2.6.3	Key Measurements That Are Needed	64
<b>Acknowledgment</b>		65
<b>References</b>		65

---

### 6.2.1 Introduction

The degassing of Earth redistributes volatile elements in Earth from the interior to the surface. Although the volatile elements only account for a trivial mass fraction, they play major roles in Earth's evolution. For example, H<sub>2</sub>O content in the mantle affects mantle viscosity and hence mantle convection dynamics. Both H<sub>2</sub>O and CO<sub>2</sub> can affect mantle partial melting, a major process for crustal formation and mantle differentiation. Significant

amount of volatile elements has been degassed from Earth's mantle to the surface, contributing to air, oceans, and sediments. The surface volatiles are critical to life, climate, weathering, sedimentary processes, and subduction zone volcanism.

Numerous investigators have traced the degassing history using volatile inventories and isotopes. Many models have been developed to quantify the degassing history. Often, the most important constraints, especially on the timescale of the degassing process, come from the noble gas isotopes although they are

minor in terms of volatile mass. Hence, much space in this chapter is devoted to the noble gases. This section will introduce mantle degassing processes, definitions, basic concepts, and the literature. [Section 6.2.2](#) will review important physical properties of the volatiles (partition coefficients and solubilities) during mantle degassing. [Section 6.2.3](#) will present essential geochemical data regarding the volatiles. [Section 6.2.4](#) will cover the degassing and atmospheric evolution models. [Section 6.2.5](#) will discuss some unresolved issues. [Section 6.2.6](#) will be a summary of the current status of the field.

### 6.2.1.1 Mantle Degassing Processes

Mantle rocks contain low concentration of volatile components, either absorbed in mineral interior or concentrated at grain boundaries (e.g., [Baxter et al., 2007](#); [Hiraga et al., 2004](#)). Mantle degassing is generally thought to be closely coupled with mantle partial melting and the early magma ocean. At mid-ocean ridges and hot spot regions, mantle upwelling leads to decompressional partial melting. Volatile components (noble gases, H<sub>2</sub>O, C, N<sub>2</sub>, etc.) are incompatible and partition preferentially into the melt. The quantification of this step requires knowledge of the partition coefficients. During partial melting, the volatile elements are coupled with other incompatible elements, meaning volatile and nonvolatile elements are coupled in this stage.

At the mantle source region of partial melting, where the pressure is high, all the volatile components can be dissolved in the melt because gas solubilities are high at high pressures. As the melt rises to shallow enough depth, the pressure eventually becomes low enough so that dissolved volatiles become oversaturated and gas bubbles form in the melt. The gas bubbles, being less dense than the melt, gradually rise and escape from the melt into surface reservoirs, such as ocean water. The gas may also leak into fractures and gradually percolate through rocks to reach the surface. Because mid-ocean ridges are typically below 2500–3000 m of water, the pressure is still significant. Hence, degassing is not complete, especially for H<sub>2</sub>O whose solubility is much greater than the noble gases, N<sub>2</sub>, and CO<sub>2</sub>. With incomplete degassing, the degree of degassing of an individual volatile component is related to its solubility. The lower the solubility is, the higher the degree of degassing. Furthermore, because volatile components enter bubbles through diffusion, the kinetics of nucleation and diffusion likely also play some role in determining the degree of degassing. In this stage, volatile and nonvolatile elements are decoupled.

Unambiguous evidence is available for the occurrence of mantle degassing and for its contribution to gases in surface reservoirs (air, oceans, and crust, AOC), including (1) mid-ocean ridge basalts (MORBs) at hundreds of bars (as well as subaerial basalts), which are often vesicular with high-pressure gas in the vesicles (e.g., [Hekinian et al., 1973](#); [Sarda and Graham, 1990](#)), (2) <sup>3</sup>He flux from the mantle, which can be observed and quantified in ocean water ([Bianchi et al., 2010](#); [Bieri et al., 1964](#); [Craig et al., 1975](#); [Lupton, 1983](#)), and (3) <sup>40</sup>Ar in air, which must be from mantle degassing through time because essentially all <sup>40</sup>Ar is produced gradually by decay of <sup>40</sup>K (e.g., [Ozima and Podosek, 2002](#); [Turekian, 1959](#)). For some species, the flux or total contribution from the mantle can be quantified.

Even though mantle degassing certainly contributed to volatiles in AOC, whether there are other important nonmantle sources has been debated, especially by planetary scientists (e.g., [Balsiger et al., 1995](#); [Chyba, 1987](#); [Hartogh et al., 2011](#); [Meibom et al., 2007](#); [Meier et al., 1998](#)). For most solid Earth geochemists, the default assumption for Earth's atmosphere has been that they are from degassing of the interior, unless there is evidence to show otherwise (or inconsistencies and paradoxes resulting from the assumption). This paradigm has been gradually shifting as more lines of evidence show that at least for some species the mantle may not contain enough volatiles to supply surface volatiles, as can be seen in later parts of this chapter.

Mantle degassing is probably countered by the reverse process, the regassing of the mantle by subduction of surface rocks that carry volatiles. The regassing fluxes are difficult to quantify because of the obstacle to estimate what fraction of a given volatile component in the subduction slab returns to the surface through volcanism and what fraction actually goes down to the deep mantle. Occasionally, the effect of recycling can be seen from gas budget in mantle reservoirs.

Although mantle degassing is physically closely coupled with mantle partial melting, the depletion of gaseous species is not necessarily coupled with the depletion of nongaseous species. That is because the nongaseous elements mostly stay in the oceanic crust, whereas gaseous species leave the oceanic lithosphere all together. The subduction of the oceanic lithosphere returns the oceanic crust with high concentrations of incompatible elements back to the mantle, whereas the gaseous species are often not recycled, or they are recycled through a different path (e.g., by subduction of sediments or by alteration of oceanic crust).

### 6.2.1.2 Definition of Reservoirs

In discussing Earth degassing, for simplicity, the relevant parts of Earth are divided into reservoirs. Some reservoirs are physically real and continuous, such as air or oceans. Some reservoirs are hypothetical constructs.

Two different definitions of the atmosphere can be found in literature ([Ozima and Podosek, 2002](#)). One equates the atmosphere to Earth's air. The other is a more general definition in which the atmosphere includes not only the air but also volatiles in other surface reservoirs, including the hydrosphere, the biosphere, and crustal rocks ([Rubey, 1951](#)). In the discussion in the succeeding texts, air and atmosphere will be distinguished, with the atmosphere including volatiles in all surface reservoirs.

AOC will be used to refer to air + oceans + biosphere + crust. Hence, the atmosphere means all volatiles in AOC.

BSE (bulk silicate Earth) will be used to refer to the whole Earth except the core. That is, BSE includes the mantle and AOC. In other words, if AOC were mixed back to the mantle to get a homogeneous silicate Earth, it would be the BSE. If there was nonmantle contribution to the atmosphere (such as remnant initial air, impact degassing, and cometary injection of H<sub>2</sub>O), that would be counted as part of the present-day BSE. On the other hand, helium lost to outer space is added back to BSE.

UPM (undegassed primitive mantle) refers to the part of the mantle that is undegassed and unperturbed, with primordial volatile concentrations plus radiogenic growth at the

primordial parent-to-daughter ratio. If all atmosphere comes from mantle degassing, the composition of UPM would be the same as that of BSE. However, when allowing the possibility of initial atmosphere or impact degassing as a source for AOC, BSE composition does not have to be the same as the present-day primitive undegassed mantle.

DMM (degassed MORB mantle) refers to the degassed mantle. As will be discussed later, the mass fraction of DMM is much greater than that of the upper mantle (e.g., Zhang and Zindler, 1989; also later discussion). MORBs are variable, and there is N-MORB (normal MORB) and E-MORB (enriched MORB). In this chapter, MORB means N-MORB. [Figure 1](#) compares Earth's physical structure on the one hand and the DMM and UPM on the other hand. That is, part of the lower mantle must also be degassed. However, whether the mass of DMM is the same for all gases and isotopes is not certain because of the complicated convection, dynamics, and hence degassing history of the mantle. Due to degassing when basaltic melts erupt, DMM is expected to have lower noble gas concentrations compared to primitive undegassed mantle. Furthermore, because degassing lowers the concentration of the nonradiogenic isotope, the radiogenic-to-nonradiogenic isotopic ratio grows more rapidly with time in DMM than in primitive undegassed mantle, leading to higher radiogenic/nonradiogenic isotopic ratios in DMM.

In [Figure 1\(b\)](#), UPM is shown as a physical entity in the lower part of the lower mantle. However, UPM is a hypothetical construct, and whether such a physically continuous entity exists is uncertain. It is possible that every part of the mantle has been degassed to some degree (van Keken and Ballentine, 1999; van Keken et al., 2002) and might be treated as a mixture between the DMM and UPM (sometimes needing a recycled component, such as subducted MORB). If so, the meaning of DMM and UPM reservoirs would be the collections of the decomposed end-members of every part of the mantle.

OIB (ocean island basalt) mantle source refers to the mantle source from which OIBs are generated. The isotopic signatures in OIB can be used to trace the OIB mantle. OIBs are often thought to represent mantle plumes originating deeper than MORBs (but see Foulger, 2005), approaching UPM. High-quality noble gas data are also available for a Devonian continental plume, the Kola plume (Yokochi and Marty, 2004, 2005; Tolstikhin et al., 2002), and these data are also included in the discussion in the succeeding texts. Often, the least-radiogenic OIB is used to represent isotopic signatures of UPM. However, there is also uncertainty in this (see later discussion about [Figure 4](#)).

### 6.2.1.3 Closed-System Degassing Versus Open-System Behavior

In the literature, quantitative mantle degassing and atmosphere evolution models often assumed that Earth has been a closed system in terms of degassing (e.g., Allegre et al., 1986/87; Hart et al., 1985; Sarda et al., 1985; Staudacher and Allegre, 1982; Zhang, 1997; Zhang and Zindler, 1989, 1993) except for He. In the context of closed-system degassing models, essentially all volatiles in AOC come from mantle degassing (e.g., Allegre et al., 1986/87; Hart et al., 1985; Zhang, 1997; Zhang and Zindler, 1989). That is, degassing is assumed to begin at a time when the initial gas content in AOC was negligible (e.g., right after a giant impact that drove away all the gases from Earth's surface), and extraterrestrial addition during the degassing process (such as contributions from impact degassing from planetesimals including comets) is also negligible. Because volatile contents in AOC can be estimated fairly well, the closed-system assumption provides strong constraints to degassing models.

Some authors have proposed open-system degassing to allow a nonmantle source for the atmosphere (e.g., Marty, 1989) to explain some specific features (such as air Ne), but

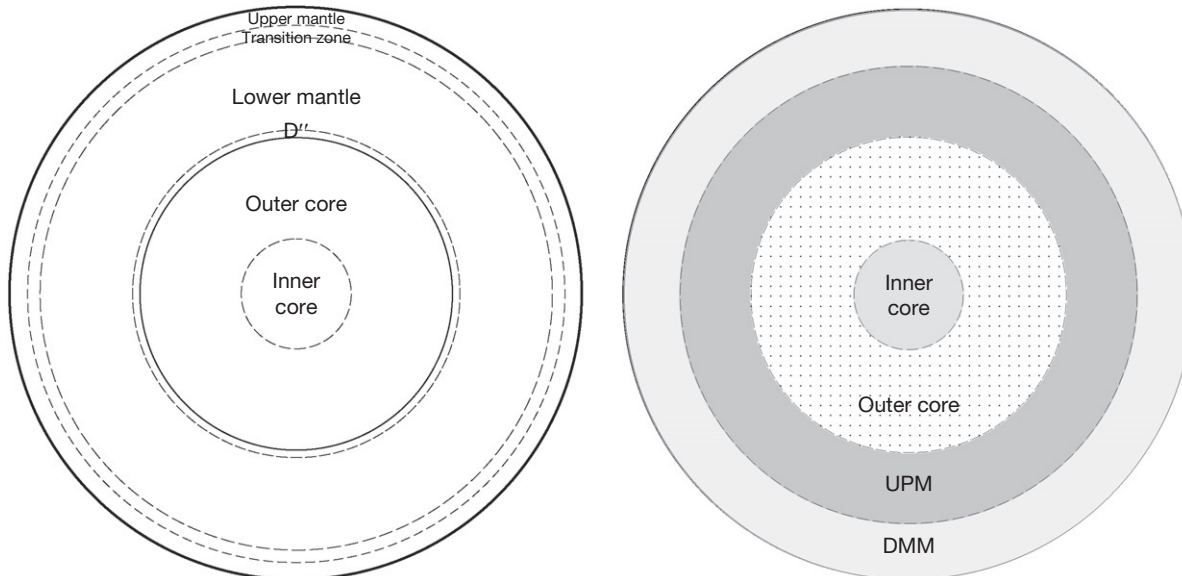


**Figure 1** Earth structure. The left-hand side shows the upper mantle, transition zone, lower mantle, D'' layer, outer core, and inner core. The right-hand side shows that the DMM (degassed MORB mantle) is larger than the upper mantle. In this drawing, the mass of DMM is about two times that of the upper mantle plus the transition zone. UPM, undegassed primitive mantle.

did not present quantitative models for mantle degassing and atmosphere evolution because without the closed-system assumption, there were not enough constraints. Initially, the open-system degassing assumption did not gain much support because the Ne isotopic data could also be explained in some other way. With the accumulation of more data, more gas species appear to require both mantle and nonmantle sources. In this chapter, whether degassing and atmosphere evolution may be viewed as closed system or open system will be critically evaluated.

The accretion history of Earth and other terrestrial planets is discussed by Dauphas and Morbidelli (see [Chapter 6.1](#)). Because Earth is formed by accretion (or collision) of planetesimals (thought to be mostly chondritic materials), one may argue that all volatiles on and in Earth are extraterrestrial. However, in the context of understanding mantle degassing, it is important to distinguish (1) volatiles that were delivered to Earth's interior by planetesimals and became part of the primordial mantle (or the solid Earth) and (2) volatiles that were brought in by planetesimals but were immediately released to the atmosphere by impact degassing ([Lange and Ahrens, 1982](#)) or by cosmic dusts (e.g., [Farley, 1995](#)). (The part that was immediately lost to outer space is irrelevant to the discussion here.) In the former case, the volatiles become part of the primordial mantle, and mantle degassing brings the volatiles to the surface. However, in the latter case, referred to as impact degassing (including cometary injection), there is extra gain of volatiles for the atmosphere in addition to mantle degassing, and the extra volatiles are referred to as nonmantle or extraterrestrial volatiles in this chapter. If the nonmantle volatiles do not contribute significantly to Earth's atmosphere, then closed-system degassing assumption is fine. Otherwise, open-system degassing models are necessary.

Continuous cometary injection, especially during the first 700 My of solar system formation, may or may not have contributed significant volatiles to Earth for some gases (e.g., [Chyba, 1987](#); [Dauphas et al., 2000](#); [Hartogh et al., 2011](#); [Hutsemekers et al., 2009](#); [Meier et al., 1998](#); [Zhang, 2002](#)). More generally, volatiles brought to Earth by various impacts (including planetesimals and comets) may have contributed to Earth's atmosphere (e.g., [Lange and Ahrens, 1982](#); also see [Chapter 6.1](#)). The largest impacts may also erode an existing atmosphere ([Ahrens, 1993](#)). Currently, no quantitative models are available to incorporate the effect of mantle degassing, initial gas, and volatiles delivered by impact degassing of planetesimals and comets. In modeling the evolution of the atmosphere, the hypothetical starting point is often the time when a protoatmosphere was eroded with essentially zero initial gas.

#### 6.2.1.4 Brief Literature Overview

The composition of Earth's atmosphere is different from solar composition, not only in terms of lighter gases that could escape easily but also in terms of heavier gases (e.g.,  $^{36}\text{Ar}$ ,  $^{84}\text{Kr}$ , and  $^{130}\text{Xe}$ ). Although  $^{84}\text{Kr}/^{130}\text{Xe}$  ratio in air is similar to solar, the various nonradiogenic Xe isotope ratios are very different from the solar ratios. It was recognized early that Earth's atmosphere is different from solar nebula gas; rather, the  $\text{H}_2\text{O}:\text{CO}_2:\text{SO}_2$  ratios in the atmosphere (including hydrosphere and sediment) are similar to those in volcanic gases ([Rubey, 1951](#)). Hence, Earth's atmosphere is not simply from

accretion or gravitational grab of solar nebula gas, but is secondary (e.g., [Brown, 1952](#); [Rubey, 1951, 1955](#)), including at least degassing from the interior of Earth and modifications on the surface (e.g.,  $\text{O}_2$  from photosynthesis).

Noble gases, even though with only low abundance, have played a major role in understanding mantle degassing and atmosphere evolution. Specifically, the many radiogenic isotopes of noble gases are critical in evaluating noble gas budgets in various reservoirs and in constraining the timing (and dynamics) of degassing.

[Turekian \(1959\)](#) constructed a continuous degassing model for  $^{40}\text{Ar}$  from the solid Earth to air assuming that the degassing rate is proportional to the amount of  $^{40}\text{Ar}$  in the solid Earth, which is often adopted in later degassing models with some variation. [Schwartzman \(1973\)](#) treated  $^{40}\text{Ar}$  degassing by assuming that  $^{40}\text{Ar}$  and K behaved coherently, meaning that as K is transferred to the crust,  $^{40}\text{Ar}$  is coherently transferred to air. Because degassing involves melt-gas separation and crustal formation does not, meaning  $^{40}\text{Ar}$  and K do not have to behave coherently, the approach of [Schwartzman \(1973\)](#) was not followed by later workers. [Ozima \(1975\)](#) developed continuous and early catastrophic degassing models and concluded that Ar isotopes require early catastrophic degassing.

Helium concentration excess in seawater was reported by [Bieri et al. \(1964\)](#) and [Clarke et al. \(1969\)](#), indicating that the mantle is currently degassing. Craig and coworkers made key contributions in understanding the distribution of He and other noble gases in Earth (e.g., [Craig and Lupton, 1976](#); [Craig et al., 1975](#)), estimating He degassing flux from the mantle ([Craig et al., 1975](#)) and showing that  $^{20}\text{Ne}/^{22}\text{Ne}$  ratio in mantle-derived basalts can be significantly higher than the air ratio ([Craig and Lupton, 1976](#)).

Allegre and his coworkers made major contributions to the understanding of mantle degassing and atmosphere formation (e.g., [Allegre et al., 1986/87](#); [Moreira and Allegre, 2002](#); [Moreira et al., 1995, 1996, 1998](#); [Sarda et al., 1985, 1988, 2000](#); [Staudacher, 1987](#); [Staudacher and Allegre, 1982, 1989](#); [Staudacher et al., 1986, 1989, 1990](#); [Trieloff et al., 2000](#); [Valbracht et al., 1997](#)). They reported the majority of the Ne, Ar, and Xe isotopic data in mantle-derived rocks and also contributed significantly to He isotopic data. Furthermore, they developed numerous quantitative mantle degassing models. [Staudacher and Allegre \(1982\)](#) reported systematic Xe isotopic data in MORB and OIB and presented a model for the degassing history of Earth, arriving at a mean degassing time of 10–25 My. [Sarda et al. \(1985\)](#) obtained systematic Ar isotopic data in MORB and OIB and extended the degassing model of [Staudacher and Allegre \(1982\)](#) to include Ar, finding that degassing of Ar operated on a longer timescale compared to Xe. [Allegre et al. \(1986/87\)](#) modeled Xe, Ar, and He degassing history and found that half of Earth's mantle is extensively outgassed, and He degassing operated on a longer timescale than Ar and than Xe. [Sarda et al. \(1988\)](#) reported high-quality Ne isotopic data in mantle-derived rocks and showed that Ne in the mantle is very different from air Ne, but approaching solar Ne plus additional nucleogenic  $^{21}\text{Ne}$  (see also [Marty, 1989](#)). [Moreira et al. \(1998\)](#) inferred the end-member isotope ratios of  $^{21}\text{Ne}/^{22}\text{Ne}$ ,  $^{40}\text{Ar}/^{36}\text{Ar}$ , and  $^{129}\text{Xe}/^{130}\text{Xe}$  in MORB mantle.

Other groups also made critical contributions. [Phinney et al. \(1978\)](#) discovered high  $^{20}\text{Ne}/^{22}\text{Ne}$  and  $^{21}\text{Ne}/^{22}\text{Ne}$  ratios,

excess  $^{129}\text{Xe}$ , and fission  $^{131-136}\text{Xe}$  in well gases. Honda et al. (1991) measured solar Ne isotopes in OIBs (see also Hiyagon et al., 1992; Moreira et al., 2001; Valbracht et al., 1997). Caffee et al. (1999) reported the presence of excess  $^{124-128}\text{Xe}$  in well gases. Holland et al. (2009) detected Kr isotope anomalies in well gases. Marty and coworkers (Marty, 1989, 1995, 2012; Marty and Dauphas, 2003; Marty and Humbert, 1997; Marty and Tolstikhin, 1998; Marty et al., 2011) made crucial contributions to numerous aspects of degassing, especially nitrogen and carbon degassing.

Various other groups have proposed different degassing models from the models of Allegre and coworkers. Hart et al. (1985) outlined a closed-system evolution model for Ar in Earth. Zhang and Zindler (1989) constructed a solubility-controlled degassing model for mantle degassing. Zhang and Zindler (1993) explored the recycling of  $\text{CO}_2$  and  $\text{N}_2$  into the mantle. Tolstikhin and O'Nions (1994) explained the missing xenon as well as Xe isotope fractionation by rapid early degassing of xenon in the context of solubility-controlled degassing and subsequent hydrodynamic escape. Porcelli and Wasserburg (1995a,b) developed a steady-state degassing model. Zhang (1997) tried to evaluate the various mantle degassing models. Honda and McDougall (1998) explained the different  $^3\text{He}/^{22}\text{Ne}$  ratios in MORB and OIB by solubility-controlled degassing. There were also other conceptual models with less quantification and sometimes few quantitative constraints (e.g., Ahrens, 1993; Chyba, 1987; Lange and Ahrens, 1982; Lee et al., 2010; Marty, 1989).

Most quantitative degassing models were developed in the 1980s and 1990s. Later work has considerably expanded the database of mantle noble gases and volatiles with some conceptual advancements (e.g., Furi et al., 2010; Hanyu et al., 2007; Holland et al., 2009; Honda et al., 2011; Jackson et al., 2009; Kurz et al., 2009; Moreira and Allegre, 2002; Moreira et al., 2001; Raquin and Moreira, 2009; Raquin et al., 2008; Starkey et al., 2009; Stroncik et al., 2007; Tolstikhin et al., 2002; Trieloff et al., 2000, 2002; Yokochi and Marty, 2004, 2005). However, with the accumulation of ever more data, constructing a quantitative degassing model that is consistent with all available data does not become easier; instead, it becomes increasingly more difficult.

## 6.2.2 Partitioning and Solubility of Volatile Components

As introduced in Section 6.2.1.1, mantle degassing begins with volatiles partitioning into the melt during mantle partial melting. In this process, the partition coefficients between the melt and minerals in the mantle residue control the behavior of the volatile components. Subsequently, as the melt ascends to shallower depth (lower pressures), the volatiles become oversaturated, leading to bubble nucleation, growth, rise, and escape (degassing). For example, if a tholeiitic melt contains 1000 ppm of  $\text{CO}_2$ , oversaturation would be reached at  $\leq 200$  MPa pressure (or  $\leq 6.6$  km depth below ocean ridge). This degassing step is largely controlled by the solubilities of the volatile components. Nucleation and diffusion kinetics (Zhang, 2008) likely also play a role during degassing since it has been shown repeatedly that mid-ocean ridge basalts are often oversaturated (e.g., Dixon et al., 1988; Soule et al., 2012). However, the kinetic details are not easy to be incorporated into quantitative mantle degassing models. In this section,

partition coefficients and solubilities are summarized. The summary of the diffusion data of volatile components in silicate melts can be found in recent reviews by Behrens (2010), Zhang and Ni (2010), and Zhang et al. (2010).

### 6.2.2.1 Partition Coefficients

A number of authors made efforts to measure partition coefficients of noble gas elements between minerals and melts (e.g., a number of papers before 2000; Brooker et al., 2003; Heber et al., 2007). The partition coefficients (defined as the concentration in the mineral(s) to that in the melt) are expected to be very small because noble gases are the archetypal elements for not forming bonds or minerals. Hence, even a small amount of fluid or melt inclusions in the crystal may compromise the measured concentration in the mineral and hence compromise the partition data significantly. Early experimental data (before 2000) on partition coefficients of noble gases between minerals and melt were high, and it is generally agreed that the early data suffered from these problems (Ozima and Podosek, 2002). Recently, Brooker et al. (2003) and Heber et al. (2007) determined the partition coefficients between clinopyroxene and melts and between olivine and melts. The data are shown in Figure 2 and demonstrate that the noble gases are indeed highly incompatible, rivaling the most incompatible elements. Therefore, during mantle partial melting at mid-ocean ridges with degree of partial melting at about 12% (Klein and Langmuir, 1987; Niu, 1997), essentially all noble gases will enter the melt phase. The partition data in Figure 2 do not exhibit smooth trends (unlike the solubility data in Figure 3), an indication that the data may need further improvement.

The partition of  $\text{H}_2\text{O}$  has been investigated both experimentally (e.g., review by Kohn and Grant, 2006) and through studies of covariation of 'elemental' ratios in basalts (Michael, 1988, 1995). The partition coefficient of  $\text{H}_2\text{O}$  during mantle partial melting is similar to that of Ce (Michael, 1988, 1995). Because  $\text{H}_2\text{O}$  is not much degassed at mid-ocean ridge depth, the roughly constant  $\text{H}_2\text{O}/\text{Ce}$  ratio is often used to estimate  $\text{H}_2\text{O}$  concentrations in different mantle reservoirs.

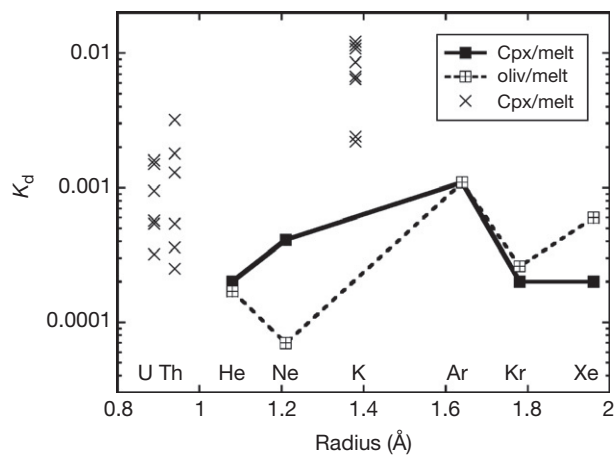


**Figure 2** Partition coefficients of noble gas elements (K, U, and Th) between mantle minerals and melts. Zero-charge 'ionic' radii of noble gases are from Zhang and Xu (1995), and ionic radii of  $\text{K}^+$ ,  $\text{U}^{4+}$ , and  $\text{Th}^{4+}$  are from Shannon (1976), all for octahedral coordination. For the noble gases, partition data are the preferred data in Heber et al. (2007). K, U, and Th partition data are from Brooker et al. (2003).

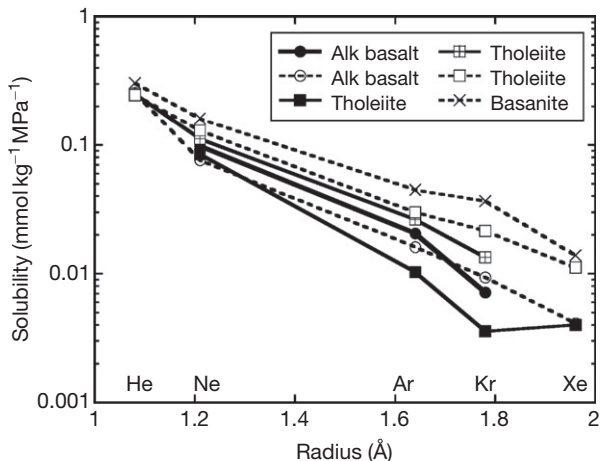


**Figure 3** Solubility of noble gases in mafic melts. Zero-charge ‘ionic’ radii of noble gases are from Zhang and Xu (1995). Solubility data are from Paonita (2005). Note that the solubility is given in  $10^{-3} \text{ mol kg}^{-1} \text{ MPa}^{-1}$ .

The partition coefficients of  $\text{CO}_2$  and  $\text{N}_2$  are not known, but both volatiles are generally thought to be highly incompatible, similar to the noble gases. It has been found that  $\text{CO}_2$  has a partition coefficient similar to Nb during mantle partial melting (e.g., Cartigny et al., 2008; Saal et al., 2002; Salters and Stracke, 2004).

It is also important to compare the partition coefficients of radioactive parent and radiogenic daughter to examine whether the parent-to-daughter ratio in the partial melt is higher or lower than in the mantle residue. Hence, the partition coefficients of K, U, and Th (Brooker et al., 2003) are also shown in Figure 2. Assuming the data are reliable, K is more compatible than Ar, and U and Th are more compatible than He. Hence, in the mantle residue, the parent-to-daughter ratios are higher than in primordial mantle. More importantly, with the subduction of the oceanic lithosphere, much of the incompatible nonvolatile elements are returned back to the mantle, but the gaseous elements are degassed and are much more difficult to recycle back to the mantle. Hence, even with similar degree of incompatibility, it is expected that the volatile elements will be depleted more than the nonvolatile elements. For example, even though Ar partition coefficient is similar to that of U as shown in Figure 2, using Ar/U ratio to estimate Ar concentrations in DMM and UPM would require careful handling of the degassing effect.

### 6.2.2.2 Solubilities

Contrary to the case for the partition coefficients of volatile components, the solubilities of volatiles in basaltic melts are fairly well known for  $\text{H}_2\text{O}$ ,  $\text{CO}_2$ , and noble gases (e.g., Iacono-Marziano et al., 2010; Jambon et al., 1986; Paonita, 2005). All experimental data show that the solubility of the noble gases in melts decreases from the lighter noble gas elements to the heavier ones, a trend opposite to that in water. The temperature and pressure dependence of per-MPa solubility is not major. Selected solubility data for noble gases are shown in Figure 3, with solubility per unit pressure decreasing almost exponential with atomic radii of noble gases (i.e.,  $\ln(\text{solubility})$  is almost linear with atomic radii). The molar ratios of the solubilities of He/Ne/Ar/Kr/Xe are about 1:0.43:0.10:0.051:0.031 (Iacono-Marziano et al., 2010; Jambon

et al., 1986; Paonita, 2005), with He solubility being about 32 times Xe solubility.

$\text{H}_2\text{O}$  solubility in basaltic melts is well known, and the per-MPa solubility depends strongly on pressure due to  $\text{H}_2\text{O}$  speciation in silicate melts (Stolper, 1982; Zhang, 1999) and slightly on melt composition (Lesne et al., 2011b) and temperature. Hence, there is no single ratio to characterize the relation between  $\text{H}_2\text{O}$  solubility and He solubility. At 1473 K and mid-ocean ridge pressure of 25 MPa, the total  $\text{H}_2\text{O}$  solubility in basaltic melt (in  $\text{mol kg}^{-1} \text{ MPa}^{-1}$ ) is 54 times that of He, whereas at 0.1 MPa (Liu et al., 2005), the total  $\text{H}_2\text{O}$  solubility is 670 times that of He (Zhang et al., 2007).

$\text{CO}_2$  solubility does not vary much from rhyolitic to basaltic melts (e.g., Blank et al., 1993; Dixon et al., 1995; Zhang et al., 2007), but does increase from tholeiitic to alkali basaltic melts (Dixon, 1997; Lesne et al., 2011a). For tholeiitic melt,  $\text{CO}_2$  solubility is about 0.5 times He solubility on molar basis (Dixon, 1997; Lesne et al., 2011a). For alkali basaltic melt,  $\text{CO}_2$  solubility is about the same as He solubility on molar basis (Dixon, 1997; Lesne et al., 2011a).

$\text{N}_2$  solubility depends on oxygen fugacity ( $f\text{O}_2$ ). At  $\log f\text{O}_2 \geq \text{IW-1}$  (relevant to terrestrial degassing),  $\text{N}_2$  solubility is independent of  $f\text{O}_2$  and is about 1.5 times Ar solubility (Libourel et al., 2003; Miyazaki et al., 2004). At  $\log f\text{O}_2 \geq \text{IW-1}$ , as  $f\text{O}_2$  decreases further,  $\text{N}_2$  solubility increases strongly by orders of magnitude (Libourel et al., 2003), whereas solubilities of noble gases are roughly independent of  $f\text{O}_2$ .

During degassing at mid-ocean ridges or for OIBs, gas concentrations and hence concentration ratios are fractionated. For many mass balance calculations, reliable elemental ratios are often needed. To minimize the effect of fractionation during degassing, a pair of gases with similar solubilities are used to form a ratio, and the ratio is estimated in basaltic glasses. For example,  $\text{CO}_2/\text{He}$  and  $\text{N}_2/\text{Ar}$  molar ratios are two often-used ratios thought to be roughly constant, whereas  $\text{CO}_2/\text{N}_2$  ratio could be fractionated.

As will be discussed later, some previous mantle degassing models assumed that all gases degassed to similar degree (meaning that gas solubilities did not play a role in degassing), whereas other degassing models assumed that gas solubilities played a significant role in degassing. With solubility control, a volatile component with low solubility is expected to be degassed to a higher degree. The quantitative aspects of mantle degassing models will be discussed in a later section.

### 6.2.3 Volatile Data

#### 6.2.3.1 Beginning Comments About Noble Gases

Most of the constraints on the budget, reservoir size, and degassing history of Earth come from the minor and trace gases in the atmosphere: the noble gases. Several characters of the noble gases make them excellent tracers of the degassing process and the escape process, including the following:

1. The noble gases are ‘real’ gases. Once they are degassed, they mostly stay in air, whereas other volatile components can be mostly in rocks (such as  $\text{CO}_2$  in carbonates) or in oceans ( $\text{H}_2\text{O}$ ). The noble gases can be absorbed into minerals in rocks and dissolved in water, but the effect is not as major as other gases.

2. Noble gases all have two or more stable isotopes: xenon has 9 stable isotopes, krypton 6, argon 3, neon 3, and helium 2. All stable isotopes of noble gases and their relative abundances can be found in Ozima and Podosek (1983, 2002) and Porcelli and Turekian (see Chapter 6.16), which also provide excellent overview of the noble gases and Earth degassing. The stable and nonradiogenic isotopes can be fractionated during escape and hence can indicate the degree of escape to outer space.
3. Numerous stable isotopes of noble gases are radiogenic-nucleogenic-fissiogenic (for simplicity, they will be collectively referred to as radiogenic in this chapter):  $^4\text{He}$ ,  $^{21}\text{Ne}$ ,  $^{40}\text{Ar}$ ,  $^{83}\text{Kr}$ ,  $^{84}\text{Kr}$ ,  $^{86}\text{Kr}$ ,  $^{129}\text{Xe}$ ,  $^{131}\text{Xe}$ ,  $^{132}\text{Xe}$ ,  $^{134}\text{Xe}$ , and  $^{136}\text{Xe}$ , providing crucial constraints including the timing of mantle degassing and the degree of degassing.
4. The properties of noble gases are relatively simple, and hence, they can often be traced reliably.

Because of these wonderful properties, the noble gases have been heavily studied, and volumes have been written about noble gases in Earth sciences (e.g., Ozima and Podosek, 1983, 2002; Porcelli et al., 2002; also see Chapter 3.7). The other gases do not provide much constraint on the timing of degassing, but their budget reveals their own individual degassing and possible recycling history. All the individual gas systems will be summarized in this data section. In summarizing the data, care is taken to use model-independent estimates or to clearly specify the assumptions adopted in making the estimates although comments and explanations are also provided.

Measured noble gas isotope ratios in mantle-derived rocks are often contaminated by atmospheric noble gases (e.g., noble gases in seawater or air). For helium, this problem is negligible because most air helium has escaped, leading to negligible concentrations compared to mantle-derived rocks (but helium in continental crust can be a source of contamination for basalts in continental regions). Hence, helium isotopes in oceanic basalts and mantle xenoliths are often taken to represent mantle signature. For neon, with the consensus that mantle neon is close to solar, it is possible to correct for atmospheric contamination and obtain the true mantle  $^{21}\text{Ne}/^{22}\text{Ne}$  ratio by extrapolation to solar  $^{20}\text{Ne}/^{22}\text{Ne} = 13.8$  or to the maximum observed  $^{20}\text{Ne}/^{22}\text{Ne} \approx 13.0$  (Sarda et al., 2000; Yokochi and Marty, 2004). Atmospheric contamination could occur in the laboratory, or since or as the mantle sample was brought to the surface, or by subducted atmospheric component into the mantle. All of these contaminations are removed when correction is made in estimating  $^{21}\text{Ne}/^{22}\text{Ne}$  at a fixed  $^{20}\text{Ne}/^{22}\text{Ne}$ . For Ar and Xe (Kr data are very limited), atmospheric contamination is ubiquitous, and no simple correction scheme is available. Although using a mixing model by a plot of a specific isotope ratio with  $^{20}\text{Ne}/^{22}\text{Ne}$  may help to constrain the atmospheric contamination component, various uncertainties mean that only very rough estimates for Ar and Xe isotope ratios are possible if correcting to  $^{20}\text{Ne}/^{22}\text{Ne} = 13.0$ , and no reliable correction can be made if correcting to  $^{20}\text{Ne}/^{22}\text{Ne} = 13.8$ .

Another issue is that even after obtaining the mantle signature (by correcting for atmospheric contamination), that signature can still be due to mixing of different mantle reservoirs (such as MORB mantle and OIB mantle).

### 6.2.3.2 He

The He system provides the best constraint on the current degassing rate, the presence of primordial gas (not recycled gas) inside Earth, and true mantle isotope ratios. There are two stable He isotopes,  $^3\text{He}$  and  $^4\text{He}$ .  $^4\text{He}$  (its nucleus is the  $\alpha$ -particle) is the decay product of  $^{238}\text{U}$  (each  $^{238}\text{U}$  decays to eight  $^4\text{He}$  and one  $^{206}\text{Pb}$ ),  $^{235}\text{U}$  (each  $^{235}\text{U}$  decays to seven  $^4\text{He}$  and one  $^{207}\text{Pb}$ ), and  $^{232}\text{Th}$  (each  $^{232}\text{Th}$  decays to six  $^4\text{He}$  and one  $^{208}\text{Pb}$ ). In addition,  $^{146}\text{Sm}$  (extinct),  $^{147}\text{Sm}$ , and  $^{190}\text{Pt}$  also contribute minor amount of  $^4\text{He}$ .  $^3\text{He}$  is primordial. (Cosmogenic and nucleogenic  $^3\text{He}$  is insignificant in mantle rocks although one has to be careful to avoid surface cosmogenic  $^3\text{He}$  accumulation during sampling and measurements (Chen et al., 2007; Ozima and Podosek, 2002).) Once He is degassed from the mantle to air, it is rapidly lost to outer space due to the small mass of  $^3\text{He}$  and  $^4\text{He}$ , with preferential loss of  $^3\text{He}$ . Hence, He content in air is very small and reflects the steady-state concentration due to degassing from the interior and gravitational loss from air.

In literature, He isotope ratio is often expressed as  $^3\text{He}/^4\text{He}$  (with the radiogenic isotope in the denominator), and less commonly as  $^4\text{He}/^3\text{He}$ . Because radiogenic isotope is used as the numerator in all other isotopic systems, for consistency,  $^4\text{He}/^3\text{He}$  will be used in this chapter.

Because of the loss of He from air to outer space, the total amount of degassed He is not directly known and the small amount of He in air does not provide a constraint on mantle degassing. Furthermore, due to (1) the preferential loss of  $^3\text{He}$  compared to  $^4\text{He}$  and (2) the partial degassing of  $^4\text{He}$  from the crust,  $^4\text{He}/^3\text{He}$  ratio in air is high and does not provide any constraint on mantle degassing. Owing to the low concentration of He in air and in ocean water and other surface reservoirs, the recycling of He back to the mantle is negligible, and measured  $^4\text{He}/^3\text{He}$  ratios in mantle-derived oceanic basaltic glasses typically are not contaminated by air and represent mantle signature, which is a blessing. However, crustal He concentration (due to decay of  $^{238}\text{U}$ ,  $^{235}\text{U}$ , and  $^{232}\text{Th}$ ) can be significant, so that He in crustal fluids may not be pure mantle signature. Porcelli and Halliday (2001) evaluated whether the core could serve as a source for mantle helium, with inconclusive result. Wheeler et al. (2006) argued that U concentration in Earth's core is low and hence cannot provide much additional  $^4\text{He}$  to the mantle.

The primordial  $^4\text{He}/^3\text{He}$  ratio in Earth is often thought to be similar to that measured on Jupiter,  $6000 \pm 180$  (Mahaffy et al., 1998).  $^4\text{He}/^3\text{He}$  ratio in MORB is fairly consistent, about  $89\,350 \pm 11\,170$  ( $1\sigma$  error hereafter) (Graham, 2002), indicating a roughly uniform DMM.  $^4\text{He}/^3\text{He}$  ratio in OIB is more variable, but usually, significantly lower than that in MORB, frequently interpreted to mean higher  $^3\text{He}$  concentration and hence lower degree of degassing for OIB mantle.

The radiogenic part of  $^4\text{He}$  (signified as  $^4\text{He}^*$ ) in UPM can be estimated well. The mass of BSE is  $4.04 \times 10^{24}$  kg. Using U and Th concentrations in BSE as 21.8 and 83.4 ppb (hereafter, ppb and ppm are concentrations by weight) with 15% relative error (see Chapter 3.1) and a closure age of 4.46 Ga (Allegre et al., 2008; Wetherill, 1975; Zhang, 1998), the total production of  $^4\text{He}^*$  in BSE (without loss to outer space) is  $(6.56 \pm 0.98) \times 10^{18}$  mol, and the concentration of  $^4\text{He}^*$  in

UPM is  $(1.62 \pm 0.24) \times 10^{-6}$  mol kg $^{-1}$ , or  $(6.50 \pm 0.97)$  ppb ([Table 1](#)). This concentration is also the minimum concentration of  $^4\text{He}$  in BSE.

To estimate total  $^4\text{He}$  (including radiogenic and nonradioactive) in UPM requires knowledge of the initial nonradioactive  $^4\text{He}$ . One method to estimate the initial nonradioactive  $^4\text{He}$  is from primordial  $^4\text{He}/^3\text{He}$  ratio and the present  $^4\text{He}/^3\text{He}$  ratio in UPM. Some years ago, it was thought that the present-day  $^4\text{He}/^3\text{He}$  ratio in UPM could be approximated by the lowest  $^4\text{He}/^3\text{He}$  in OIB, such as Hawaii and Iceland basalts. This assumption has been challenged in at least two fronts.

1. Although the low  $^4\text{He}/^3\text{He}$  ratio in OIB is often interpreted to mean a less degassed mantle compared to MORB mantle, the concentration of  $^3\text{He}$  in OIB (even in undersea Loihi basaltic glass) is often less than that in MORB. This long-standing ‘helium paradox’ has been used to argue that OIB mantle is more degassed ([Anderson, 1998a,b](#)), but others prefer to interpret the low  $^3\text{He}$  concentration in OIB as due to magma chamber processes (e.g., [Graham, 2002; Hilton et al., 2000](#)), such as open-system degassing of plume melts ([Gonnermann and Mukhopadhyay, 2007; Moreira and Sarda, 2000](#)). There has also been discussion of  $^3\text{He}$  contribution to OIB mantle source by the outer core ([Brandon et al., 1998, 1999](#)), but the jury is still out ([Brandon et al., 2007](#)).

2. Low  $^4\text{He}/^3\text{He}$  ratios (or high  $^3\text{He}/^4\text{He}$ ) in Hawaii and Iceland are associated with  $^{143}\text{Nd}/^{144}\text{Nd}$ ,  $^{87}\text{Sr}/^{86}\text{Sr}$ ,  $^{176}\text{Hf}/^{177}\text{Hf}$ , and  $^{187}\text{Os}/^{188}\text{Os}$  isotope ratios characteristic of depleted mantle ([Albarede, 2008; Ellam and Stuart, 2004; Jackson et al., 2007](#)), almost as depleted as in DMM. For example, [Figure 4](#) shows  $^4\text{He}/^3\text{He}$  versus  $^{143}\text{Nd}/^{144}\text{Nd}$  in various OIB samples, and no data are clustered near the expected UPM (large open square). The samples of MORB (DMM), Azores, Reunion, and Kerguelen do form a trend toward the expected UPM, but Hawaii and Iceland are often regarded as the best plume samples for primitive He signatures. Only one sample in the Iceland plume (Baffin Islands, Cape Searle, sample CS/17; [Stuart et al., 2003](#)) is near the expected UPM. The fact that low  $^4\text{He}/^3\text{He}$  ratios (and hence presumably primordial) are mostly associated with depleted Sr–Nd–Hf–Os isotopes similar to MORB (see also [Richard et al., 1996](#)) is another paradox in He isotope systematics. As will be seen, He and Ne isotope ratios are correlated. Hence, this paradox is referred to as the ‘volatile paradox.’ One solution is that  $^4\text{He}/^3\text{He}$  ratios measured in OIB are not necessarily candidates for UPM or BSE ([Albarede, 2008; Ellam and Stuart, 2004](#)). Another solution to this paradox is to assume that Earth is superchondritic, with  $^{143}\text{Nd}/^{144}\text{Nd}$  ratio of  $0.512\,97 \pm 0.000\,10$  in BSE or UPM ([Boyett and Carlson, 2005, 2006; Jackson et al., 2010](#)). However, the full consequence of the superchondritic Earth assumption has

**Table 1** He budget and degassing flux

	Concentration in UPM (mol kg $^{-1}$ )	Concentration in DMM (mol kg $^{-1}$ )	Global degassing flux (mol year $^{-1}$ )	Z
$^4\text{He}^*$	$(1.62 \pm 0.24) \times 10^{-6}$			
$^4\text{He}$	$(2.31 \pm 0.69) \times 10^{-6}$	$(9.2 \pm 3.0) \times 10^{-8}$	$(4.7 \pm 1.1) \times 10^7$	24
$^3\text{He}$	$\sim 1.16 \times 10^{-10}$	$\sim 1.03 \times 10^{-12}$	$527 \pm 102$	106

( $^4\text{He}/^3\text{He}$ ) is  $89\,350 \pm 11\,170$  in DMM ([Graham, 2002](#)) and 20000 in UPM (see text). Z = ratio of (needed mean degassing rate to produce the atmosphere including the escaped He)/(present-day degassing rate).

Source: [Graham \(2002\)](#), [Bianchi et al. \(2010\)](#), and this work.

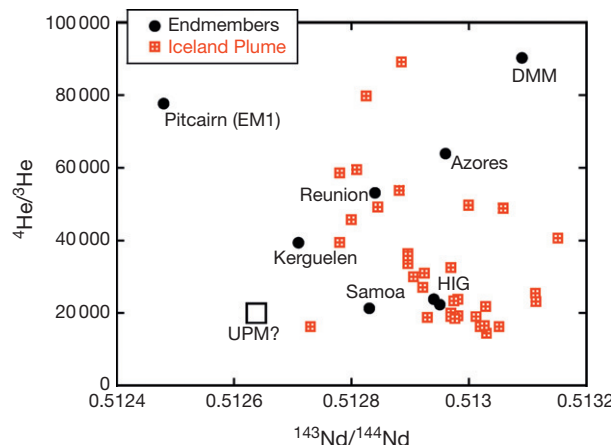


**Figure 4**  $^4\text{He}/^3\text{He}$  versus  $^{143}\text{Nd}/^{144}\text{Nd}$  in mantle-derived basalts. End-members of Azores, HIG (Hawaii–Iceland–Galapagos), Kerguelen, Pitcairn, Reunion, and Samoa are from [Jackson et al. \(2009\)](#). Iceland plume data include not only modern Iceland basalts but also Tertiary basalts of North Atlantic Large Igneous Province with age  $\leq 62$  Ma. The data are from [Graham et al. \(1998\)](#), [Marty et al. \(1998a,b\)](#), [Hilton et al. \(1999\)](#), [Peate et al. \(2003\)](#), [Stuart et al. \(2003\)](#), [Ellam and Stuart \(2004\)](#), and [Jackson et al. \(2010\)](#).

not been examined. For example, based on the Sr-Nd mantle array,  $^{87}\text{Sr}/^{86}\text{Sr}$  ratio in UPM corresponding to  $^{143}\text{Nd}/^{144}\text{Nd} = 0.51297 \pm 0.00010$  would be  $0.7030 \pm 0.0004$ , very close to the ratio in DMM (0.7020). That would mean only about 10% Sr has been transported from primordial DMM to continental crust, which is not consistent with independent estimate of about 50% (e.g., McDonough and Sun, 1995; Salters and Stracke, 2004). It is hence necessary to examine all the consequences of a superchondritic Sm/Nd ratio before adopting it for the primitive mantle. Albarede (2008) speculated that He isotope ratio variations in the mantle are due to diffusion between fertile reservoir and refractory reservoir. Lee et al. (2010) explained the low  $^4\text{He}/^3\text{He}$  in mantle plumes with depleted Sr-Nd-Hf-Os isotopes characteristic of DMM by the upside-down differentiation model in which deep partial melts during the early Earth evolution sank into the lower mantle and were later sampled by OIB.

If OIB does not sample UPM, there is no good way to estimate the  $^4\text{He}/^3\text{He}$  ratio and  $^4\text{He}$  and  $^3\text{He}$  concentrations in UPM. In order to provide some constraint, here OIB with the least-radiogenic  $^4\text{He}/^3\text{He}$  is still assumed to represent UPM. Taking  $^4\text{He}/^3\text{He}$  in UPM to be  $\sim 20\,000$  (Jackson et al., 2009; Figure 4), radiogenic  $^4\text{He}$  would be  $(20\,000 - 6000)/20\,000 = 70\%$  of the total  $^4\text{He}$ ,  $^4\text{He}$  concentration in UPM would be  $(2.31 \pm 0.35) \times 10^{-6} \text{ mol kg}^{-1}$ , or  $(9.3 \pm 1.4) \text{ ppb}$ , and  $^3\text{He}$  concentration in UPM would be  $\sim 1.16 \times 10^{-10} \text{ mol kg}^{-1}$  ( $\sim 0.35 \text{ ppt}$ ). If on the other hand, the present-day  $^4\text{He}/^3\text{He}$  in BSE is taken to be 14 300, which is the lowest  $^4\text{He}/^3\text{He}$  in  $\sim 60 \text{ Ma}$  Iceland plume picrites (Starkey et al., 2009; Stuart et al., 2003), then radiogenic  $^4\text{He}$  would be  $(14\,300 - 6000)/14\,300 = 58\%$  of the total  $^4\text{He}$ ,  $^4\text{He}$  concentration in UPM would be  $(2.8 \pm 0.4) \times 10^{-6} \text{ mol kg}^{-1}$ , or  $(11.2 \pm 1.7) \text{ ppb}$ , and  $^3\text{He}$  concentration in UPM would be  $\sim 2.0 \times 10^{-10} \text{ mol kg}^{-1}$ , or  $\sim 0.59 \text{ ppt}$ . Because no corresponding Ne, Ar, and Xe isotopic data are available for  $^4\text{He}/^3\text{He}$  ratio of  $\sim 14\,300$ , this extreme condition will not be considered much anymore. It seems that a  $^4\text{He}$  concentration of  $(2.31 \pm 0.69) \times 10^{-6} \text{ mol kg}^{-1}$ , or  $9.3 \pm 2.8 \text{ ppb}$  (with 6.5 ppb being the minimum), covers all these possibilities. The total amount of  $^4\text{He}$  in BSE without loss to outer space would be  $(9.3 \pm 2.8) \times 10^{18} \text{ mol}$ . It is estimated that about 40–60% of this amount has been degassed (see later discussion on  $^{40}\text{Ar}$ ), meaning  $\sim 5 \times 10^{18} \text{ mol}$  of  $^4\text{He}$  (about 5000 times the present-day amount in air) has been degassed and then lost to outer space (Table 2).

**Table 2** He concentration ( $\text{mol kg}^{-1}$ ) in UPM as a function of  $^4\text{He}/^3\text{He}$  in UPM

Assumed $^4\text{He}/^3\text{He}$ in UPM	Concentration in UPM		Degree of degassing from DMM	
	$^4\text{He}$	$^3\text{He}$	$^4\text{He}$ (%)	$^3\text{He}$ (%)
20 000	$2.31 \times 10^{-6}$	$1.16 \times 10^{-10}$	96.0	99.1
14 300	$2.8 \times 10^{-6}$	$2.0 \times 10^{-10}$	96.7	99.5

Primordial  $^4\text{He}/^3\text{He}$  ratio is assumed to be 6000.

Source: Mahaffy PR, Donahue TM, Atreya SK, Owen TC, and Niemann HB (1998) Galileo probe measurements of D/H and  $^3\text{He}/^4\text{He}$  in Jupiter's atmosphere. *Space Science Reviews* 84: 251–263.

The concentration of  $^3\text{He}$  and  $^4\text{He}$  in DMM can be estimated from the following: degassing rate of  $^3\text{He}$  and  $^4\text{He}$  (Bianchi et al., 2010; see also Cartigny et al., 2008; Jean-Baptiste 1992; Saal et al., 2002), MORB production rate  $21 \text{ km}^3$  (Crisp, 1984), and average degree of partial melting 12% (Klein and Langmuir, 1987; Niu, 1997). The new estimate of global  $^3\text{He}$  degassing rate from new global dataset of helium isotopes and World Ocean Circulation Experiment is  $527 \pm 102 \text{ mol year}^{-1}$  (Bianchi et al., 2010), about a factor of 2 lower than the earlier estimate by Craig et al. (1975) and Lupton (1983). Because many mantle fluxes are based on the  $^3\text{He}$  flux, this change is significant and will affect estimation of other parameters. The global  $^4\text{He}$  degassing rate is about  $89\,350 \times 527 = (4.7 \pm 1.1) \times 10^7 \text{ mol year}^{-1}$ . At this rate, the estimated amount of degassed  $^4\text{He}$  ( $\sim 5 \times 10^{18} \text{ mol year}^{-1}$ ) would take 106 billion years. In other words, the mean  $^4\text{He}$  degassing rate over Earth history is  $\sim 24$  times the current degassing rate. Let  $Z$  be the ratio of the needed mean degassing rate to generate the atmosphere (including lost He) to the observed mantle degassing rate. The values of  $Z$  for  $^3\text{He}$  and  $^4\text{He}$  are listed in Table 1.

From the He degassing rate, the calculated concentrations in DMM are  $(9.2 \pm 3.0) \times 10^{-8} \text{ mol kg}^{-1}$ , or  $(0.37 \pm 0.09) \text{ ppb}$ , for  $^4\text{He}$  and  $(1.03 \pm 0.20) \times 10^{-12} \text{ mol kg}^{-1}$ , or  $(0.0031 \pm 0.0006) \text{ ppt}$ , for  $^3\text{He}$ . Adopting  $^4\text{He}/^3\text{He}$  ratios in UPM to be 20 000, then the degree of degassing for DMM is 96.0% for  $^4\text{He}$  and 99.1% for  $^3\text{He}$ , somewhat higher than the estimate of Zhang and Zindler (1989; 88% and 97.5%), mostly due to the updated and lower  $^3\text{He}$  flux (only about 46% of the earlier estimate by Craig et al., 1975).

### 6.2.3.3 Ne

The Ne isotopic system provides the best evidence for the solar affinity of Ne in the primordial mantle. Furthermore, this system offers a method to correct for atmospheric contamination so that true mantle Ne signature can be fairly reliably deduced.

There are three stable Ne isotopes ( $^{20}\text{Ne}$ ,  $^{21}\text{Ne}$ , and  $^{22}\text{Ne}$ ), of which  $^{20}\text{Ne}$  and  $^{22}\text{Ne}$  are nonradiogenic and  $^{21}\text{Ne}$  is nucleogenic by mainly the following reaction:  $^{18}\text{O} + ^4\text{He} \rightarrow ^{21}\text{Ne} + ^1\text{n}$ , where  $^4\text{He}$  is from  $\alpha$ -decay. Therefore, the production of nucleogenic  $^{21}\text{Ne}$  is related to that of radiogenic  $^4\text{He}$ , with  $^{21}\text{Ne}^*/^4\text{He}^* = (4.5 \pm 0.8) \times 10^{-8}$  (Leya and Wieler, 1999; Yatsevich and Honda, 1997), where \* signifies nucleogenic or radiogenic. From the total production of  $^4\text{He}^*$  in BSE,  $(6.56 \pm 0.98) \times 10^{18} \text{ mol}$  (Section 6.2.3.2), the total production of  $^{21}\text{Ne}^*$  in BSE is  $(2.95 \pm 0.68) \times 10^{11} \text{ mol}$ .

$^{20}\text{Ne}/^{22}\text{Ne}$  and  $^{21}\text{Ne}/^{22}\text{Ne}$  ratios in air are 9.80 and 0.0290 (Ozima and Podosek, 2002).  $^{20}\text{Ne}/^{22}\text{Ne}$  ratio in air is higher than the so-called meteoritic or planetary neon ( $^{20}\text{Ne}/^{22}\text{Ne} = 7.4\text{--}8.9$ ; Anders and Grevesse, 1989; Black and Pepin, 1969; also see Huss et al., 1996) but lower than solar neon ( $^{20}\text{Ne}/^{22}\text{Ne} = 13.8$ ). Nonradiogenic Ne in air is assumed to be fractionated solar Ne. The exact nonradiogenic  $^{21}\text{Ne}/^{22}\text{Ne}$  ratio in air as fractionated product of solar Ne is not known due to the range of possibilities in mass fractionation. Using various fractionation laws (including the equilibrium fractionation law, kinetic fractionation law, power law, and exponential law), the nonradiogenic  $^{21}\text{Ne}/^{22}\text{Ne}$  ratio in air is in a narrow range of 0.0276–0.0279, meaning

$3.2 \times 10^{11}$  to  $4.1 \times 10^{11}$  mol of nucleogenic  $^{21}\text{Ne}^*$  in air, greater than total  $^{21}\text{Ne}^*$  production in BSE. That would be a neon paradox. However, using the hydrodynamic escape model of Pepin (1991), the nonradiogenic  $^{21}\text{Ne}/^{22}\text{Ne}$  ratio in air can be as high as 0.0288, leading to  $5.9 \times 10^{10}$  mol of nucleogenic  $^{21}\text{Ne}^*$  in air, only  $\sim 20\%$  of the total  $^{21}\text{Ne}^*$  production in BSE. Another calculation is to assume about 40% of the total  $^{21}\text{Ne}^*$  is in air based on the degree of degassing for  $^{40}\text{Ar}$  (see later), leading to  $\sim 0.0286$  for the nonradiogenic  $^{21}\text{Ne}/^{22}\text{Ne}$  ratio in air.

The present degassing rate of mantle Ne (excluding contamination by recent or ancient air) can be estimated from  $^3\text{He}$  degassing rate ( $527$  mol year $^{-1}$ ; see previous section) and the uncontaminated  $^3\text{He}/^{22}\text{Ne}$  ratio in MORB and OIB. Assume that mantle degassing is mostly due to MORB degassing. The uncontaminated  $^3\text{He}/^{22}\text{Ne}$  ratio in MORB is about  $10.2 \pm 1.6$  (Honda and McDougall, 1998), leading to  $^{22}\text{Ne}$  degassing rate of  $52$  mol year $^{-1}$ ,  $^{20}\text{Ne}$  degassing rate of  $672$  mol year $^{-1}$ , and  $^{21}\text{Ne}$  degassing rate of  $3.3$  mol year $^{-1}$ , and the concentrations of  $^{22}\text{Ne}$ ,  $^{20}\text{Ne}$ , and  $^{21}\text{Ne}$  in DMM are about  $1.05 \times 10^{-13}$ ,  $1.37 \times 10^{-12}$ , and  $7.0 \times 10^{-15}$  mol kg $^{-1}$  (or  $2.32$ ,  $27.4$ , and  $0.146$  ppq). At these rates, it would take  $4.3 \times 10^{12}$ ,  $2.6 \times 10^{12}$ , and  $5.7 \times 10^{12}$  years to supply enough  $^{20}\text{Ne}$ ,  $^{21}\text{Ne}$ , and  $^{22}\text{Ne}$  in air. Because of the correlation between  $^{21}\text{Ne}$  and  $^4\text{He}$  production, the large time difference (by a factor of more than 20) to supply air  $^{21}\text{Ne}$  ( $2.6 \times 10^{12}$  years) and to supply the hypothetical  $^4\text{He}$  in air ( $1.1 \times 10^{11}$  years) is a paradox. One solution to the paradox is that a significant amount of  $^{21}\text{Ne}$  in air was initially there or was from a nonmantle origin. This argument will be reinforced from other lines of evidence later in this section.

Nonradiogenic Ne isotope ratio ( $^{20}\text{Ne}/^{22}\text{Ne}$ ) in mantle-derived rocks is clearly higher than the air ratio of  $9.80$  (Honda et al., 1991; Marty, 1989; Sarda et al., 1988). Ne is the only noble gas element with clear difference in nonradiogenic isotope ratio between mantle-derived rocks and air. Although Kr and Xe in well gases also have different nonradiogenic isotope ratios from those in air, suggesting that Kr and Xe isotopes in the mantle may also differ from air ratios, the differences cannot be resolved clearly in mantle-derived rocks at present.

Air contamination to measured Ne isotope ratios in mantle-derived rocks is often major. However, the Ne system provides a way (three-isotope plot, see Figure 5) to remove air contamination and hence to obtain true mantle ratios. As discussed earlier, the correction also removes the effect of recycled surface Ne into the mantle. In a  $^{21}\text{Ne}/^{22}\text{Ne}$  versus  $^{20}\text{Ne}/^{22}\text{Ne}$  plot, data for MORB and for specific ocean islands form linear trends with air neon at one end (Figure 5). The trends are interpreted to be due to mixing between air Ne and mantle Ne. The true mantle end-member may be pinned down if the primordial  $^{20}\text{Ne}/^{22}\text{Ne}$  ratio is known. Ne isotopic data from well gases are also included in Figure 5, which cannot be attributed to simple mixing between air and another end-member.

Within  $2\sigma$  uncertainty, the maximum  $^{20}\text{Ne}/^{22}\text{Ne}$  ratio so far measured in mantle samples approaches but does not exceed  $13.0$ . Hence, the mantle end-member (i.e., the high  $^{20}\text{Ne}/^{22}\text{Ne}$  ratio and  $^{21}\text{Ne}/^{22}\text{Ne}$  ratio end-member) of Ne isotope arrays in Figure 5 is expected to have a  $^{20}\text{Ne}/^{22}\text{Ne}$  ratio of  $13.0$  or higher. Because  $^{20}\text{Ne}/^{22}\text{Ne}$  is  $13.8$  for solar Ne and because there are no identifiable reservoirs with  $^{20}\text{Ne}/^{22}\text{Ne} \approx 13.0$ , often, mantle

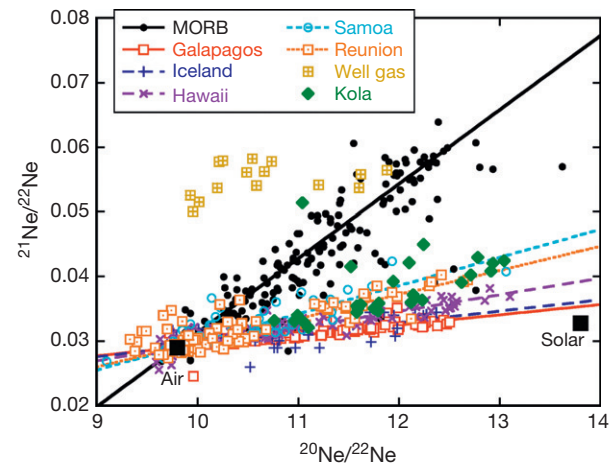


**Figure 5** Plot of selected Ne isotope data. For clarity, error bars are not shown, and data with large error bars (e.g., error on  $^{21}\text{Ne}/^{22}\text{Ne}$  is  $>0.01$ ) are not included. The two large solid squares are for air (9.80, 0.0290) and solar wind (13.8, 0.0328). Data sources: Sarda et al. (1988, 2000), Staudacher et al. (1990), Hiyagon et al. (1992), Poreda and Farley (1992), Honda et al. (1993), Moreira et al. (1995, 1996, 1998, 2001), Moreira and Allegre (2002), Valbracht et al. (1996, 1997), Niedermann and Bach (1998), Dixon et al. (2000), Trieloff et al. (2000, 2002), Hanyu et al. (2001, 2007), Shaw et al. (2001), Yokochi and Marty (2004, 2005), Ballentine et al. (2005), Stroncik et al. (2007), Jackson et al. (2009), Kurz et al. (2009), Parai et al. (2009), and Raquin et al. (2008).

Ne is assumed to be solar with  $^{20}\text{Ne}/^{22}\text{Ne}=13.8$ . Adopting  $^{20}\text{Ne}/^{22}\text{Ne}=13.8$  has the advantage that it is a clear solar component. However, because this requires relatively large extrapolation from actual data, when effort is made to correct for air contamination on Ar and Xe isotope ratios using data of  $^{20}\text{Ne}/^{22}\text{Ne}$  and Ar or Xe isotope ratios, the correction cannot be reliably made to obtain Ar and Xe isotope ratios in the mantle end-member. On the other hand, the possibility that mantle Ne end-member has a  $^{20}\text{Ne}/^{22}\text{Ne}=13.0$  cannot be ruled out even though such an end-member would be fractionated solar Ne, not simple solar Ne. Adopting a lower primordial  $^{20}\text{Ne}/^{22}\text{Ne}$  ratio of  $13.0$  has the advantage that it allows reasonable constraint on self-consistent estimates of Ar and Xe isotope ratios in different mantle reservoirs (requiring less extrapolation) using  $^{20}\text{Ne}/^{22}\text{Ne}$  to correct for atmospheric contamination. Hence, the discussion in the succeeding texts mostly uses correction to  $^{20}\text{Ne}/^{22}\text{Ne}=13.0$ , although sometimes, results for correction to  $^{20}\text{Ne}/^{22}\text{Ne}=13.8$  are also shown. If future new  $^{20}\text{Ne}/^{22}\text{Ne}$  data populate the gap between  $13.0$  and  $13.8$ , it would be time to firmly adopt  $13.8$  as the mantle  $^{20}\text{Ne}/^{22}\text{Ne}$  ratio, and these data with associated Ar and Xe isotope data would also allow new constraints on Ar and Xe isotope ratios.

Assuming  $^{20}\text{Ne}/^{22}\text{Ne}=13.0$  for primordial mantle neon, by extrapolating the trends to  $^{20}\text{Ne}/^{22}\text{Ne}=13.0$ , uncontaminated  $^{21}\text{Ne}/^{22}\text{Ne}$  in mantle-derived rocks can be estimated (Figure 5), denoted as  $(^{21}\text{Ne}/^{22}\text{Ne})_{13.0}$ . Similarly,  $(^{21}\text{Ne}/^{22}\text{Ne})_{13.8}$  can be defined. Because air contamination of  $^4\text{He}/^3\text{He}$  ratio is negligible, and because radiogenic  $^{21}\text{Ne}$  and radiogenic  $^4\text{He}$  are related, a plot of  $(^{21}\text{Ne}/^{22}\text{Ne})_{13.0}$  versus  $^4\text{He}/^3\text{He}$  can be used to examine various mantle signatures. Figure 6(b) displays such data for MORB and several hotspot regions, and there is good positive correlation between  $(^{21}\text{Ne}/^{22}\text{Ne})_{13.0}$  and  $^4\text{He}/^3\text{He}$ ,

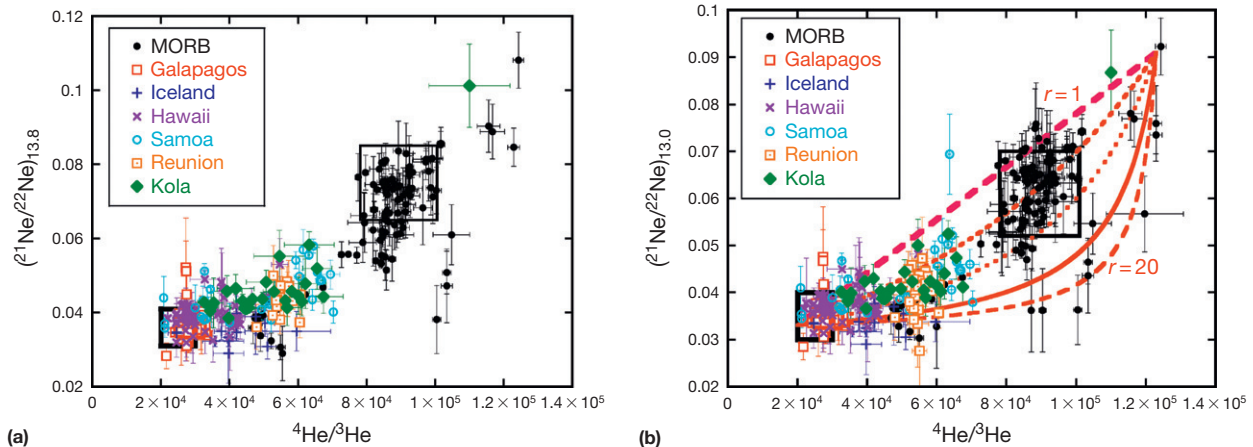


**Figure 6** Extrapolated  $^{21}\text{Ne}/^{22}\text{Ne}$  (to either  $^{20}\text{Ne}/^{22}\text{Ne} = 13.8$  or  $13.0$ ) versus  $^{4}\text{He}/^{3}\text{He}$  in selected mantle-derived rocks. In calculating  $(^{21}\text{Ne}/^{22}\text{Ne})_{13.8}$  or  $13.0$ , only data with  $^{20}\text{Ne}/^{22}\text{Ne} > 10.0$  are used. See Figure 5 for data sources. Points for which the error on  $^{21}\text{Ne}/^{22}\text{Ne}$  is greater than  $0.01$  are excluded. The two large open squares with heavy black lines in each figure are for DMM and the least-radiogenic OIB. The heavy curves in (b) are mixing curves with  $r = (^3\text{He}/^{22}\text{Ne})_{\text{DMM}} / (^3\text{He}/^{22}\text{Ne})_{\text{UPM}} = 1, 2, 4, 10, \text{ and } 20$ .

demonstrating self-consistency in treating the mantle as undegassed and degassed reservoirs. This plot may be viewed as a version of mantle array for noble gases, similar to the  $^{143}\text{Nd}/^{144}\text{Nd}$  versus  $^{87}\text{Sr}/^{86}\text{Sr}$  mantle array (see Chapter 3.3). There is clear curvature in  $(^{21}\text{Ne}/^{22}\text{Ne})_{13.0}$  versus  $^{4}\text{He}/^{3}\text{He}$ , indicating that  $(^3\text{He}/^{22}\text{Ne})$  in DMM is 1.5–4 times that in UPM, roughly consistent with the results of Honda and McDougall (1998). In DMM, both  $(^{21}\text{Ne}/^{22}\text{Ne})_{13.0}$  and  $^{4}\text{He}/^{3}\text{He}$  are high, and in HIG (Hawaii, Iceland, and Galapagos) hot spots, both ratios are low. The least-radiogenic OIB sources in terms of  $^{4}\text{He}/^{3}\text{He}$  are also the least radiogenic in terms of  $(^{21}\text{Ne}/^{22}\text{Ne})_{13.0}$  (heavy box at the lower-left region of Figure 6(a) and 6(b)). There are samples with even lower  $^{4}\text{He}/^{3}\text{He}$  ratios (early Tertiary Iceland plume rocks; Starkey et al., 2009; Stuart et al., 2003), but no corresponding Ne isotopic data are available. Low  $(^{21}\text{Ne}/^{22}\text{Ne})_{13.0}$  values in Figure 6(b) are used to represent UPM. There are also MORB samples with higher and correlated  $^{4}\text{He}/^{3}\text{He}$  (up to  $1.24 \times 10^5$ ) and  $^{21}\text{Ne}/^{22}\text{Ne}$  (up to 0.092 at  $^{20}\text{Ne}/^{22}\text{Ne} = 13.0$  or 0.110 at  $^{20}\text{Ne}/^{22}\text{Ne} = 13.8$ ) than typical MORB samples, which seem to be true signature for a more degassed mantle (meaning that DMM is not uniform) although not much is mentioned in literature. Table 3 summarizes Ne isotopes in air and in the mantle.

Because it is important to have self-consistent  $^{21}\text{Ne}/^{22}\text{Ne}$  and  $^{4}\text{He}/^{3}\text{He}$  ratios in DMM and UPM in modeling mantle degassing, the correlation between  $^{21}\text{Ne}/^{22}\text{Ne}$  and  $^{4}\text{He}/^{3}\text{He}$  (Figure 6) is used to estimate the end-member ratios. For the UPM end-member, data with  $^{4}\text{He}/^{3}\text{He}$  between 20000 and 40000 are divided into ten bins, with each bin spanning a  $^{4}\text{He}/^{3}\text{He}$  range of 2000. In each bin, the weighted averages of  $^{4}\text{He}/^{3}\text{He}$  and  $^{21}\text{Ne}/^{22}\text{Ne}$  and errors are calculated. These averages with errors are then plotted (Figure 7(a)) and are fitted using weighted linear least squares (York, 1969).  $(^{21}\text{Ne}/^{22}\text{Ne})_{13.0}$  is then calculated to be  $0.0340 \pm 0.0003$  at  $^{4}\text{He}/^{3}\text{He} = 20000$  as the ratio in UPM. For the DMM end-member, after removing some outliers, MORB data with  $^{4}\text{He}/^{3}\text{He}$  between 78000 and 124000 are divided into 23 bins (but some bins do not contain data and some bins contain only one data point). Then the same procedure is used to

**Table 3** Ne isotope ratios in air and solar wind

Sample	$^{20}\text{Ne}/^{22}\text{Ne}$	$^{21}\text{Ne}/^{22}\text{Ne}$
Solar	13.80	0.0328
Air	9.80	0.0290

Source: Graham DW (2002) Noble gas isotope geochemistry of mid-ocean ridge and ocean island basalts: Characterization of mantle source reservoirs. *Reviews in Mineralogy and Geochemistry* 47: 247–317.

obtain  $(^{21}\text{Ne}/^{22}\text{Ne})_{13.0} = 0.0646 \pm 0.0003$  at  $^{4}\text{He}/^{3}\text{He} = 89\,350$  (Figure 7(b)). The data are shown in Tables 4 and 5.

Adopting  $(^3\text{He}/^{22}\text{Ne})_{\text{DMM}} / (^3\text{He}/^{22}\text{Ne})_{\text{UPM}} = 2.28$  (mixing curves in Figure 6(b)), then  $(^3\text{He}/^{22}\text{Ne})_{\text{UPM}} = 4.5$ , and  $^{22}\text{Ne}$  concentration in UPM can be estimated from  $^3\text{He}$  in UPM ( $1.16 \times 10^{-10} \text{ mol kg}^{-1}$ ) to be  $2.6 \times 10^{-11} \text{ mol kg}^{-1}$ . Another estimate is as follows. Since the total production of  $^{21}\text{Ne}^*$  in BSE is  $(2.95 \pm 0.68) \times 10^{11} \text{ mol}$  as obtained earlier, knowing the primordial  $^{21}\text{Ne}/^{22}\text{Ne}$  ratio (solar ratio or fractionated solar ratio) and the  $^{21}\text{Ne}/^{22}\text{Ne}$  ratio in UPM, the total amount of primordial  $^{22}\text{Ne}$  in the whole mantle can also be found to as

$$^{22}\text{Ne} = ^{21}\text{Ne}^* / [(^{21}\text{Ne}/^{22}\text{Ne})_{\text{UPM}} - (^{21}\text{Ne}/^{22}\text{Ne})_0] \quad [1]$$

from which the concentration of  $^{22}\text{Ne}$  in UPM can be estimated to be  $3.4 \times 10^{-11} \text{ mol kg}^{-1}$ , which is roughly consistent with the estimate based on  $(^3\text{He}/^{22}\text{Ne})_{\text{UPM}}$ , giving some confidence in the estimates.  $^{22}\text{Ne}$  concentration in UPM is taken to be the average:  $(3.0 \pm 0.4) \times 10^{-11} \text{ mol kg}^{-1}$ .

The calculated Ne budgets are listed in Table 6. According to the results, DMM has been degassed 99.65% compared to UPM in terms of  $^{22}\text{Ne}$ . Furthermore, from Table 6, estimated  $^{22}\text{Ne}$  concentration in UPM is only about 1/5 of that needed to produce Ne in air, which reinforces the Ne-deficiency paradox raised earlier.

Because Ne isotope ratios (both the radiogenic and non-radiogenic) in the mantle are different from those in air and because there is gradual degassing, Ne isotope ratios in air must

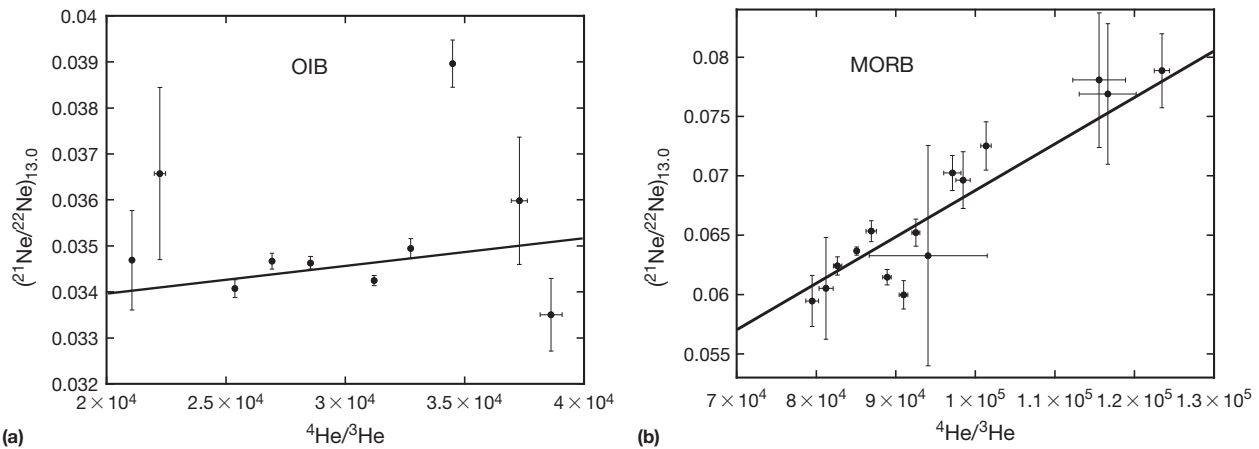


**Figure 7** Obtaining  $(^{21}\text{Ne}/^{22}\text{Ne})_{13.0}$  in UPM and DMM that are internally consistent with  $^{4}\text{He}/^{3}\text{He}$ .

**Table 4** Ne budget in air

	$^{21}\text{Ne}^*$	$^{20}\text{Ne}$	$^{21}\text{Ne}$	$^{22}\text{Ne}$
Total (mol)	$(0.59 - 3.2) \times 10^{11}$	$2.91 \times 10^{15}$	$8.62 \times 10^{12}$	$2.97 \times 10^{14}$
Z		$\sim 971$	$\sim 579$	$\sim 1211$

Nonradiogenic air has  $^{21}\text{Ne}/^{22}\text{Ne} \approx 0.0276 - 0.0288$ . Z = ratio of needed mean degassing rate to produce the escaped He/present-day degassing rate. Source: Ozima M and Podosek FA (2002) *Noble Gas Geochemistry*. Cambridge: Cambridge University Press.

**Table 5** Ne isotope ratios in mantle reservoirs

Assuming mantle $^{20}\text{Ne}/^{22}\text{Ne} = 13.0$ , $(^{4}\text{He}/^{3}\text{He})_{DDM} = 89350$ , and $(^{4}\text{He}/^{3}\text{He})_{UPM} = 20000$		Assuming mantle $^{20}\text{Ne}/^{22}\text{Ne} = 13.8$ , $(^{4}\text{He}/^{3}\text{He})_{DDM} = 89350$ , and $(^{4}\text{He}/^{3}\text{He})_{UPM} = 20000$	
DMM	UPM	DMM	UPM
$^{21}\text{Ne}/^{22}\text{Ne}$	$0.0646 \pm 0.0003$	$0.0340 \pm 0.0003$	$0.0702 \pm 0.0004$
$(^{21}\text{Ne}/^{22}\text{Ne})_0$	$0.03186$	$0.03186$	$0.0328$

$(^{21}\text{Ne}/^{22}\text{Ne})_0$  is the primordial  $^{21}\text{Ne}/^{22}\text{Ne}$  ratio related to solar ratio using exponential fractionation law (Hart and Zindler, 1989).

Source: Graham (2002) and this work.

**Table 6** Ne budget in mantle reservoirs

	$^{20}\text{Ne}$	$^{21}\text{Ne}$	$^{22}\text{Ne}$
Air distributed to DMM <sup>a</sup> ( $\text{mol kg}^{-1}$ )	$1.41 \times 10^{-9}$	$4.18 \times 10^{-12}$	$1.44 \times 10^{-10}$
Estimated concentration in UPM <sup>b</sup> ( $\text{mol kg}^{-1}$ )	$3.9 \times 10^{-10}$	$1.94 \times 10^{-12}$	$3.00 \times 10^{-11}$
Estimated concentration in DMM ( $\text{mol kg}^{-1}$ )	$1.37 \times 10^{-12}$	$7.0 \times 10^{-15}$	$1.05 \times 10^{-13}$
Degassing flux ( $\text{mol year}^{-1}$ )	672	3.3	52

<sup>a</sup>Mass of DMM is taken to be 51% of the whole mantle for this calculation.

<sup>b</sup>Assume  $(^{20}\text{Ne}/^{22}\text{Ne})_{\text{mantle}} = 13.0$ .

have evolved with time. Three possibilities are discussed in the succeeding texts:

- There was no initial neon in air and all neon in air is from mantle degassing, but degassed neon has been fractionated

isotopically (similar to the depletion of  $^3\text{He}$  relative to  $^4\text{He}$  in air) suddenly at some point of time, or gradually. Degassed nucleogenic  $^{21}\text{Ne}$  would also be lost to outer space. In this scenario, average Ne concentration by distributing air into DMM (Table 6) should be smaller than Ne concentration in the UPM (Table 6), opposite to the data in Table 6. Furthermore, nucleogenic  $^{21}\text{Ne}$  production is barely enough to provide nucleogenic  $^{21}\text{Ne}$  in air, further against the escape scenario. Moreover, the current degassing flux is already extremely low to produce air Ne (e.g., when compared to He and  $^{40}\text{Ar}$ ), also against the escape scenario. Hence, this scenario is not preferred.

- There was 'primordial' Ne (or initial Ne) in air, which could be leftover of an early atmosphere (due to accretion degassing or mantle degassing). In this scenario, the amount and isotopic composition of the primordial Ne in air are related as follows:

$$\begin{aligned} & \frac{^{22}\text{Ne}_{\text{air},0}}{^{22}\text{Ne}_{\text{air,today}}} \left( \frac{^{20}\text{Ne}}{^{22}\text{Ne}} \right)_{\text{air},0} + \frac{^{22}\text{Ne}_{\text{mantle}}}{^{22}\text{Ne}_{\text{air,today}}} \left( \frac{^{20}\text{Ne}}{^{22}\text{Ne}} \right)_{\text{mantle}} \\ &= \left( \frac{^{20}\text{Ne}}{^{22}\text{Ne}} \right)_{\text{air,today}} \end{aligned} \quad [2]$$



where  $^{22}\text{Ne}_{\text{mantle}}$  is the amount of  $^{22}\text{Ne}$  in today's air that is from mantle degassing. Let  $F = ^{22}\text{Ne}_{\text{air},0} / ^{22}\text{Ne}_{\text{air,today}}$  (the fraction of  $^{22}\text{Ne}$  in the initial air compared to today's air), then

$$F \left( \frac{^{20}\text{Ne}}{^{22}\text{Ne}} \right)_{\text{air},0} + (1 - F) \left( \frac{^{20}\text{Ne}}{^{22}\text{Ne}} \right)_{\text{mantle}} = 9.80 \quad [3]$$

The relation between  $F$  and  $(^{20}\text{Ne}/^{22}\text{Ne})_{\text{air},0}$  is shown in **Figure 8** for the case of  $(^{20}\text{Ne}/^{22}\text{Ne})_{\text{mantle}} = 13.0$ . The figure shows that at least 29.0% of  $^{22}\text{Ne}$  in air today was the initial  $^{22}\text{Ne}$  if  $(^{20}\text{Ne}/^{22}\text{Ne})_{\text{mantle}} = 13.8$  or 24.6% if  $(^{20}\text{Ne}/^{22}\text{Ne})_{\text{mantle}} = 13.0$ . The percentage of the initial amount of  $^{22}\text{Ne}$  in air is likely significantly higher because  $(^{20}\text{Ne}/^{22}\text{Ne})_{\text{air},0}$  is unlikely zero. For example, if the initial amount of  $^{22}\text{Ne}$  in air was 50% (or even more) of the present-day amount, then  $(^{20}\text{Ne}/^{22}\text{Ne})_{\text{air},0} = 5.8$  for  $(^{20}\text{Ne}/^{22}\text{Ne})_{\text{mantle}} = 13.8$ , or 6.6 for  $(^{20}\text{Ne}/^{22}\text{Ne})_{\text{mantle}} = 13.0$ . The presence of initial  $^{22}\text{Ne}$  in air would make  $(^{21}\text{Ne}/^{22}\text{Ne})_{\text{air}}$  less radiogenic than assuming no initial  $^{22}\text{Ne}$  in air. In this scenario, average concentration in Ne concentration in the present BSE (air + oceans + crust + mantle) is greater than Ne concentration in the UPM, which is consistent with data in **Tables 6**. That is, the present BSE (including all of the atmosphere) is not necessarily the same as the primitive undegassed mantle (UPM) in terms of isotopic compositions and nonradiogenic isotope budget.

3. There is a nonmantle source (such as gradual impact degassing) for Ne in air, and  $^{20}\text{Ne}/^{22}\text{Ne}$  in that source is  $< 9.80$  ([Marty, 1989](#)). The nonmantle Ne may have come to air very early in Earth history or gradually throughout Earth history. In terms of mass balance, this scenario is the same as that of the second scenario, and **Figure 8** would hold except that the horizontal axis would be  $(^{20}\text{Ne}/^{22}\text{Ne})$  ratio in the nonterrestrial source and the vertical axis would be the ratio of  $^{22}\text{Ne}$  from the nonterrestrial source to total  $^{22}\text{Ne}$  in air today. If the nonterrestrial Ne source were chondritic Ne with  $^{20}\text{Ne}/^{22}\text{Ne} = 8.9$  or 7.4, then the fraction of nonterrestrial  $^{22}\text{Ne}$  would be 81.6% or 62.5%, and the fraction of terrestrial  $^{22}\text{Ne}$  from mantle degassing would be only 18.4% or 37.5%, which is consistent with **Table 6**.

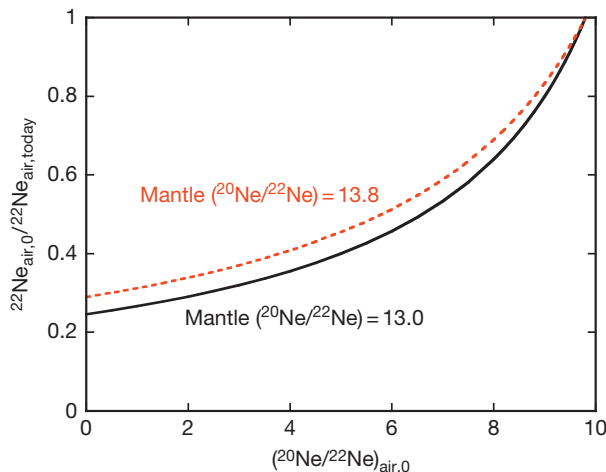


**Figure 8** The relation between the initial amount of  $^{22}\text{Ne}$  in air (expressed as a fraction of present-day  $^{22}\text{Ne}$  on the vertical axis) and initial  $^{20}\text{Ne}/^{22}\text{Ne}$  isotope ratio in air for the case of  $(^{20}\text{Ne}/^{22}\text{Ne})_{\text{mantle}} = 13.0$  or 13.8.

In summary, the observation that  $^{20}\text{Ne}/^{22}\text{Ne}$  in the mantle is higher than that in air ([Craig and Lupton, 1976](#); [Honda et al., 1991](#); [Marty, 1989](#); [Sarda et al., 1988](#)) is revolutionary in understanding the origin of air. Coupled with the deficiency of Ne in the mantle to provide Ne in air, the preferred scenario is that 70–80% of nonradiogenic Ne in air is not from mantle degassing, but from chondritic Ne ([Marty, 1989](#)). If only mantle Ne are considered, Ne isotopes in different mantle reservoirs are consistent with He isotopes. For example, the high  $^{21}\text{Ne}/^{22}\text{Ne}$  in MORB mantle and low  $^{21}\text{Ne}/^{22}\text{Ne}$  in OIB mantle are as expected based on He isotopes. The He and Ne isotope systematics can be used quantitatively to evaluate different degassing models (see later discussion). Therefore, mantle Ne is relatively simple and consistent with mantle He, but air Ne requires both mantle and nonmantle sources.

#### 6.2.3.4 Ar

The K-Ar system provides the best constraint for the mean degree of degassing for one gas species ( $^{40}\text{Ar}$ ) from the whole mantle ([Allegre et al., 1986/87](#); [Zhang, 2002](#); [Zhang and Zindler, 1989](#); see also **Chapter 6.16**). Furthermore, because the degree of degassing of DMM can be estimated, the K-Ar system also constrains the fractions of DMM and UPM over the whole mantle.

Argon has three stable isotopes of which  $^{36}\text{Ar}$  and  $^{38}\text{Ar}$  are nonradiogenic and primordial, but  $^{40}\text{Ar}$  is radiogenic due to the branch decay of  $^{40}\text{K}$  (half-life 1250 My, the branch to  $^{40}\text{Ar}$  accounts for 10.48%) with negligible primordial component. The primordial  $^{40}\text{Ar}/^{36}\text{Ar}$  ratio is about 0.0003 ([Anders and Grevesse, 1989](#)). In the present-day air, the  $^{40}\text{Ar}/^{36}\text{Ar}$  ratio is 298.6 ([Lee et al., 2006](#)), one million times the primordial ratio.  $^{40}\text{Ar}/^{36}\text{Ar}$  ratio in ancient air at 380 Ma was  $291.0 \pm 1.6$  ([Cardogan, 1977](#)). In Earth's mantle, the ratio is even higher, and the highest measured  $^{40}\text{Ar}/^{36}\text{Ar}$  ratio is 64 000 ([Burnard et al., 1997](#)). That is, essentially all  $^{40}\text{Ar}$  in Earth comes from the decay of  $^{40}\text{K}$ . Hence, by estimating K concentration in BSE, total  $^{40}\text{Ar}$  can be calculated, and the mean degree of degassing can be inferred reliably based on straightforward mass balance calculations. The estimation in the succeeding texts uses updated information, but there was little change from previous results (e.g., [Allegre et al., 1986/87](#); [Zhang, 2002](#); [Zhang and Zindler, 1989](#); see also **Chapter 6.16**).

Potassium concentration in BSE has been estimated by various authors (e.g., [Allegre et al., 1995b](#); [Arevalo et al., 2009](#); [Jochum et al., 1983](#); [Zindler and Hart, 1986](#)), and the results are similar. Adopting the most recent estimate of  $280 \pm 60$  ppm ([Arevalo et al., 2009](#)), there are  $(2.89 \pm 0.62) \times 10^{22}$  mol of K, and  $(3.38 \pm 0.72) \times 10^{18}$  mol of  $^{40}\text{K}$  in present-day BSE (using  $^{40}\text{K}$  atomic abundance of 0.0117%; [Anders and Grevesse, 1989](#)). Assuming Earth began to quantitatively retain  $^{40}\text{Ar}$  since 4.46 Ga ([Wetherill, 1975](#); [Zhang, 1998, 2002](#)), total  $^{40}\text{Ar}$  production in BSE is  $(3.84 \pm 0.82) \times 10^{18}$  mol, 59% of the total molar  $^{4}\text{He}$  production. The mean concentration of  $^{40}\text{Ar}$  in BSE and UPM is  $(9.5 \pm 2.0) \times 10^{-10}$  mol kg<sup>-1</sup>, or 38.1 ± 8.2 ppb. Changing the age from 4.46 Ga to 4.50 Ga in the proceeding calculation would increase total  $^{40}\text{Ar}$  production by ~2%, insignificant compared to other errors. K concentration in Earth's core is at least an order of magnitude lower than in BSE ([Corgne et al., 2007](#)), and the mass of the core is only 48% of the mass of

BSE. Hence, the production of  $^{40}\text{Ar}$  due to K in the core and possible transfer of this  $^{40}\text{Ar}$  to BSE can be ignored.

Total  $^{40}\text{Ar}$  in air is  $1.64 \times 10^{18}$  mol (Ozima and Podosek, 1983, 2002), representing  $(43 \pm 9)\%$  of all  $^{40}\text{Ar}$  in the whole Earth (and also in the BSE). There is about  $2.0 \times 10^{16}$  mol  $^{40}\text{Ar}$  in oceans (Broecker and Peng, 1982).  $^{40}\text{Ar}$  in the continental crust can be estimated as follows: The mean concentration of K in the continental crust is 1.69 wt% (Arevalo et al., 2009). Adopting the mass of continental crust as  $2.085 \times 10^{22}$  kg (Peterson and DePaolo, 2007) and the mean age of continents as 2.5 Ga (Hawkesworth et al., 2010), total  $^{40}\text{Ar}$  production in the continental crust is  $3.32 \times 10^{17}$  mol, some of which has already been lost to air (as evidenced by younger K-Ar ages of most rocks compared to other ages). For the purpose of this calculation, assume 30–70% of  $^{40}\text{Ar}$  in the crust was already lost to air. Then, total  $^{40}\text{Ar}$  in air, oceans, and continental crust is  $(1.83 \pm 0.20) \times 10^{18}$  mol, representing  $(47.7 \pm 11.4)\%$  of the total  $^{40}\text{Ar}$  in the BSE.

If the whole mantle has been degassed to a similar degree (one-reservoir model), then the degree of degassing of the mantle would be about  $(47.7 \pm 11.4)\%$ . In the context of a two-mantle-reservoir models with one highly degassed reservoir (DMM) and one undegassed reservoir (UPM), the mass of DMM is at least  $(47.7 \pm 11.4)\%$  of the whole mantle and hence must be more than the upper mantle alone (Figure 1).

The high degree of degassing (48%) for  $^{40}\text{Ar}$  demonstrates that mantle degassing must be more than just an early degassing pulse (e.g., during magma ocean stage) because total  $^{40}\text{Ar}$  production in the first 100 My is only  $2.3 \times 10^{17}$  mol, much less than  $^{40}\text{Ar}$  in air ( $1.64 \times 10^{18}$  mol). Therefore, a very short mean degassing time such as 10–25 My inferred for Xe isotopes (Staudacher and Allegre, 1982) does not work for  $^{40}\text{Ar}$ , meaning that different gases degassed at different timescales, consistent with solubility-controlled degassing.

The concentration of  $^{40}\text{Ar}$  in DMM at present may be estimated to be  $(6.5 \pm 2.5) \times 10^{-8}$  mol  $\text{kg}^{-1}$ , or  $2.6 \pm 1.0$  ppb, from  $^4\text{He}$  concentration in DMM  $((9.2 \pm 3.0) \times 10^{-8}$  mol  $\text{kg}^{-1}$  inferred from degassing flux in a previous section), and the  $^{40}\text{Ar}/^4\text{He}$  molar ratio of  $0.70 \pm 0.15$  (or mass ratio of  $7.0 \pm 1.5$ ) is estimated from MORB samples (Graham, 2002; Raquin et al., 2008). This means that DMM has been degassed by  $93.2 \pm 3.0\%$  for  $^{40}\text{Ar}$ , higher than the estimate of 82% by Zhang and Zindler (1989). The mean degree of degassing for  $^{40}\text{Ar}$  must be smaller than that for  $^{36}\text{Ar}$  and  $^{38}\text{Ar}$  because  $^{40}\text{Ar}$  is continuously produced in the mantle, meaning that early degassing did not affect  $^{40}\text{Ar}$  as much as  $^{36}\text{Ar}$ , and recently produced  $^{40}\text{Ar}$  in the mantle has not had much chance to degas.

Considering the  $^{40}\text{Ar}$  concentration in DMM, the mass fractions of DMM over the whole mantle can be found as  $(0.477 \pm 0.114)/(0.932 \pm 0.030) = 0.512 \pm 0.123 = (51.2 \pm 12.3)\%$ , and that of UPM is  $0.488 \pm 0.123$ . Note that both DMM and UPM are end-members and do not have to represent two separate physical entities; they can be present as a fraction in every mantle piece, with the overall mass fractions of UPM to DMM being 48.8:51.2. These fractions specifically apply to  $^{40}\text{Ar}$ . It is possible that they also apply to other isotopes and gas species, but that is not necessary unless the DMM is one uniform physically defined reservoir (meaning a specific physical region of the mantle is the DMM, Figure 1(b)). If the mantle is degassed to various degrees and DMM is just an end-member

**Table 7** Mass of mantle reservoirs from K-Ar systematics

Reservoir	BSE	UPM	DMM+AOC
Mass (kg)	$4.035 \times 10^{24}$	$\sim 1.96 \times 10^{24}$	$\sim 2.08 \times 10^{24}$

See text.

for the variously degassed mantle pieces, then DMM for other gases most likely would be more than  $(51.2 \pm 12.3)\%$  of the whole mantle because  $^{40}\text{Ar}$  was not initially present and is gradually produced over geologic time. Interestingly, the estimated mass fraction of the depleted mantle is also about 50% (see Chapter 3.3), similar to that of the degassed mantle, and supporting the notion that the DMM is a physical reservoir (Table 7).

The  $^{40}\text{Ar}/^{36}\text{Ar}$  ratio in AOC+DMM can be estimated from total  $^{40}\text{Ar}$  production in DMM ( $1.97 \times 10^{18}$  mol) and  $^{36}\text{Ar}$  in air ( $5.51 \times 10^{15}$  mol) to be 357. Even if the whole BSE is assumed to supply  $^{36}\text{Ar}$  in air (but assuming neither initial nor nonmantle  $^{36}\text{Ar}$ ), the maximum  $^{40}\text{Ar}/^{36}\text{Ar}$  ratio in the present-day BSE would be only  $693 \pm 149$  (or  $\leq 842$ ). The estimate of the limit is robust, and its accuracy only depends on the estimate of K concentration in the BSE (because the amount of  $^{36}\text{Ar}$  in air is well known). Next,  $^{40}\text{Ar}/^{36}\text{Ar}$  ratios in DMM and UPM are estimated, and the ratio in UPM is compared to that in AOC+DMM. If  $(^{40}\text{Ar}/^{36}\text{Ar})_{\text{AOC+DMM}} = (^{40}\text{Ar}/^{36}\text{Ar})_{\text{UPM}}$  within error, Ar degassing can be treated in the framework of closed-system degassing. Otherwise, extra sources are necessary.

Measured  $^{40}\text{Ar}/^{36}\text{Ar}$  ratios in mantle-derived rocks are highly variable (Figure 9). Much of the variation is attributed to variable degrees of atmospheric contamination. In MORB, the  $^{40}\text{Ar}/^{36}\text{Ar}$  ratio ranges from 300 to 64 000, and in OIB, the ratio ranges from 300 to 12 000. Although  $^{20}\text{Ne}/^{22}\text{Ne}$  ratios in mantle samples are similar to the solar ratio,  $^{38}\text{Ar}/^{36}\text{Ar}$  ratios in MORB and OIB are similar to the air ratio (0.1880), not the solar ratio (Raquin and Moreira, 2009). Hence,  $^{38}\text{Ar}/^{36}\text{Ar}$  ratios in mantle-derived rocks cannot be used to assess contamination by air Ar in a way similar to Ne isotopes.

In order to remove atmospheric contamination from true mantle ratios, Figure 9 plots  $^{40}\text{Ar}/^{36}\text{Ar}$  versus  $^{20}\text{Ne}/^{22}\text{Ne}$  in MORB and OIB, where the  $^{20}\text{Ne}/^{22}\text{Ne}$  ratio is used as a measure of air contamination. The diagram shows that one end-member is indeed air with  $^{20}\text{Ne}/^{22}\text{Ne} = 9.80$  and  $^{40}\text{Ar}/^{36}\text{Ar} = 298.6$ . For MORB, mixing with air seems to generate a roughly linear trend, with  $^{40}\text{Ar}/^{36}\text{Ar}$  ratio being  $35\,000 \pm 7\,000$  at  $^{20}\text{Ne}/^{22}\text{Ne} = 13.0$  and  $44\,000$  at  $^{20}\text{Ne}/^{22}\text{Ne} = 13.8$  (see also Moreira et al., 1998). For OIB samples, the mixing trend is curved and the mantle end-members are not well defined. The best-defined OIB trend is for Galapagos hot spot (Figure 9(b); see also recent work on Iceland by Mukhopadhyay, 2012), which approaches the lowest  $^{40}\text{Ar}/^{36}\text{Ar}$  for a given  $^{20}\text{Ne}/^{22}\text{Ne}$  (Hawaiian data are scattered, but some Hawaiian basalts show even lower  $^{40}\text{Ar}/^{36}\text{Ar}$  at  $^{20}\text{Ne}/^{22}\text{Ne} = 13.0$ ). Even for this well-defined trend, it is still impossible to estimate  $(^{40}\text{Ar}/^{36}\text{Ar})_{13.8}$  reliably by extrapolation, except that  $(^{40}\text{Ar}/^{36}\text{Ar})_{13.8}$  is almost certainly  $> 5000$ , and it could be as high as 40 000. Adopting mantle  $^{20}\text{Ne}/^{22}\text{Ne} = 13.0$ ,  $^{40}\text{Ar}/^{36}\text{Ar}$  in Galapagos mantle is  $\sim 4000$ . Marty et al. (1998b) inferred from Devonian Kola carbonatites that  $^{40}\text{Ar}/^{36}\text{Ar}$  in plume mantle is  $5000 \pm 1000$ . There are few points with  $^{40}\text{Ar}/^{36}\text{Ar}$  ratio  $\leq 842$ . The lowest  $^{40}\text{Ar}/^{36}\text{Ar}$  in all OIB rocks at

$^{20}\text{Ne}/^{22}\text{Ne} = 13.0$  is about 1700 (Figure 9(a)). This ratio is much higher than the  $^{40}\text{Ar}/^{36}\text{Ar}$  ratio in BSE ( $\sim 357$ ).

The large discrepancy between  $^{40}\text{Ar}/^{36}\text{Ar}$  ratio in AOC + DMM based on the closed-system mass balance calculations (i.e., assuming all  $^{36}\text{Ar}$  in air is from degassing of DMM) and measured  $^{40}\text{Ar}/^{36}\text{Ar}$  in OIB at high  $^{20}\text{Ne}/^{22}\text{Ne}$  is here referred to as an ‘argon paradox.’ One solution to the argon paradox is to assume that the few OIB points with very low  $^{40}\text{Ar}/^{36}\text{Ar}$  ratio at high  $^{20}\text{Ne}/^{22}\text{Ne}$  (these few are mostly Hawaiian samples, e.g., there is one point with  $^{20}\text{Ne}/^{22}\text{Ne} = 12.1$  and  $^{40}\text{Ar}/^{36}\text{Ar} = 425$ ; Valbracht et al., 1997) are representative of UPM. To verify this, careful He–Ne–Ar studies must be carried out so that  $^{20}\text{Ne}/^{22}\text{Ne}$  can be used to indicate contamination, and uncontaminated  $^{40}\text{Ar}/^{36}\text{Ar}$  can be plotted against  $^{4}\text{He}/^{3}\text{He}$  (in a figure similar to Figure 6) to find the  $^{40}\text{Ar}/^{36}\text{Ar}$  ratio of UPM at  $^{4}\text{He}/^{3}\text{He} = 20\,000$ . Another solution is to assume that  $^{36}\text{Ar}$  in air is not entirely from mantle degassing, meaning that the closed-system assumption does not work for  $^{36}\text{Ar}$  and that UPM does not have the same composition of AOC + DMM in terms of  $^{36}\text{Ar}$  and  $^{38}\text{Ar}$ . Although this possibility has not been raised before, it is not so unthinkable because Ne isotope systematics can be explained by nonmantle Ne. Adopting  $^{40}\text{Ar}/^{36}\text{Ar} = 4000$  to represent UPM, no more than about

$357/4000 \approx 9\%$  of air  $^{36}\text{Ar}$  is from mantle degassing, and 91% is extraterrestrial or was initially in air. The third solution to the argon paradox is to assume that none of the OIB sources is close to UPM, not a preferred solution.

Mantle  $^{40}\text{Ar}$  degassing rate can be estimated to be  $(3.3 \pm 1.0) \times 10^7 \text{ mol year}^{-1}$  from the  $^{40}\text{Ar}/^{4}\text{He}$  molar ratio in DMM ( $0.70 \pm 0.15$ ; Graham, 2002; Raquin et al., 2008), and  $^{4}\text{He}$  degassing rate of  $(4.7 \pm 1.1) \times 10^7 \text{ mol year}^{-1}$  (see Section 6.2.3.2). At this rate, it would take  $5 \times 10^{10}$  years to supply all  $^{40}\text{Ar}$  in air, which is only a factor of 2 different from the time to supply the hypothetical  $^{4}\text{He}$  in air at the current  $^{4}\text{He}$  degassing rate, demonstrating self-consistency. Because all  $^{40}\text{Ar}$  in air must be supplied by mantle degassing, the mean degassing rate for  $^{40}\text{Ar}$  over Earth’s history is about 11 times higher than today’s degassing rate.

Global  $^{36}\text{Ar}$  degassing rate is about  $943 \text{ mol year}^{-1}$  using the  $^{40}\text{Ar}/^{36}\text{Ar}$  ratio of 35 000. At this rate, it would take  $(5.8 \pm 1.0) \times 10^{12}$  years to supply all  $^{36}\text{Ar}$  in air. That is, the required mean degassing rate to generate air  $^{36}\text{Ar}$  is 1300 times higher than the present degassing rate, a situation similar to Ne (Table 4), again supporting the notion that there is significant nonmantle  $^{36}\text{Ar}$ .

Ar isotope ratios and concentrations in Earth reservoirs are summarized in Table 8. The  $^{40}\text{Ar}/^{36}\text{Ar}$  ratio and  $^{36}\text{Ar}$

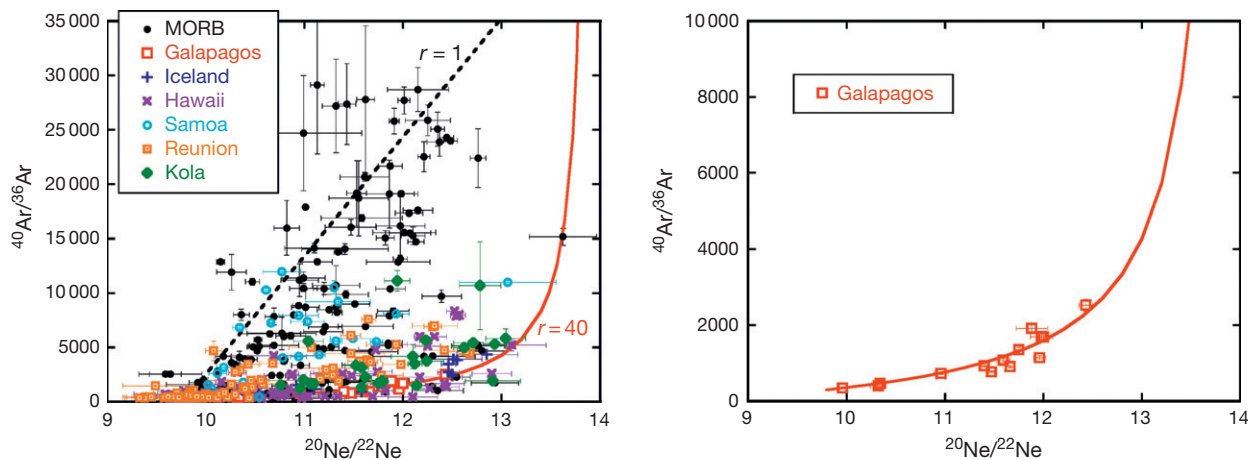


**Figure 9**  $^{40}\text{Ar}/^{36}\text{Ar}$  versus  $^{20}\text{Ne}/^{22}\text{Ne}$  for basalts from different locations. For each location, the trend is attributed to air contamination of mantle samples. Data for Galapagos are shown individually. The correlation may be used to estimate air contamination of Ar isotopes. For example, if mantle  $^{20}\text{Ne}/^{22}\text{Ne}$  ratio is about 13.0,  $^{40}\text{Ar}/^{36}\text{Ar}$  values for OIB are clearly lower than the ratio in normal MORB, and the lowest value is about 2500. Data sources: Staudacher et al. (1990), Hiyagon et al. (1992), Poreda and Farley (1992), Honda et al. (1993), Moreira et al. (1995, 1998), Moreira and Allegre (2002), Valbracht et al. (1997), Niedermann and Bach (1998), Sarda et al. (2000), Trieloff et al. (2000, 2002), Hanyu et al. (2001, 2007), and Raquin et al. (2008).

**Table 8** Ar budget and isotope ratio in air, BSE, and mantle reservoirs

	Air	DMM	AOC + DMM	UPM	BSE
$^{40}\text{Ar}$ ( $10^{18}$ mol)	1.644	$\sim 0.13$	$\sim 1.97$	$\sim 1.87$	$3.84 \pm 0.82$
$^{40}\text{Ar}$ ( $\text{mol kg}^{-1}$ )		$(6.5 \pm 2.5) \times 10^{-8}$	$(9.5 \pm 2.0) \times 10^{-7}$	$(9.5 \pm 2.0) \times 10^{-7}$	$(9.5 \pm 2.0) \times 10^{-7}$
$^{40}\text{Ar}/^{36}\text{Ar}$	298.6	$35\,000 \pm 5\,000$	$\sim 357 (< 842)$	$\sim 4000?$	
$^{36}\text{Ar}$ ( $\text{mol kg}^{-1}$ )		$\sim 1.8 \times 10^{-12}$	$> 1.4 \times 10^{-9}$	$\sim 2.4 \times 10^{-10}?$	
$^{36}\text{Ar}$ ( $10^{15}$ mol)	5.51	$\sim 0.0037$	$> 5.51$	0.47?	
References	Ozima and Podosek (2002), Lee et al. (2006)	Moreira et al. (1998), Trieloff et al. (2000), and this work	Allegre et al. (1983), Zhang and Zindler (1989), and this work	This work	

The mass of UPM is assumed to be 49% of BSE (see text).  $^{40}\text{Ar}$  degassing flux is  $(3.3 \pm 1.0) \times 10^7 \text{ mol year}^{-1}$ .

concentration in UPM are highly uncertain. Based on estimated  $^{36}\text{Ar}$  concentration in UPM (from  $^{40}\text{Ar}$  concentration in UPM and estimated  $^{40}\text{Ar}/^{36}\text{Ar}$  ratio in UPM) and that in DMM, the degree of degassing for  $^{36}\text{Ar}$  from DMM is  $\sim 99.5\%$ , similar to that obtained by Zhang and Zindler (1989).

### 6.2.3.5 Kr

There are six stable isotopes of Kr of which three receive very minor ( $\leq 0.014\%$ ) fission contribution by  $^{244}\text{Pu}$  and  $^{238}\text{U}$ , which currently cannot be resolved. That is, all six stable isotopes of Kr can be treated as primordial (nonradiogenic). The Kr isotope system has not received much attention in literature. Recently, Holland et al. (2009) presented high-precision measurements of Kr isotope ratios in well gases and found that there is interesting variation. On a  $^{86}\text{Kr}/^{82}\text{Kr}$  versus  $^{84}\text{Kr}/^{82}\text{Kr}$  plot, the Kr isotopes lie along a mixing trend between air Kr and chondritic Kr (AVCC), away from solar Kr. Whether well gas Kr is representative of mantle Kr is not known. The difference between air and chondritic Kr isotopes is small, with AVCC Kr more fractionated than air Kr compared to solar Kr; that is, AVCC Kr is more enriched in the heavier isotopes than air Kr by about 0.3% per atomic mass unit. The small difference means that (1) only when the measurement precision is extremely high, it is possible to resolve the difference, and (2) even if mantle Kr is AVCC Kr, degassing would not have noticeably affected Kr isotope ratios in air.

### 6.2.3.6 Xe

The I–Pu–U–Xe system provides the best constraint on the xenon closure age of Earth, the timing of degassing, the intensity of early degassing, and the early loss of gases from Earth. There are nine stable isotopes of xenon ( $^{124}\text{Xe}$ ,  $^{126}\text{Xe}$ ,  $^{128}\text{Xe}$ ,  $^{129}\text{Xe}$ ,  $^{130}\text{Xe}$ ,  $^{131}\text{Xe}$ ,  $^{132}\text{Xe}$ ,  $^{134}\text{Xe}$ , and  $^{136}\text{Xe}$ ) of which  $^{129}\text{Xe}$  received radiogenic contribution from extinct nuclide  $^{129}\text{I}$  (half-life is 15.7 My) and  $^{136}\text{Xe}$ ,  $^{134}\text{Xe}$ ,  $^{132}\text{Xe}$ , and  $^{131}\text{Xe}$  received not only fissionogenic contribution from extinct nuclide  $^{244}\text{Pu}$  (half-life is 80 My) but also minor contribution from extant nuclide  $^{238}\text{U}$  (half-life is 4468 My) (Fields et al., 1969; Ozima and Podosek, 2002; Wetherill, 1953; Zhang, 2002; see also Chapter 6.16).

The Xe isotope system is complicated in a number of ways. The sheer number of isotopes involved is one of them. Also, two extinct nuclides ( $^{129}\text{I}$  and  $^{244}\text{Pu}$ ) and one extant nuclide

( $^{238}\text{U}$ ) have contributed to the radiogenic isotopes of xenon. The decay of  $^{129}\text{I}$  to  $^{129}\text{Xe}$  is simple, but fission from  $^{244}\text{Pu}$  and  $^{238}\text{U}$  to  $^{136}\text{Xe}$ – $^{134}\text{Xe}$ – $^{132}\text{Xe}$ – $^{131}\text{Xe}$  is less so. The complexity means much information is contained in the Xe isotopes, and various authors have tried to mine such information.

Unlike the case for radiogenic  $^{40}\text{Ar}$  for which the primordial component is negligible, for all xenon isotopes, the primordial components are major and must be accurately known for the inference of the radiogenic contribution. However, the primordial nonradiogenic isotope ratios of xenon in air are different from those in other reservoirs (such as solar). Sophisticated mass fractionation models have been developed to derive the nonradiogenic xenon isotope composition from solar xenon (or U–Xe; Pepin and Phinney, 1978) with which the radiogenic components are inferred. Table 9 lists relevant Xe data.

Xe isotopes in air, coupled with a robust constraint of the overall degree of mantle degassing using  $^{40}\text{Ar}$ , can constrain the Xe closure age of Earth (Allegre et al., 1995a; Staudacher and Allegre, 1982; Wetherill, 1975; Zhang, 1998, 2002). The concept of Xe closure age for the whole Earth is similar to that of Ar closure of a mineral in isotopic dating. The basic argument is as follows. Estimated iodine (only one stable isotope  $^{127}\text{I}$ ) concentration in BSE ranges from 7 ppb (O'Neill and Palme, 1998; also see Chapter 3.1) to 10 ppb (Deruelle et al., 1992; McDonough and Sun, 1995). Therefore, total  $^{127}\text{I}$  in BSE ranges from  $2.26 \times 10^{17}$  to  $3.23 \times 10^{17}$  mol. The half-life of  $^{129}\text{I}$  is 15.7 My, and all initial  $^{129}\text{I}$  has decayed to  $^{129}\text{Xe}$ . The initial  $^{129}\text{I}/^{127}\text{I}$  ratio in meteorite Bjurböle at 4.56 Ga (Hudson et al., 1989) is  $(1.10 \pm 0.03) \times 10^{-4}$  (Swindle and Podosek, 1988). If BSE was closed at 4.56 Ga, the amount of initial  $^{129}\text{I}$ , that is, the amount of radiogenic  $^{129}\text{Xe}$ , would be  $2.5 \times 10^{13}$  to  $3.6 \times 10^{13}$  mol in BSE, about 100 times more than the amount in air ( $2.8 \times 10^{11}$  mol, Table 9), much larger than the expected factor of 2 between total production and the amount in air. This difference can be reconciled if BSE is allowed to close at a time later than 4.56 Ga because  $^{129}\text{I}$  has a very short half-life. Furthermore, starting from 4.56 Ga, total fissionogenic  $^{136}\text{Xe}$ ,  $^{134}\text{Xe}$ ,  $^{132}\text{Xe}$ , and  $^{131}\text{Xe}$  in BSE would be  $\sim 3.7 \times 10^{11}$ ,  $3.4 \times 10^{11}$ ,  $3.2 \times 10^{11}$ , and  $0.9 \times 10^{11}$  mol from  $^{238}\text{U}$  concentration in BSE and  $(^{244}\text{Pu}/^{238}\text{U})_{4.56\text{ Ga}} = 0.0068$  (Hudson et al., 1989), only about  $5.7 \pm 0.2$  times the amount of fissionogenic  $^{136}\text{Xe}$  in air (Table 9). The inconsistency between the factors of 5.7 and  $\sim 100$  can also be reconciled if BSE is allowed to close at a time later than 4.56 Ga because the short

**Table 9** Xenon isotope ratios and budget in air

Xe isotope	Xe isotopic ratio in air, relative to $^{130}\text{Xe}$	Primordial Xe isotope ratio in air, relative to $^{130}\text{Xe}$	Amount of Xe isotope in air ( $10^{10}$ mol)	Amount of radiogenic Xe in air ( $10^{10}$ mol)
$^{124}\text{Xe}$	$0.02337 \pm 0.00008$	$0.02337 \pm 0.00008$	1.462	$\equiv 0$
$^{126}\text{Xe}$	$0.02180 \pm 0.00011$	$0.02180 \pm 0.00011$	1.364	$\equiv 0$
$^{128}\text{Xe}$	$0.4715 \pm 0.0007$	$0.4715 \pm 0.0007$	29.51	$\equiv 0$
$^{129}\text{Xe}$	$6.4958 \pm 0.0058$	$6.053 \pm 0.029$	406.5	$27.7 \pm 1.8$
$^{130}\text{Xe}$	$\equiv 1$	$\equiv 1$	62.58	$\equiv 0$
$^{131}\text{Xe}$	$5.2127 \pm 0.0059$	$5.187 \pm 0.071$	326.2	$1.59 \pm 0.44$
$^{132}\text{Xe}$	$6.6068 \pm 0.0053$	$6.518 \pm 0.013$	413.5	$5.56 \pm 0.83$
$^{134}\text{Xe}$	$2.5628 \pm 0.0037$	$2.47 \pm 0.013$	160.4	$5.81 \pm 0.81$
$^{136}\text{Xe}$	$2.1763 \pm 0.0022$	$2.075 \pm 0.013$	136.2	$6.32 \pm 0.82$

half-life of  $^{129}\text{I}$  (15.7 My) leads to rapid decrease of the amount of  $^{129}\text{I}$  in BSE. The closure age of Xe is when the initial amounts of  $^{129}\text{I}$ ,  $^{244}\text{Pu}$ , and  $^{238}\text{U}$  in the primordial DMM are about the right amounts to produce radiogenic Xe isotopes in air. When all of these constraints are combined in a total inversion regression to obtain a self-consistent closure age of Xe, Zhang (1998) obtained a 4.45 Ga using an iodine concentration from McDonough and Sun (1995). If the lower iodine concentration of Palme and O'Neill (see Chapter 3.1) is used, the Xe closure age becomes  $\sim 4.46$  Ga.

To obtain Xe isotope ratios in mantle reservoirs, it is necessary to remove contamination by air Xe. The contamination by air does not have to be recent and could happen through ancient recycled crustal material into the mantle (i.e., Xe recycling from the surface to the mantle is treated as contamination). Theoretically, the many nonradiogenic isotopic ratios ( $^{124}\text{Xe}/^{130}\text{Xe}$ ,  $^{126}\text{Xe}/^{130}\text{Xe}$ , and  $^{128}\text{Xe}/^{130}\text{Xe}$ ) can be used to accurately correct for atmospheric contamination if small differences in mantle samples and in air can be measured precisely. However, in terms of these nonradiogenic isotope ratios, Xe in mantle-derived basalts is indistinguishable from air Xe within measurement precision.

On the other hand, high-precision measurements of nonradiogenic Xe isotopes in well gases (Caffee et al., 1999; Holland et al., 2009; Phinney et al., 1978) revealed slightly

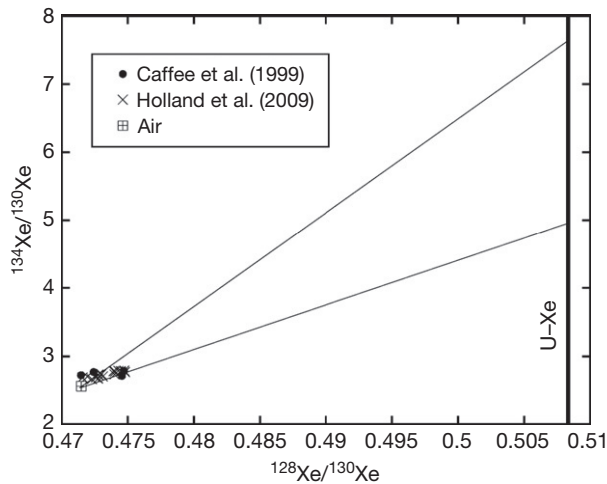


**Figure 10**  $^{134}\text{Xe}/^{130}\text{Xe}$  versus  $^{128}\text{Xe}/^{130}\text{Xe}$  in well gases. Data are from Caffee et al. (1999) and Holland et al. (2009).  $^{128}\text{Xe}/^{130}\text{Xe}$  ratio of U-Xe is from Pepin and Phinney (1978).

higher  $^{124}\text{Xe}/^{130}\text{Xe}$ ,  $^{126}\text{Xe}/^{130}\text{Xe}$ , and  $^{128}\text{Xe}/^{130}\text{Xe}$  isotope ratios than those in air. The trends defined by the data are not too different from a mixing trend between air and either one of the following Xe components: solar Xe, AVCC Xe, Q-Xe, or U-Xe (Holland et al., 2009). If well gas xenon is treated as a mixture between air xenon and DMM xenon using  $^{129}\text{Xe}/^{130}\text{Xe}$  or  $^{134}\text{Xe}/^{130}\text{Xe}$  versus nonradiogenic xenon isotope ratios such as  $^{128}\text{Xe}/^{130}\text{Xe}$  (Figure 10) and if nonradiogenic xenon in DMM is assumed to be U-Xe (Tolstikhin and O’Nions, 1994; Dauphas, 2003), then  $^{129}\text{Xe}/^{130}\text{Xe}$  ratio in DMM would be between 14 and 17 and the  $^{134}\text{Xe}/^{130}\text{Xe}$  ratio would be between 5.0 and 7.5, which are much higher than currently adopted  $^{129}\text{Xe}/^{130}\text{Xe}$  and  $^{134}\text{Xe}/^{130}\text{Xe}$  ratios in DMM (e.g., Trieloff and Kunz, 2005; see Table 10). In the future, if nonradiogenic Xe isotopes in mantle-derived rocks (MORB and OIB) can be resolved from air Xe, it would provide a way to correct for air contamination and reveal real Xe isotope ratios in the mantle (similar to Ne isotopes) and would significantly change the understanding of Xe isotopic behavior in the mantle.

Because there is no resolvable difference between air and mantle-derived basalts in terms of nonradiogenic Xe isotopes, the discussion in the succeeding texts assumes that nonradiogenic Xe isotopes in DMM and UPM are the same as that in air, and  $^{129}\text{Xe}/^{130}\text{Xe}$ ,  $^{131}\text{Xe}/^{130}\text{Xe}$ ,  $^{132}\text{Xe}/^{130}\text{Xe}$ ,  $^{134}\text{Xe}/^{130}\text{Xe}$ , and  $^{136}\text{Xe}/^{130}\text{Xe}$  ratios in DMM and UPM are obtained using  $^{20}\text{Ne}/^{22}\text{Ne}$  to correct for air contamination.

MORB and OIB show clear excess in  $^{129}\text{Xe}$  (from decay of  $^{129}\text{I}$ ) and  $^{131}\text{Xe}$ - $^{132}\text{Xe}$ - $^{134}\text{Xe}$ - $^{136}\text{Xe}$  (from fission of  $^{244}\text{Pu}$  and  $^{238}\text{U}$ ). Because  $^{136}\text{Xe}$  receives more fissiogenic contribution than  $^{134}\text{Xe}$ ,  $^{132}\text{Xe}$ , and  $^{131}\text{Xe}$  (Ozima, and Podosek, 2002; Wetherill, 1953), when discussing Xe isotope trends,  $^{129}\text{Xe}/^{130}\text{Xe}$  and  $^{136}\text{Xe}/^{130}\text{Xe}$  are often used (but Holland et al. (2009) reported  $^{134}\text{Xe}/^{130}\text{Xe}$  rather than  $^{136}\text{Xe}/^{130}\text{Xe}$  ratios; see Figure 10). Selected Xe isotopic data are shown in Figure 11: in a plot of  $^{129}\text{Xe}/^{130}\text{Xe}$  versus  $^{136}\text{Xe}/^{130}\text{Xe}$ , all MORB and OIB samples fall into a single linear trend passing through air Xe, interpreted to be due to mixing between air (with lower  $^{129}\text{Xe}/^{130}\text{Xe}$  and  $^{136}\text{Xe}/^{130}\text{Xe}$  ratios) and mantle end-members. To constrain which high ratio (the highest measured ratio or some extrapolated higher ratio) is representative of each mantle reservoir, one rough approach is to use  $^{20}\text{Ne}/^{22}\text{Ne}$  to correct for air contamination (Figure 12).

For MORB mantle, Moreira et al. (1998) obtained that if corrected to  $^{20}\text{Ne}/^{22}\text{Ne} = 13.0$ , then  $^{129}\text{Xe}/^{130}\text{Xe}$  ratio in DMM is 7.8 and if corrected to  $^{20}\text{Ne}/^{22}\text{Ne} = 13.8$ , then  $^{129}\text{Xe}/^{130}\text{Xe}$  ratio in DMM is 8.2. Similarly, other Xe isotopes with

**Table 10** Xenon isotope ratios in the mantle

Xe isotope	Xe isotopic ratios at $^{20}\text{Ne}/^{22}\text{Ne} = 13.0$		$^{20}\text{Ne}/^{22}\text{Ne} = 13.8$	Radiogenic production in BSE ( $10^{10}$ mol)	Xe isotope ratios in BSE (closed system)
	DMM	Hawaii–Iceland			
$^{129}\text{Xe}$	~7.8	~6.9	~8.2	63.5	~6.57 ( $\leq 7.07$ )
$^{130}\text{Xe}$	$\equiv 1$	$\equiv 1$	$\equiv 1$	0	$\equiv 1$
$^{131}\text{Xe}$	~5.32	~5.25	~5.35	3.76	~5.22 ( $\leq 5.25$ )
$^{132}\text{Xe}$	~6.91	~6.70	~7.01	13.9	~6.63 ( $\leq 6.74$ )
$^{134}\text{Xe}$	~2.90	~2.67	~3.01	15.0	~2.59 ( $\leq 2.71$ )
$^{136}\text{Xe}$	~2.60	~2.31	~2.72	16.2	~2.21 ( $\leq 2.33$ )

After Pepin (1991), Moreira et al. (1998), Ozima and Podosek (2002), Trieloff and Kunz (2005), and this work.

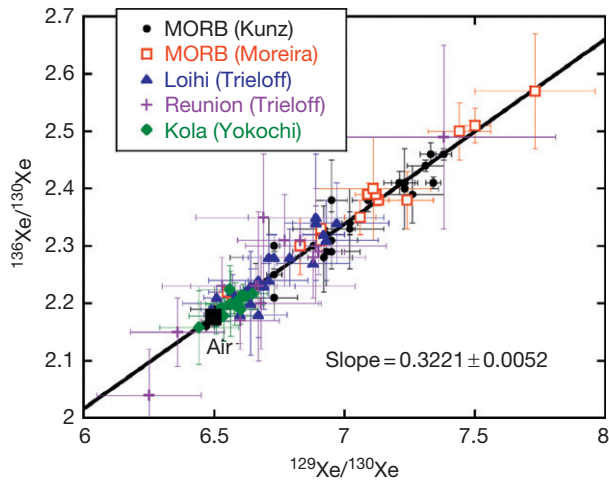


**Figure 11** Selected Xe isotope data in MORB and OIB samples. Data sources: Kunz et al. (1998), Moreira et al. (1998), Trieloff et al. (2000, 2002), and Yokochi and Marty (2005). The large black square is the composition of air. For clarity, other data (often with larger error bars) are not shown.

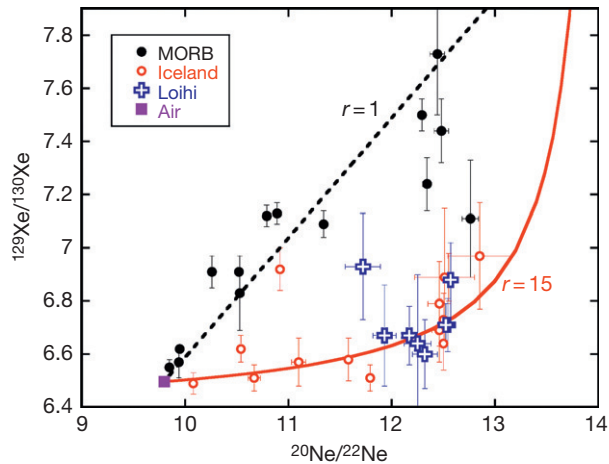


**Figure 12** Selected data for  $^{129}\text{Xe}/^{130}\text{Xe}$  versus  $^{20}\text{Ne}/^{22}\text{Ne}$  to assess air contamination to Xe isotope ratios. Data sources: MORB (Moreira et al., 1998); Iceland and Loihi (Trieloff et al., 2000).

radiogenic contribution can be estimated. For OIB samples, the  $^{129}\text{Xe}/^{130}\text{Xe}$  versus  $^{20}\text{Ne}/^{22}\text{Ne}$  relation is curved (Figure 12).  $^{129}\text{Xe}/^{130}\text{Xe}$  ratio at  $^{20}\text{Ne}/^{22}\text{Ne} = 13.0$  can be estimated (Table 10), but obtaining the ratio at  $^{20}\text{Ne}/^{22}\text{Ne} = 13.8$  requires too much extrapolation.

From Figures 11 and 12,  $^{129}\text{Xe}/^{130}\text{Xe}$  and  $^{136}\text{Xe}/^{130}\text{Xe}$  ratios in OIB mantle are lower than those in MORB mantle, which is consistent with many mantle degassing models (e.g., Zhang and Zindler, 1989), but not with the steady-state degassing model (see later discussion). The difference in  $^{129}\text{Xe}/^{130}\text{Xe}$  ratio between air and DMM (MORB mantle) demonstrates that mantle degassing was very early before  $^{129}\text{I}$  has decayed away (e.g., before 4.3 Ga); otherwise,  $^{129}\text{Xe}/^{130}\text{Xe}$  in air would be the same as that in the mantle. The difference in  $^{129}\text{Xe}/^{130}\text{Xe}$  ratio between MORB and OIB means that the mantle reservoirs have been separated for a very long time and have not been homogenized in the last 4.3 Ga.

Some authors (Caffee et al., 1999; Kunz et al., 1998; Yokochi and Marty, 2005) estimated the contribution to fission  $^{136}\text{Xe}$  from  $^{244}\text{Pu}$  and  $^{238}\text{U}$  by decomposing measured Xe isotopes into air,  $^{244}\text{Pu}$  fission, and  $^{238}\text{U}$  fission Xe, with or without solar Xe end-members, and obtained that  $^{244}\text{Pu}$  contributed to <20% of the total fission  $^{136}\text{Xe}$  (the rest due to  $^{238}\text{U}$  fission) in well gas Xe and 30–50% of fission  $^{136}\text{Xe}$  in MORB Xe. Because (1) air Xe itself also contains fission  $^{136}\text{Xe}$  (assuming primordial Xe is U-Xe), (2) at least some air Xe is from degassing, and (3) mantle xenon might have a solar component (Figure 10), the true  $^{244}\text{Pu}$  contribution to total fission  $^{136}\text{Xe}$  in Earth cannot be obtained using this approach. Theoretically, for a chondritic Earth closed since 4.55 Ga,  $^{244}\text{Pu}$  fission  $^{136}\text{Xe}$  would make 96.2% of the total fission  $^{136}\text{Xe}$ . If closure occurred later, the contribution by  $^{244}\text{Pu}$  would decrease. Hence, the accurate determination of this fraction is very important in constraining Earth degassing.

Because the closure age of BSE in terms of Xe loss can be constrained,  $^{129}\text{Xe}/^{130}\text{Xe}$  and  $^{136}\text{Xe}/^{130}\text{Xe}$  ratios in BSE can be constrained in a similar way as  $^{40}\text{Ar}/^{36}\text{Ar}$ . Using 4.46 Ga as the Xe closure age of BSE, total radiogenic  $^{129}\text{Xe}$ ,  $^{131}\text{Xe}$ ,  $^{132}\text{Xe}$ ,  $^{134}\text{Xe}$ , and  $^{136}\text{Xe}$  can be estimated. Using the amount of  $^{130}\text{Xe}$  in air (ignoring  $^{130}\text{Xe}$  in DMM and UPM) and the nonradioactive primordial Xe isotope ratios, the upper limit of isotope ratios in BSE can be obtained. Assuming mass of UPM is 49% of BSE, the likely isotope ratios in BSE can be estimated. They are listed in the last column of Table 10. The upper limits (by distributing air  $^{130}\text{Xe}$  to the whole mantle) are not too far off the high ends of measured isotopic values in OIB sources (Table 10; Figures 11 and 12), but the preferred ratios (by distributing air  $^{130}\text{Xe}$  to DMM) are too low. Hence, there is also an issue whether OIB represents UPM or whether the closed-system assumption is valid.

The concentration of  $^{130}\text{Xe}$  in DMM may be very roughly estimated using  $^{130}\text{Xe}/^{3}\text{He}$  molar ratio (0.0014) in popping rocks (Sarda and Graham, 1990) to be  $\sim 1.4 \times 10^{-15} \text{ mol kg}^{-1}$ , or 0.00019 ppt. The concentration of  $^{130}\text{Xe}$  in UPM may be very roughly estimated using  $^{130}\text{Xe}/^{3}\text{He}$  molar ratio (0.012) in Loihi samples (Sarda and Graham, 1990) to be  $\sim 1.4 \times 10^{-12} \text{ mol kg}^{-1}$ , 0.188 ppt. Hence, DMM is  $(1 - 0.00019/0.188) = 99.90\%$  degassed in terms of  $^{130}\text{Xe}$ , similar to 99.92% by Zhang and Zindler (1989). Based on this estimate,  $^{130}\text{Xe}$  is more degassed than  $^{22}\text{Ne}$ , which is more degassed than  $^{3}\text{He}$ .

Using the closed-system assumption, the concentration of  $^{130}\text{Xe}$  in BSE, estimated by dividing the amount of air  $^{130}\text{Xe}$  by the mass of DMM, would be  $3.0 \times 10^{-13} \text{ mol kg}^{-1}$ , or 0.039 ppt, smaller than 0.188 ppt. The fact that  $^{130}\text{Xe}$  in air divided by mass of DMM is smaller than the estimated  $^{130}\text{Xe}$  in UPM is consistent with loss of  $^{130}\text{Xe}$  from air (which is also needed to fractionate Xe isotopes in air). Because the  $^{130}\text{Xe}/^{3}\text{He}$  ratios are based on limited samples, the reliability of these estimates is not high. Note that for  $^{36}\text{Ar}$ , the estimated concentration in BSE using the closed-system assumption is much higher than that in UPM, opposite to the case of  $^{130}\text{Xe}$ .

### 6.2.3.7 N<sub>2</sub>

The total amount of N<sub>2</sub> in AOC is  $(1.80 \pm 0.14) \times 10^{20} \text{ mol}$  (Zhang and Zindler, 1993). The N<sub>2</sub> concentration in the present-day DMM can be estimated from the N<sub>2</sub>/<sup>40</sup>Ar molar

ratio of  $124 \pm 40$  in DMM (Marty and Dauphas, 2003), and the  $^{40}\text{Ar}$  concentration of  $(6.5 \pm 2.5) \times 10^{-8} \text{ mol kg}^{-1}$  in DMM to be  $(8.1 \pm 4.0) \times 10^{-6} \text{ mol kg}^{-1}$ , or  $0.23 \pm 0.12 \text{ ppm}$ . Assuming all surface N<sub>2</sub> originated from DMM, distributing surface N<sub>2</sub> to DMM plus N<sub>2</sub> still in the present-day DMM leads to  $(2.66 \pm 0.22) \text{ ppm N}_2$  in AOC+DMM or initial DMM.

The degassing flux of N<sub>2</sub> can be estimated from the N<sub>2</sub>/ $^{40}\text{Ar}$  molar ratio of  $124 \pm 40$  in DMM (Marty and Dauphas, 2003), and the  $^{40}\text{Ar}$  degassing flux of  $(3.3 \pm 1.0) \times 10^7 \text{ mol year}^{-1}$  (see Section 6.2.3.4) to be  $(4.1 \pm 1.8) \times 10^9 \text{ mol year}^{-1}$ . Hence, at the current degassing rate, surface N<sub>2</sub> would be supplied in  $(4.4 \pm 2.0) \times 10^{10} \text{ years}$ , or the required mean degassing rate is ten times the present degassing rate.

N<sub>2</sub> concentration in UPM can be estimated to be  $2.1 \pm 0.7 \text{ ppm}$  from the N<sub>2</sub>/ $^{40}\text{Ar}$  molar ratio of  $80 \pm 20$  in BSE (Marty and Dauphas, 2003; this ratio is very close to the air ratio of 83.6), and  $^{40}\text{Ar}$  concentration of  $38.1 \pm 8.2 \text{ ppb}$ , which is consistent with estimation of initial N<sub>2</sub> concentration in DMM ( $2.66 \pm 0.22 \text{ ppm}$ ). All N<sub>2</sub> in air seems to be degassed from the mantle, and no extra source (such as impact degassing or cometary injection) is needed, meaning that the closed-system assumption works well for N<sub>2</sub>. Using a weighted mean concentration of  $2.61 \pm 0.21 \text{ ppm}$  for N<sub>2</sub> in BSE, the total amount of N<sub>2</sub> in BSE can be estimated to be  $(3.76 \pm 0.30) \times 10^{20} \text{ mol}$  of which 48% is in air. The concentrations are summarized in Table 11.

From the concentration of N<sub>2</sub> in DMM and UPM, the degree of degassing for N<sub>2</sub> in DMM is  $(1 - 0.23/2.61) \approx 91.2 \pm 4.6\%$ , with  $(8.8 \pm 4.6)\%$  still remaining in DMM. The fraction of remaining N<sub>2</sub> in DMM is significantly higher than that for  $^{36}\text{Ar}$  ( $\sim 0.9\%$ , Table 8), although N<sub>2</sub> and Ar have similar solubilities. (The degree of degassing of N<sub>2</sub> is not compared to that of  $^{40}\text{Ar}$  because  $^{40}\text{Ar}$  is radiogenic.) This difference has been attributed to the recycling of N<sub>2</sub> back to the mantle (Zhang and Zindler, 1993).

Nitrogen isotopes are consistent with the earlier mentioned results. The  $^{15}\text{N}/^{14}\text{N}$  ratio is 0.003676 in air, 0.00364 in the mantle (Marty and Humbert, 1997),  $(6.77 \pm 0.26) \times 10^{-3}$  in comets (Manfroid et al., 2009), 0.00356 in enstatite chondrites, 0.00383 in CI chondrites (Pepin, 1991), 0.0023 in Jupiter (Owen et al., 2001),  $(2.178 \pm 0.024) \times 10^{-3}$  for solar wind, and  $(2.268 \pm 0.028) \times 10^{-3}$  for protosolar nebula (Marty et al., 2011; Meibom et al., 2007). The similarity between air and mantle  $^{15}\text{N}/^{14}\text{N}$  ratios and their large difference from cometary  $^{15}\text{N}/^{14}\text{N}$  ratio preclude significant contribution of cometary injection to N<sub>2</sub> in air. Even though nitrogen isotopes allow impact degassing as a source for air N<sub>2</sub>, the N<sub>2</sub> budget in various reservoirs ( $2.66 \pm 0.22 \text{ ppm}$  in AOC+DMM and  $2.1 \pm 0.7 \text{ ppm}$  in UPM) would only allow minor contribution of impact degassing to air N<sub>2</sub>. Hence, N<sub>2</sub> seems to be a well-behaved volatile component that can be modeled by closed-system degassing.

**Table 11** Estimated N<sub>2</sub> concentrations in various reservoirs

	DMM	DMM+AOC	UPM	BSE
N <sub>2</sub> conc (ppm)	$0.23 \pm 0.12$	$2.66 \pm 0.22$	$2.1 \pm 0.7$	$2.61 \pm 0.21$

### 6.2.3.8 CO<sub>2</sub>

Carbon in Earth can be present in various forms: in the fluid form as CO<sub>2</sub>, CO, and CH<sub>4</sub> (plus other C-H compounds); in the form of carbonates; in reduced elemental form as graphite or diamond; or possibly in the form of Fe<sub>3</sub>C (Frost and McCammon, 2008). The properties of these forms are very different, for example, graphite and diamond are not volatile unless oxidized. Furthermore, there might be significant concentration of C in the core (Dasgupta and Walker, 2008; Nakajima et al., 2009; also see Chapter 3.15), meaning that the core is almost certainly the most significant reservoir of carbon. For example, assuming 6 wt% of C in the core (Dasgupta and Walker, 2008), the amount of carbon in the core would be as high as  $9.7 \times 10^{24} \text{ mol}$ ,  $> 1000$  times the amount of carbon in AOC. Hayden and Watson (2008) proposed that carbon in the core might slowly leak into the mantle. If so, C/ $^3\text{He}$  ratio in the mantle would have increased with time, and BSE would not be a closed system for carbon.

The total amount of carbon in AOC is well known, about  $(7 \pm 1) \times 10^{21} \text{ mol}$  (Holland, 1978; Hunt, 1972; Zhang and Zindler, 1993). CO<sub>2</sub>/ $^3\text{He}$  molar degassing ratio in MORB (including N-MORB and E-MORB) is  $(2.2 \pm 0.7) \times 10^9$  (Javoy and Pineau, 1991; Marty and Tolstikhin, 1998). The various stable forms of carbon such as diamond, graphite, and carbonates mean that the observed C/ $^3\text{He}$  ratio is lower than the C/ $^3\text{He}$  ratio in mantle source rocks (e.g., graphite might be retained in the mantle during mantle partial melting). CO<sub>2</sub> degassing rate has been estimated before with good consistency. However, the estimates were often pinned to the  $^3\text{He}$  degassing flux, which has been revised down recently by about a factor of 2 (Bianchi et al., 2010; Cartigny et al., 2008; Jean-Baptiste 1992; Saal et al., 2002), necessitating a revision of mantle carbon degassing flux. Using  $^3\text{He}$  flux of  $527 \pm 102 \text{ mol year}^{-1}$  (Bianchi et al., 2010), and CO<sub>2</sub>/ $^3\text{He}$  molar degassing ratio of  $(2.2 \pm 0.7) \times 10^9$  in MORB, the present-day mantle CO<sub>2</sub> degassing flux is  $(1.2 \pm 0.4) \times 10^{12} \text{ mol year}^{-1}$ , about half of  $2.3 \times 10^{12} \text{ mol year}^{-1}$  in many previous estimates (e.g., Marty and Tolstikhin, 1998; Zhang and Zindler, 1993). Although Cartigny et al. (2008) estimated CO<sub>2</sub> ridge flux to be  $2.3 \times 10^{12} \text{ mol year}^{-1}$  using a different method based on CO<sub>2</sub>/Nb mass ratio ( $\sim 530$ ; note that Cartigny et al. (2008) reevaluated the value of this ratio) in MORB, they used an average Nb concentration of 3.31 ppm in MORB, which is almost certainly too high because it implies 0.4 ppm Nb in DMM at 12% partial melting (Klein and Langmuir, 1987; Niu, 1997), twice the estimation of 0.21 ppm by Salters and Stracke (2004). If 0.21 ppm in DMM is used, then the estimated ridge CO<sub>2</sub> degassing flux would be  $\sim 1.2 \times 10^{12} \text{ mol year}^{-1}$ , the same as that estimated from the CO<sub>2</sub>/ $^3\text{He}$  ratio. Therefore, there is good consistency in the estimated new CO<sub>2</sub> flux of  $(1.2 \pm 0.4) \times 10^{12} \text{ mol year}^{-1}$  using different methods.

Carbon concentrations in mantle reservoirs have also been estimated before (e.g., Zhang and Zindler, 1993). Again, the estimates were pinned to the  $^3\text{He}$  degassing flux and hence need revision. The concentration of CO<sub>2</sub> in DMM can be estimated to be  $104 \pm 46 \text{ ppm}$  (meaning C concentration of  $28 \pm 12 \text{ ppm}$ ) from the degassing flux of CO<sub>2</sub> and the magma production rate of  $21 \text{ km}^3 \text{ year}^{-1}$  and the average degree of partial melting of  $(12 \pm 3)\%$ . This estimate is lower than most

**Table 12** Carbon budget

	<i>AOC</i>	<i>DMM</i>	<i>AOC+DMM</i>	<i>UPM</i>
Amount of C (mol)	$(7 \pm 1) \times 10^{21}$	$(4.8 \pm 2.1) \times 10^{21}$	$(11.8 \pm 2.3) \times 10^{21}$	$\sim 6.8 \times 10^{23}$
CO <sub>2</sub> conc (ppm)		104 ± 46	254 ± 51	~15 300
C conc (ppm)		28 ± 12	69 ± 14	~4200
C/ <sup>3</sup> He (molar ratio)		$(2.2 \pm 0.7) \times 10^9$		$\sim 3 \times 10^9$

previous estimates by a factor of 2 as expected. Using the CO<sub>2</sub>/Nb ratio approach (Cartigny et al., 2008), with Nb concentration of 0.21 ppm in DMM (Salters and Stracke, 2004), CO<sub>2</sub> concentration would be ~111 ppm (or C concentration of ~30 ppm), consistent with the CO<sub>2</sub>/<sup>3</sup>He ratio approach. The estimates by Saal et al. (2002) and Salters and Stracke (2004) were lower than author's estimate here because they used a lower CO<sub>2</sub>/Nb ratio, which was discussed in Cartigny et al. (2008). Helo et al. (2011) reported CO<sub>2</sub> concentration as high as 0.9 wt% in melt inclusions in plagioclase from Juan de Fuca MORB. Such high CO<sub>2</sub> concentration would require either an unusual mantle source or a very low degree of partial melting (e.g., close to 2% from an E-MORB source) or a normal degree of partial melting but with very high degree of crystal fractionation.

Using the concentration of CO<sub>2</sub> in DMM, the total amount of degassable C in DMM is estimated to be  $(4.8 \pm 2.1) \times 10^{21}$  mol. Therefore, total CO<sub>2</sub> in DMM + AOC is  $(11.8 \pm 2.3) \times 10^{21}$  mol. Mean CO<sub>2</sub> concentration in AOC + DMM is 254 ± 51 ppm (or 69 ± 14 ppm C, Table 12).

Given the present-day CO<sub>2</sub> degassing flux, total carbon in AOC would be supplied in 5.8 billion years, only slightly longer than the age of Earth. However, because it is expected that early degassing was much more rapid, the total degassed amount of CO<sub>2</sub> is almost certainly more than the amount in AOC. For example, based on the amount of <sup>40</sup>Ar in air, the mean degassing rate of <sup>40</sup>Ar is 11 times the present-day degassing rate. Considering that early degassing would not have degassed much <sup>40</sup>Ar because <sup>40</sup>Ar concentration was low in the early mantle and increased gradually due to radiogenic production, the mean degassing rate of CO<sub>2</sub> is expected to be more than 11 times the present degassing rate. That the estimated total degassed CO<sub>2</sub> is much more than the amount of CO<sub>2</sub> on Earth's surface may be referred to as a 'carbon paradox' (the first carbon paradox). One solution to the paradox is to recycle carbon back to the mantle (Zhang and Zindler, 1993). Because <sup>3</sup>He is not recycled back to the mantle, the recycling of C from the crust to the mantle would gradually increase C/<sup>3</sup>He in DMM. Hence, measured C/<sup>3</sup>He ratios in modern MORB samples are expected to be much higher than the primordial ratio.

However, measured C/<sup>3</sup>He ratios in OIB samples are about the same of slightly higher than the ratio in MORB (Marty and Tolstikhin, 1998), raising the question whether OIB source reflects UPM in terms of C/<sup>3</sup>He ratio. Furthermore, CO<sub>2</sub> concentration in UPM may be estimated from <sup>3</sup>He concentration ( $\sim 1.16 \times 10^{-10}$  mol kg<sup>-1</sup>) in UPM and C/<sup>3</sup>He molar ratio ( $3 \times 10^9$ ; Marty and Tolstikhin, 1998) in plume samples to be ~0.35 mol kg<sup>-1</sup>, or ~1.53 wt% CO<sub>2</sub> (or 0.42 wt% of C). This new estimate is extremely high and is ~60 times the concentration in AOC + DMM. That means, not only there is no non-mantle source for surface carbon, but also degassed CO<sub>2</sub> is trivial compared to CO<sub>2</sub> in UPM. Another way to estimate

CO<sub>2</sub> concentration in UPM is to use the CO<sub>2</sub>/Nb ratio, which is about 530 (Cartigny et al., 2008; note that the ratio of 530 is 2.3 times the ratio estimated by Salters and Stracke, 2004). Using Nb concentration of 0.658 ppm in UPM (McDonough and Sun, 1995), CO<sub>2</sub> concentration in UPM is 349 ± 87 ppm, which is not too different from the mean CO<sub>2</sub> concentration of 254 ± 51 ppm in AOC + DMM, but lower than the estimate from the C/<sup>3</sup>He ratio by a factor of 44. (Using Nb concentration of 0.588 ppm in UPM from Palme and O'Neill would lead to 312 ± 78 ppm.) The extremely high CO<sub>2</sub> concentration in UPM estimated using the C/<sup>3</sup>He method, meaning the extremely high C/<sup>3</sup>He ratio in OIB, is here termed the second carbon paradox. The paradox can also be stated as the large difference of estimated CO<sub>2</sub> concentration in UPM using the CO<sub>2</sub>/<sup>3</sup>He method versus the CO<sub>2</sub>/Nb ratio. One approach must be incorrect. One solution to this paradox is that C/<sup>3</sup>He ratios measured in OIB samples are not representative of UPM. That is, the result from the CO<sub>2</sub>/Nb ratio approach is accepted as reliable. Then the inferred CO<sub>2</sub> concentration in UPM is in reasonably good agreement with that for AOC+DMM, meaning that the BSE has been a closed system for carbon. The only issue would be to explain why C/<sup>3</sup>He ratios measured in OIB samples are not representative of UPM. On the other hand, because Nb is not volatile whereas CO<sub>2</sub> has a low solubility and hence is easily lost by degassing (whereas H<sub>2</sub>O has a much higher solubility), the CO<sub>2</sub>/Nb ratio approach may not be as reliable as the H<sub>2</sub>O/Ce approach. In this case, accepting the result from the C/<sup>3</sup>He ratio approach as reliable, a solution to the paradox is for carbon concentration in UPM (OIB source) to increase gradually with time by carbon input from the core (Hayden and Watson, 2008), or more directly, OIB source comes from core–mantle boundary where carbon concentration is high. The latter interpretation would support mantle plume generation at core–mantle boundary with a core component (Brandon et al., 1998, 1999, 2007). The third solution, which is less likely, is for DMM to be more reduced than plume samples so that most carbon in DMM is not present in the form of degassable CO<sub>2</sub>, but as elemental carbon or some other nondegassable form.

### 6.2.3.9 H<sub>2</sub>O

The total amount of H<sub>2</sub>O in AOC is well known, about  $(1.64 \pm 0.10) \times 10^{21}$  kg (Tables 13 and 14), or  $(9.10 \pm 0.55) \times 10^{22}$  mol. Distributing this amount to DMM leads to 789 ± 200 ppm.

One method to estimate H<sub>2</sub>O content in different mantle reservoirs is to use the roughly constant H<sub>2</sub>O/Ce ratio in mantle-derived basalts. The H<sub>2</sub>O/Ce mass ratio is 150 ± 75 (Michael, 1988, 1995; Saal et al., 2002; Salters and Stracke, 2004). In the present-day DMM, Ce concentration is estimated to be 0.772 ppm (Salters and Stracke, 2004), leading to

$116 \pm 58$  ppm H<sub>2</sub>O in DMM. Adding surface H<sub>2</sub>O, the average H<sub>2</sub>O concentration in DMM+AOC is  $905 \pm 208$  ppm (or H concentration of  $101 \pm 23$  ppm, similar to 120 ppm obtained by Palme and O'Neill, see Chapter 3.1). If all surface H<sub>2</sub>O comes from mantle degassing (i.e., the closed-system assumption), this would be the primary H<sub>2</sub>O concentration in the mantle.

On the other hand, H<sub>2</sub>O content in UPM can be estimated using the H<sub>2</sub>O/Ce ratio method. In the UPM, Ce concentration is well constrained, 1.675–1.786 ppm in UPM (McDonough and Sun, 1995; also see Chapter 3.1). Using the higher estimate for Ce concentration, H<sub>2</sub>O concentration in UPM is only  $268 \pm 134$  ppm, much lower than the mean H<sub>2</sub>O concentration in DMM+AOC. The inconsistency in estimated H<sub>2</sub>O concentrations in the UPM and in AOC+DMM is hereafter referred to as the 'H<sub>2</sub>O paradox.' Possible solutions to the H<sub>2</sub>O paradox include the following:

1. The H<sub>2</sub>O/Ce ratio is not constant and hence the ratio approach is not reliable. For example, Michael (1995) showed that the H<sub>2</sub>O/Ce ratio in Northern Atlantic MORB ranges from 200 to 350, whereas the ratio in other MORBs ranges from 120 to 230. However, even using the highest H<sub>2</sub>O/Ce ratio of 350 and Ce concentration in UPM, the H<sub>2</sub>O content in UPM would only be 586 ppm, still lower than  $905 \pm 208$  ppm for DMM+AOC. The H<sub>2</sub>O/Ce ratio may also be variable because H<sub>2</sub>O is affected by degassing if the degassing depth is shallow (such as subaerial degassing), whereas Ce is not. Hence, it is possible that the estimated H<sub>2</sub>O content in UPM using H<sub>2</sub>O/Ce ratio is not correct, but this alone would not be able to explain the large discrepancy.
2. A larger fraction of the mantle has been degassed for H<sub>2</sub>O, compared to <sup>40</sup>Ar. This is possible because H<sub>2</sub>O in the mantle was present initially, whereas <sup>40</sup>Ar is gradually produced by the decay of <sup>40</sup>K. Therefore, early degassing affected H<sub>2</sub>O more but did not affect <sup>40</sup>Ar much. For example, if 80% of the whole mantle is allowed to be degassed in terms of H<sub>2</sub>O, H<sub>2</sub>O concentration in AOC+DMM would be  $\sim 624$  ppm,

**Table 13** H<sub>2</sub>O in air, oceans, and crust

Reservoir	H <sub>2</sub> O (kg)	Percentage (%)
Oceans	$1.37 \times 10^{21}$	83.5
Ice caps and glaciers	$4.34 \times 10^{19}$	2.65
Groundwater	$1.53 \times 10^{19}$	0.93
Lakes	$1.25 \times 10^{17}$	0.0076
Rivers	$1.7 \times 10^{15}$	0.00011
Atmosphere vapor	$1.55 \times 10^{16}$	0.00095
Soil moisture	$6.5 \times 10^{16}$	0.0040
Continental and oceanic crust	$(2.09 \pm 1.00) \times 10^{20}$	$(12.7 \pm 6.1)$
Total	$(1.64 \pm 0.10) \times 10^{21}$	100

Source: Holland HD (1978) *The Chemistry of the Atmosphere and Oceans*. New York: Wiley; Drever (1997). *The Geochemistry of Natural Waters*. New Jersey: Prentice-Hall.

**Table 14** H<sub>2</sub>O budget

	AOC	DMM	AOC+DMM	UPM
Amount of H <sub>2</sub> O (mol)	$(9.1 \pm 0.6) \times 10^{22}$			
H <sub>2</sub> O conc (ppm)		$116 \pm 58$	$905 \pm 208$	$268 \pm 134$
H conc (ppm)		$13.0 \pm 6.5$	$101 \pm 23$	$30 \pm 15$

which would still be higher than the estimated H<sub>2</sub>O content in UPM. That is, this option alone is not enough.

3. A significant amount of ocean H<sub>2</sub>O is not from mantle degassing but from accretion impact degassing or cometary injection or meteorites (mostly chondrites) that came to Earth in its long history. Possible contribution by comets has been debated: Chyba (1987) suggested that cometary injection could be a main source of ocean water. Balsiger et al. (1995) and Meier et al. (1998) reported consistent <sup>2</sup>H/<sup>1</sup>H ratio in comets measured independently to be  $\sim 0.00032$ , about two times the ratio in ocean water ( $(1.558 \pm 0.001) \times 10^{-4}$ ) and in primordial mantle water ( $(1.433 \pm 0.030) \times 10^{-4}$ ; Kingsley et al., 2002; Kyser and O'Neil, 1984 similar to that in carbonaceous chondrites ( $1.4 \pm 0.1) \times 10^{-4}$ ; Kerridge, 1985). From these measurements, it was thought that about 93% of ocean water is from mantle degassing and only about 7% originated from cometary injection (Dauphas et al., 2000; Hutsemekers et al., 2009; Zhang, 2002). However, recently, Hartogh et al. (2011) reported that the <sup>2</sup>H/<sup>1</sup>H ratio of a Jupiter-family comet (originated from the Kuiper Belt) is  $(1.61 \pm 0.24) \times 10^{-4}$ , which is similar to <sup>2</sup>H/<sup>1</sup>H in ocean water, allowing (though not proving) significant (but unconstrained) contribution of these comets to ocean water. If all the discrepancy in H<sub>2</sub>O budget is attributed to delivery of water to Earth's surface by bombardments of asteroids and Jupiter-family comets, then about 80% of ocean water would be from asteroids and Jupiter-family comets and only about 20% is from mantle degassing.

It is also possible that the solution to the H<sub>2</sub>O paradox involves all of the earlier mentioned factors.

Taking H<sub>2</sub>O concentration to be  $268 \pm 134$  ppm in UPM and  $116 \pm 58$  ppm in DMM, the degree of degassing for H<sub>2</sub>O from DMM would be  $(57 \pm 30)\%$ . Because there is large uncertainty in the value, including unspecified uncertainty in the H<sub>2</sub>O concentration in UPM and the mass fraction of DMM in terms of H<sub>2</sub>O degassing, the significance of this value, either in terms of the solubility-controlled degassing model or in terms of possible H<sub>2</sub>O recycling back to the mantle, is not discussed.

#### 6.2.3.10 Summary of Various Paradoxes and Uncertainties

Although much progress has been made, mantle degassing and atmosphere evolution are not fully understood yet. There are aspects in volatile budgets and isotopic ratios that are inconsistent with the usual assumption about degassing and Earth's volatile evolution. To highlight these inconsistencies, they are referred to as paradoxes and summarized in the succeeding texts:

1. Even though OIB (especially Hawaii–Iceland–Galapagos) mantle sources have low and correlated <sup>4</sup>He/<sup>3</sup>He and <sup>21</sup>Ne/<sup>22</sup>Ne, consistent with the assumption that they approach UPM, the Sr–Nd–Hf–Os isotopes in these OIBs

indicate that they are almost as depleted as MORB mantle ([Figure 4](#)). Because the volatiles are consistent (at least for He and Ne for which atmospheric contamination is either negligible or can be reliably corrected) and because there are already various helium paradoxes ([Anderson, 1998a,b](#)), this paradox is referred to as the ‘volatile paradox.’ This paradox may be related to differences between mantle degassing and mantle depletion and OIB’s not representing UPM. Another possible solution to the paradox is to adopt a superchondritic primitive mantle.

2. A long-standing neon paradox is that  $^{20}\text{Ne}/^{22}\text{Ne}$  ratios in the mantle are different from the air ratio, indicating that air cannot be directly and entirely due to mantle degassing. Furthermore, the total nucleogenic production of  $^{21}\text{Ne}$  in the mantle might not be enough to provide air  $^{21}\text{Ne}$ , and  $^{20-22}\text{Ne}$  concentrations in UPM are also too low to supply Ne in air ([Table 6](#)). The inferred low Ne concentration in UPM is reinforced by that the current  $^{20-22}\text{Ne}$  degassing rates are also too low (compared to He) to supply air Ne. This is referred to as the second ‘neon paradox.’ The hydrodynamic escape of neon to outer space can account for the first paradox but would worsen the second paradox. The two neon paradoxes can be resolved if there was nonmantle Ne (either extraterrestrial Ne or initial Ne) in air.
3. Using  $^{36}\text{Ar}$  in air and total  $^{40}\text{Ar}$  production in BSE, the upper limit of  $^{40}\text{Ar}/^{36}\text{Ar}$  in current AOC+DMM can be robustly estimated, and this estimate is significantly lower than air contamination-corrected  $^{40}\text{Ar}/^{36}\text{Ar}$  in OIB samples. In other words, there is not enough  $^{36}\text{Ar}$  in UPM to supply  $^{36}\text{Ar}$  in air. This is referred to as an ‘argon paradox.’ This paradox can be resolved if either OIB does not come from UPM or there was nonmantle  $^{36}\text{Ar}$  in air. The former option is consistent with the implication of the volatile paradox. The latter option is consistent with Ne data.
4. Estimated  $\text{H}_2\text{O}$  concentration in UPM using  $\text{H}_2\text{O}/\text{Ce}$  ratio in the mantle is too low compared to estimated  $\text{H}_2\text{O}$  concentration by adding surface  $\text{H}_2\text{O}$  content back to DMM. There does not seem to be enough  $\text{H}_2\text{O}$  in the initial mantle to supply  $\text{H}_2\text{O}$  on the surface, similar to the case of  $^{36}\text{Ar}$ . This is referred to as the  $\text{H}_2\text{O}$  paradox. This paradox can be resolved if OIB mantle does not represent UPM or there is nonmantle  $\text{H}_2\text{O}$  in oceans, such as  $\text{H}_2\text{O}$  directly delivered to the surface of Earth by asteroids and Jupiter-family comets.
5. Nonradiogenic Kr and Xe isotope ratios in well gas samples are different from those in air, suggesting that mantle degassing may not be the sole source of these gases in air. Furthermore, there seems to be too much  $^{130}\text{Xe}$  in UPM for supplying  $^{130}\text{Xe}$  in air (referred to as a xenon paradox), which is opposite to the case of Ne,  $^{36}\text{Ar}$ , and  $\text{H}_2\text{O}$ .
6. Estimated C concentration in UPM using  $\text{C}/^{3}\text{He}$  ratio in OIB is extremely high, much higher than that using the  $\text{C}/\text{Nb}$  ratio approach, or by adding surface carbon back to DMM. This is referred to as a carbon paradox. This paradox is similar to the Xe paradox and opposite to the Ne, Ar, and  $\text{H}_2\text{O}$  paradoxes. The carbon paradox can be resolved by assuming that OIB mantle does not represent UPM in terms of  $\text{C}/^{3}\text{He}$  ratio, or the core is continuously supplying carbon to UPM (the lower mantle).

In summary, among the volatile components discussed, only  $\text{N}_2$  budget, flux, and isotope data seem to provide a self-consistent picture of closed-system degassing, and for all other components, there are paradoxes. For Ne,  $^{36}\text{Ar}$ , and  $\text{H}_2\text{O}$ , the concentrations in UPM seem to be too low to supply the amount in air, whereas for Xe and  $\text{CO}_2$ , the concentrations in UPM appear to be too high compared to the amount in the atmosphere. Some of the paradoxes may be related to difficulties in estimating the concentrations and isotope ratios in UPM, some may be attributed to escape to outer space or to flux from the outer core, and some can be resolved by assuming nonmantle (initial or extraterrestrial) contribution to air. Hence, it is time to abandon or at least modify the closed-system degassing model. Furthermore, the degassing of volatile elements and the depletion of nonvolatile incompatible elements may be decoupled. Resolving all of these paradoxes will be important in future studies.

## 6.2.4 Modeling Degassing, Recycling, and Atmosphere Evolution

### 6.2.4.1 Various Mantle Degassing Models in the Literature

#### 6.2.4.1.1 General model features

There are numerous degassing models, progressing from relatively simple to fairly sophisticated through the years ([Albarede, 1998](#); [Allegre et al., 1986/87](#); [Honda and McDougall, 1998](#); [Ozima, 1975](#); [Porcelli and Wasserburg, 1995a,b](#); [Sarda et al., 1985](#); [Staudacher and Allegre, 1982](#); [Turekian, 1959](#); [Zhang and Zindler, 1989, 1993](#)), though none captures the full complexity that people now know. All the degassing models divided the mantle into two parts: either degassed mantle and undegassed mantle or upper mantle and lower mantle. Most degassing models assume that essentially all gases in AOC are from mantle degassing, and hence, the amount and isotope ratios of noble gases in AOC provide important constraints. These models are referred to closed-system degassing models in which the BSE (AOC and mantle) is assumed to be a closed system except for escape of He and early hydrodynamic escape to outer space. Possible contributions to surface volatiles by impact degassing and cometary injection and to mantle volatiles by Earth’s outer core were ignored in such degassing models.

Some models allow not only mantle degassing but also the recycling of gases from AOC back to the mantle ([Zhang and Zindler, 1993](#)) or exchange between mantle reservoirs ([Porcelli and Wasserburg, 1995a,b](#)).

In degassing models, the mantle is often divided into two reservoirs: one is degassed and depleted (DMM) and the other is undegassed and undepleted (UPM). The isotopic evolution of UPM is straightforward. Using  $^{4}\text{He}/^{3}\text{He}$  ratio as an example and ignoring minor contributions from  $^{147}\text{Sm}$ ,  $^{146}\text{Sm}$ , and  $^{190}\text{Pt}$ , the isotopic evolution of  $^{4}\text{He}/^{3}\text{He}$  in UPM can be written as (e.g., [Zhang and Zindler, 1989](#))

$$\left(\frac{^{4}\text{He}}{^{3}\text{He}}\right)_p^t = \left(\frac{^{4}\text{He}}{^{3}\text{He}}\right)_p^0 + 8\left(\frac{^{238}\text{U}}{^{3}\text{He}}\right)_p^0(1 - e^{-\lambda_{238}t}) + 7\left(\frac{^{235}\text{U}}{^{3}\text{He}}\right)_p^0(1 - e^{-\lambda_{235}t}) + 6\left(\frac{^{232}\text{Th}}{^{3}\text{He}}\right)_p^0(1 - e^{-\lambda_{235}t}) \quad [4]$$

where subscript P stands for UPM (not subscript U to avoid confusion with element U), superscript  $t$  is time measured from the beginning of degassing, and superscript 0 is the initial (at  $t=0$ ) in UPM. Once  $(^4\text{He}/^3\text{He})$  in the initial UPM and in the present-day UPM is known, the initial (or the present)  $^{238}\text{U}/^3\text{He}$  can be constrained (since  $^{238}\text{U}$ ,  $^{235}\text{U}$ , and  $^{232}\text{Th}$  concentrations in UPM are related). For example, assuming  $(^4\text{He}/^3\text{He})$  in the initial UPM is 6000 and  $(^4\text{He}/^3\text{He})$  in the present UPM is 20 000, and the beginning of degassing is 4.46 Ga, because  $(^{238}\text{U}/^{235}\text{U})_{t=0} = 137.818 \times e^{(0.155125 - 0.98485)4.46} = 3.405$  and  $(^{232}\text{Th}/^{238}\text{U})_{t=0} = (83.4/21.8) \times (238.029/232.0381) \times (137.818/138.818) \times e^{(0.049475 - 0.155125)4.46} = 2.432$  (where the value 137.818 is from [Hiess et al., 2012](#); and 83.3 and 21.8 ppb are from [Palme and O'Neil, 2004](#)), then the initial ( $^{238}\text{U}/^3\text{He}$ ) molar ratio in UPM is 1570 and the present ratio is 786.

The ratio in DMM can be written as

$$\begin{aligned} \left(\frac{^4\text{He}}{^3\text{He}}\right)_D^t &= \left(\frac{^4\text{He}}{^3\text{He}}\right)_D \\ &+ \int_0^t \left[ 8\lambda_{238} \left(\frac{^{238}\text{U}}{^3\text{He}}\right)_D^\tau + 7\lambda_{235} \left(\frac{^{235}\text{U}}{^3\text{He}}\right)_D^\tau + 6\lambda_{232} \left(\frac{^{232}\text{Th}}{^3\text{He}}\right)_D^\tau \right] d\tau \end{aligned} \quad [5]$$

where subscript D stands for DMM and  $\tau$  is an integration dummy variable. To determine how  $^4\text{He}/^3\text{He}$  in DMM would evolve with time, it is necessary to know how  $(^{238}\text{U}/^3\text{He})$  and  $(^{232}\text{Th}/^3\text{He})$  in DMM vary with time, meaning to know how  $^3\text{He}$  is degassed and U and Th are depleted in DMM. The depletion of U, Th, and K is often expressed as (e.g., [Sarda et al., 1985](#); [Zhang and Zindler, 1989](#))

$$\frac{^{238}\text{U}(t)}{^{238}\text{U}(0)} = e^{-(\lambda_{238} + \mu_U)t} \quad [6a]$$

$$\frac{^{235}\text{U}(t)}{^{235}\text{U}(0)} = e^{-(\lambda_{235} + \mu_U)t} \quad [6b]$$

$$\frac{^{232}\text{Th}(t)}{^{232}\text{Th}(0)} = e^{-(\lambda_{232} + \mu_{\text{Th}})t} \quad [6c]$$

$$\frac{^{40}\text{K}(t)}{^{40}\text{K}(0)} = e^{-(\lambda_{40} + \mu_K)t} \quad [6d]$$

where  $\mu_U$ ,  $\mu_{\text{Th}}$ , and  $\mu_K$  account for how U, Th, and K are depleted in DMM. By comparing the concentration of U in DMM ([Salters and Stracke, 2004](#)) and Palme and O'Neill (see [Chapter 3.1](#)),  $\mu_U = 0.344 \pm 0.092$ . Similarly,  $\mu_{\text{Th}} = 0.405 \pm 0.092$ , and  $\mu_K = 0.345 \pm 0.092$ .

The evolution of  $^3\text{He}/^4\text{He}_0$  ratio in DMM is often referred to as the degassing function  $g(t)$ . In the degassing models of [Staudacher and Allegre \(1982\)](#), [Sarda et al. \(1985\)](#), and [Allegre et al. \(1986/87\)](#), the degassing model is taken to be either one-term exponential function or multiple-terms such as

$$\text{for } ^{130}\text{Xe} \text{ degassing, } g(t) = e^{-\alpha t} \quad [7a]$$

$$\text{for } ^{36}\text{Ar} \text{ degassing, } g(t) = ae^{-\alpha t} + (1-a)e^{-\beta t} \quad [7b]$$

where  $\alpha$ ,  $\beta$ , and  $a$  are parameters to be determined from fitting. For He degassing, another flux term from UPM to DMM is assumed in the model of [Allegre et al. \(1986/87\)](#). In the degassing model of [Zhang and Zindler \(1989\)](#), the degassing

function for all noble gases is related to gas solubility and expressed as

$$g_i(t) = \frac{1}{1 + B_i(1 - e^{-\gamma t})} \quad [8]$$

where  $i$  stands for a specific nonradiogenic noble gas,  $\gamma$  is a universal parameter for all gases, and  $B_i$  is an element-dependent parameter inversely proportional to the solubility of  $i$ . Specific groups of degassing models are summarized in the succeeding texts.

#### 6.2.4.1.2 Bulk degassing models

[Staudacher and Allegre \(1982\)](#), [Sarda et al. \(1985\)](#), and [Allegre et al. \(1986/87\)](#) developed sophisticated mantle degassing models assuming (1) two mantle reservoirs (degassed and undegassed), (2) closed-system degassing except for He, and (3) all gases (including He, Ar, and Xe) are degassed similarly from the degassed mantle. That is, there is no fractionation of the gases during degassing, and all nonradiogenic gases are assumed to have been degassed to the same degree. On the other hand, the degree of degassing for radiogenic isotopes depends on how rapidly they have been produced and how large the primordial component was. These models are termed bulk degassing models in this chapter. The depletion and degassing functions are given in eqns [6a]–[6d], [7a], and [7b]. Because  $^{129}\text{Xe}/^{130}\text{Xe}$  ratio in DMM is significantly higher than that in air, and because  $^{129}\text{I}$  (the parent of  $^{129}\text{Xe}$ ) has a half-life of only 16 My, Xe data demand very rapid early degassing ([Staudacher and Allegre, 1982](#)). However, Ar and especially He data imply significantly slower degassing (e.g., about 43% of all mantle  $^{40}\text{Ar}$  is in air, and  $^{40}\text{Ar}$  is slowly produced by the decay of  $^{40}\text{K}$ ). [Sarda et al. \(1985\)](#) and [Allegre et al. \(1986/87\)](#) reconciled these differences by adding ad hoc additional degassing terms for each gas. They inferred that all the nonradiogenic isotopes in DMM have been degassed to 99% or more, a conclusion that still stands.

#### 6.2.4.1.3 Solubility-controlled degassing model

[Zhang and Zindler \(1989, 1993\)](#) presented a solubility-controlled degassing model (see also [Honda and McDougall, 1998](#); [Tolstikhin and O'Nions, 1994](#)). The assumptions of two mantle reservoirs and closed-system degassing are the same as those in bulk degassing models. The depletion function for K, I, U, and Th is similar to that adopted by [Staudacher and Allegre \(1982\)](#), [Sarda et al. \(1985\)](#), and [Allegre et al. \(1986/87\)](#), but the degassing function is eqn [8] (rather than eqn [7a] and [7b]), depending on solubility. In the context of the solubility-controlled degassing model, bubble growth and subsequent gas loss occur through equilibrium partitioning between bubbles (the gas phase) and the melt phase. In a way, the solubility-controlled degassing model is similar to the batch partial melting model ([Zou, 2007](#)). Hence, if the solubility of the gas is high, more gas is retained in the melt and returned to the mantle, resulting in smaller degree of degassing and slower growth of radiogenic/nonradiogenic isotope ratio in DMM. With this model, He, Ar, and Xe isotope ratios available at that time were all reconciled by a single degassing history. [Zhang and Zindler \(1993\)](#) extended the solubility-controlled degassing model to  $\text{N}_2$

and CO<sub>2</sub> degassing and concluded that recycling back to the mantle is important for these gases and modeled the evolution of these volatiles. Tolstikhin and O’Nions (1994) and Honda and McDougall (1998) also used solubility-controlled degassing model to reconcile noble gas data.

The solubility-controlled degassing models lead to the following results: (1) For a pair of gas components with similar solubilities, the measured concentration ratio (such as CO<sub>2</sub>/<sup>3</sup>He ratio or N<sub>2</sub>/Ar ratio) in basaltic glasses and vesicles should not vary much by degassing (consistent with observation), and hence, these ratios are often used to infer mantle compositions; (2) the mean degassing time depends on solubility, and is very short for <sup>130</sup>Xe (21 My) and increases to <sup>36</sup>Ar (56 My) and then to <sup>3</sup>He (310 My); and (3) the degree of degassing for nonradiogenic gas species in DMM is 97.5% for <sup>3</sup>He, 99.7% for <sup>36</sup>Ar, and 99.92% for <sup>130</sup>Xe. The solubility-controlled degassing model can roughly predict the observed <sup>3</sup>He degassing rate (Zhang and Zindler, 1989).

#### 6.2.4.1.4 Steady-state degassing model

Porcelli and Wasserburg (1995a,b) proposed the steady-state degassing model. In this model, the mantle is divided into the upper mantle (represented by MORB) and lower mantle (represented by OIB). The model assumes that noble gases in the upper mantle are due to ‘steady state’ supply from the lower mantle, mixed with subducted noble gases, plus radiogenic nuclides produced in situ in MORB mantle. For example, the model predicts that <sup>4</sup>He/<sup>3</sup>He in DMM is higher than in UPM due to <sup>4</sup>He ingrowth in DMM, which is consistent with observations. The model also predicts that <sup>129</sup>Xe/<sup>130</sup>Xe in DMM is less than or equal to that in UPM because there is no more ingrowth in DMM (<sup>129</sup>I is extinct) and mixing of subducted materials would lower <sup>129</sup>Xe/<sup>130</sup>Xe in DMM. This prediction could not be evaluated at the time because atmospheric contamination of Xe isotopes could not be corrected. Furthermore, their models do not directly address atmosphere formation, and hence, nonmantle contribution to the atmosphere is allowed.

#### 6.2.4.2 Evaluation of Some Assumptions in Degassing Models

##### 6.2.4.2.1 Closed-system assumption

The bulk degassing and solubility-controlled degassing models adopted the closed-system assumption, but many lines of evidence discussed in the data section show that the closed-system degassing assumption is untenable. The contribution of mantle degassing to air is certain (e.g., Section 6.2.1.1), but the Ne, <sup>36</sup>Ar, and H<sub>2</sub>O paradoxes seem to indicate significant contribution to atmosphere by nonmantle sources. As a result, information about UPM must be obtained independently and cannot be obtained by treating atmosphere as the complementary part of DMM.

##### 6.2.4.2.2 Testing the degassing models

Zhang (1997) and Moreira and Allegre (1998) made an effort in testing the various classes of degassing models with inconclusive results because the critical data were not available. A lot more data have become available since the degassing models were developed in 1980s and 1990s. Therefore, it is time to test the degassing models again.

Bulk degassing models predict that the degree of degassing for nonradiogenic noble gases is all the same, which is not consistent with available data reviewed in earlier sections. On the other hand, solubility-controlled degassing models predict that the degree of degassing is lowest for <sup>3</sup>He and then increases for <sup>22</sup>Ne, <sup>36</sup>Ar, and <sup>130</sup>Xe. As shown in the data section, this is consistent with the self-consistent and contamination-corrected Ne and He data (DMM is 99.1% degassed in terms of <sup>3</sup>He and 99.66% degassed in terms of <sup>22</sup>Ne). For Ar and Xe, air contamination cannot be perfectly corrected, and hence, the degree of degassing cannot be estimated so well.

The best test is probably by isotope ratios. Among the isotope data, only for the He and Ne isotope data in DMM and UPM is there internal consistency. Hence, they will be used in testing the models. Following Zhang and Zindler (1989) and Zhang (1997), S parameters are defined and explained in the succeeding equations:

$$S_{4\text{He}/^3\text{He}} = \frac{(^4\text{He}/^3\text{He})_{\text{DMM}}^T - (^4\text{He}/^3\text{He})_{\text{UPM}}^0}{(^4\text{He}/^3\text{He})_{\text{UPM}}^T - (^4\text{He}/^3\text{He})_{\text{UPM}}^0} \quad [9]$$

$$S_{21\text{Ne}/^22\text{Ne}} = \frac{(^{21}\text{Ne}/^{22}\text{Ne})_{\text{DMM}}^T - (^{21}\text{Ne}/^{22}\text{Ne})_{\text{UPM}}^0}{(^{21}\text{Ne}/^{22}\text{Ne})_{\text{UPM}}^T - (^{21}\text{Ne}/^{22}\text{Ne})_{\text{UPM}}^0} \quad [10]$$

where the superscript ‘0’ means  $t=0$  (initial) and ‘T’ means  $t=T$  (present-day). Because contamination-corrected <sup>21</sup>Ne/<sup>22</sup>Ne ratios and mantle <sup>4</sup>He/<sup>3</sup>He ratios are well-correlated (Figure 6), self-consistent  $S_{21\text{Ne}/^22\text{Ne}}$  and  $S_{4\text{He}/^3\text{He}}$  can be reliably estimated using the least-radiogenic <sup>21</sup>Ne/<sup>22</sup>Ne and <sup>4</sup>He/<sup>3</sup>He (even though these ratios may still be too high for UPM). For example, adopting  $(^{20}\text{Ne}/^{22}\text{Ne})_{\text{mantle}} = 13.0$  and using ratios in Table 5, it can be obtained that  $S_{4\text{He}/^3\text{He}} = 6.0 \pm 1$  and  $S_{21\text{Ne}/^22\text{Ne}} \approx 15 \pm 5$ , leading to

$$S_{21\text{Ne}/^22\text{Ne}} \approx (2.5 \pm 0.9)S_{4\text{He}/^3\text{He}} \quad [11]$$

Using eqns [4] and [5],  $S_{4\text{He}/^3\text{He}}$  can be written as

Because nucleogenic <sup>21</sup>Ne production is proportional to radiogenic <sup>4</sup>He production with a ratio of  $(4.5 \pm 0.8) \times 10^{-8}$  (Leya and Wieler, 1999; Yatsevich and Honda, 1997),  $S_{21\text{Ne}/^22\text{Ne}}$  can be written as

$$S_{4\text{He}/^3\text{He}} = \frac{\int_0^T \left[ 8\lambda_{238} \left( \frac{^{238}\text{U}_D^\tau}{^{238}\text{U}_D^0} \right) + 7\lambda_{235} \left( \frac{^{235}\text{U}_D^\tau}{^{238}\text{U}_D^0} \right) + 6\lambda_{232} \left( \frac{^{232}\text{Th}_D^\tau}{^{238}\text{U}_D^0} \right)_D^\tau \right] ^3\text{He}_D^0 d\tau}{8(1 - e^{-\lambda_{238}T}) + 7 \left( \frac{^{235}\text{U}}{^{238}\text{U}} \right)_p^0 (1 - e^{-\lambda_{235}T}) + 6 \left( \frac{^{232}\text{Th}}{^{238}\text{U}} \right)_p^0 (1 - e^{-\lambda_{232}T})} \quad [12]$$

$$S_{^{21}\text{Ne}/^{22}\text{Ne}} = \frac{\int_0^T \left[ 8\lambda_{238} \left( \frac{^{238}\text{U}_D^\tau}{^{238}\text{U}_D^0} \right) + 7\lambda_{235} \left( \frac{^{235}\text{U}_D^\tau}{^{238}\text{U}_D^0} \right) + 6\lambda_{232} \left( \frac{^{232}\text{Th}_D^\tau}{^{238}\text{U}_D^0} \right)_D^\tau \right] \frac{^{22}\text{Ne}_D^0}{^{22}\text{Ne}_D^\tau} d\tau}{8(1 - e^{-\lambda_{238}T}) + 7 \left( \frac{^{235}\text{U}}{^{238}\text{U}} \right)_P^0 (1 - e^{-\lambda_{235}T}) + 6 \left( \frac{^{232}\text{Th}}{^{238}\text{U}} \right)_P^0 (1 - e^{-\lambda_{232}T})} \quad [13]$$

For bulk degassing models,  ${}^3\text{He}$  and  ${}^{22}\text{Ne}$  are assumed to degas at the same relative rate, that is,  $S_{^3\text{He}/^3\text{He}} = S_{^{21}\text{Ne}/^{22}\text{Ne}}$ , resulting in  $S_{^4\text{He}/^3\text{He}} = S_{^{21}\text{Ne}/^{22}\text{Ne}}$ , which is inconsistent with He and Ne isotopic data (eqn [11]).

On the other hand, for solubility-controlled degassing models,  $S_{^{22}\text{Ne}/^{22}\text{Ne}} \approx (K_{\text{He}}/K_{\text{Ne}})$ , resulting in  $S_{^{21}\text{Ne}/^{22}\text{Ne}} \approx (K_{\text{He}}/K_{\text{Ne}})S_{^4\text{He}/^3\text{He}} \approx 2.3$ , where  $K_{\text{He}}$  and  $K_{\text{Ne}}$  are solubilities of He and Ne. This result is consistent with He and Ne isotopic data.

In theory,  $S_{^{40}\text{Ar}/^{36}\text{Ar}}$ ,  $S_{^{129}\text{Xe}/^{130}\text{Xe}}$ , and  $S_{^{136}\text{Xe}/^{130}\text{Xe}}$  may be similarly defined (Zhang and Zindler, 1989) and applied to further test various degassing models. However, (1) the different half-life of  ${}^{40}\text{K}$ ,  ${}^{129}\text{I}$ , and  ${}^{244}\text{Pu}$  compared to those of  ${}^{238}\text{U}$ ,  ${}^{235}\text{U}$ , and  ${}^{232}\text{Th}$  and (2) the difficulty to reliably estimate  ${}^{40}\text{Ar}/{}^{36}\text{Ar}$ ,  ${}^{129}\text{Xe}/{}^{130}\text{Xe}$ , and  ${}^{136}\text{Xe}/{}^{130}\text{Xe}$  in the least-radiogenic OIB to be internally consistent with  ${}^4\text{He}/{}^3\text{He}$  make it impossible at present to use the  $S_{^{40}\text{Ar}/^{36}\text{Ar}} - S_{^4\text{He}/^3\text{He}}$ ,  $S_{^{129}\text{Xe}/^{130}\text{Xe}} - S_{^4\text{He}/^3\text{He}}$ , and  $S_{^{136}\text{Xe}/^{130}\text{Xe}} - S_{^4\text{He}/^3\text{He}}$  relations.

To test the steady-state degassing model, it is noted that for radiogenic isotope ratios whose parent is now extinct, such as  ${}^{129}\text{Xe}/{}^{130}\text{Xe}$  and  ${}^{136}\text{Xe}/{}^{130}\text{Xe}$ , the steady-state degassing model requires that OIB is at least as radiogenic as MORB because (1)  ${}^{129}\text{Xe}$  has not been produced since about 4.40 Ga, meaning no in situ production of  ${}^{129}\text{Xe}$  in MORB mantle now, and (2) subducted noble gases with air signature would have lowered  ${}^{129}\text{Xe}/{}^{130}\text{Xe}$  in the MORB mantle. Plotting  ${}^{129}\text{Xe}/{}^{130}\text{Xe}$  versus  ${}^{20}\text{Ne}/{}^{22}\text{Ne}$  in MORB to assess the effect of air contamination, Loihi and Iceland (Figure 12), the trend for Iceland and Hawaii lies at much lower  ${}^{129}\text{Xe}/{}^{130}\text{Xe}$  at the same  ${}^{20}\text{Ne}/{}^{22}\text{Ne}$  than MORB. That is,  ${}^{129}\text{Xe}/{}^{130}\text{Xe}$  data in OIB (Trieloff et al., 2000) that became available after the work of Porcelli and Wasserburg (1995a,b) are significantly lower than those in MORB (Moreira et al., 1998), inconsistent with the steady-state degassing model. Another consequence of the steady-state model is that  $S_{^{21}\text{Ne}/^{22}\text{Ne}} = S_{^4\text{He}/^3\text{He}}$  because (1) at input from UPM into DMM,  ${}^4\text{He}/{}^3\text{He}$  and  ${}^{21}\text{Ne}/{}^{22}\text{Ne}$  in DMM are the same as in UPM; (2) subducted He is negligible; (3) subducted Ne is corrected away using  ${}^{20}\text{Ne}/{}^{22}\text{Ne}$ ; and (4) in situ growth of  ${}^{21}\text{Ne}$  is proportional to that of  ${}^4\text{He}$ . However, data show that  $S_{^{21}\text{Ne}/^{22}\text{Ne}} \approx 2.5S_{^4\text{He}/^3\text{He}}$  (eqn [11]), further against the steady-state model.

In summary, among bulk degassing, solubility-controlled degassing, and steady-state degassing models, by using isotopic ratios in mantle reservoirs (atmospheric data are not used because the closed-system degassing assumption needs revision), the solubility-controlled degassing model is most consistent with available data. Nonetheless, the closed-system assumption in the original solubility-controlled degassing model (Zhang and Zindler, 1989, 1993) is not consistent with newly available data. Furthermore, equilibrium solubility-controlled degassing may be too simple since MORBs are often oversaturated with gases (e.g., Dixon et al., 1988; Soule et al., 2012). That is, bubble growth kinetics, including gas diffusion, likely also plays a

role. Incorporating such effect quantitatively into future models will be a challenge.

#### 6.2.4.2.3 Does the least-radiogenic OIB represent UPM?

All degassing models in the literature assume that the least-radiogenic isotope ratios in OIB represent UPM signature. However, there is a possibility (although not a requirement) that the least-radiogenic OIBs do not represent UPM. Because it is argued in this chapter that constraints from the atmosphere cannot be used to evaluate UPM composition, if it is further allowed that the least-radiogenic OIB samples do not come from UPM, then there is no good way to obtain information about UPM. That would mean that not enough constraints are there to understand mantle degassing and atmosphere formation and evolution through degassing models. Because the evidence against OIB being from UPM is not overwhelming, in this chapter, the least-radiogenic OIB is still used to represent UPM.

#### 6.2.4.3 Other Sources of Gases for the Atmosphere

As can be seen in earlier sections, at least some of the gases in air are not entirely from mantle degassing. Indeed, various hypotheses are available for these other sources, although they are mostly conceptual rather than quantitative models. In the succeeding texts, other sources contributing to the atmosphere are discussed.

##### 6.2.4.3.1 Impact degassing

Shock experimental studies show that high-velocity impacts on volatile-rich minerals can cause considerable release of volatiles (Lange and Ahrens, 1982). For example, serpentine begins to lose  $\text{H}_2\text{O}$  at a shock pressure of  $\sim 20$  GPa (Lange and Ahrens, 1982; Lange et al., 1985), and calcite begins to lose  $\text{CO}_2$  at 10–15 GPa (Boslough et al., 1982; Lange and Ahrens, 1986). The complete release of volatiles seems to occur at  $>60$  GPa. Gazis and Ahrens (1991) shocked vitreous carbon containing initial Ar (since carbon is often the main carrier of noble gases in chondrites, e.g., Ming and Anders, 1988) and found that about 28% of the total Ar was released from vitreous carbon at a shock pressure of 4 GPa. Exactly how the volatiles were released during shock is not known, but the release is often attributed to high temperature, enhanced diffusion, development of microcracks, etc. Because the devolatilization mechanism is not known during shock experiments, the scaling law is also not known. Hence, how the experimental results may be quantitatively applied to large-scale impacts of planetesimals remains to be worked out. Furthermore, the impact history of Earth is not known in detail anyway for quantitative modeling of impact degassing as a function of time and its contribution to the atmosphere. Another

complicating factor is that giant impacts could also partially or completely erode the atmosphere, depending on the size of the giant impact (Ahrens, 1993; Walker, 1986). A simplified summary is that accretion of small planetesimals is likely to cause shock degassing, adding volatiles to the terrestrial atmosphere (i.e., coaccretion of the atmosphere and Earth), whereas impact of giant planetesimals is likely to cause both devolatilization of the planetesimal and erosion of the existing terrestrial atmosphere, with the net effect being loss (or blow off) of the terrestrial atmosphere. The critical size for blowing off 50% of Earth's atmosphere is roughly a lunar-size planetesimal (Ahrens, 1993; Ahrens et al., 2004). Hence, Earth likely lost its early atmosphere repeatedly. The last giant impacts that drove off the atmosphere would be the beginning point for terrestrial atmosphere formation from mantle degassing and impact degassing.

Although impact degassing (also termed accretion degassing) is a possibility, direct evidence for it is not available. Often, it is when data cannot be explained by mantle degassing, accretion degassing is invoked. The case for Ne is an example.  $^{20}\text{Ne}/^{22}\text{Ne}$  in air is 9.80, very different from the ratio in Earth's mantle ( $\geq 13.0$ ). That can be explained by either isotopic fractionation due to the hydrodynamic escape of mantle-degassed atmospheric Ne or mixing between mantle-degassed Ne and an extraterrestrial contribution (Marty, 1989). However, with independent estimation of Ne in UPM, the amount of Ne in UPM is not enough to provide atmospheric Ne, let alone providing extra Ne to account for the hydrodynamic Ne loss. Hence, the different  $^{20}\text{Ne}/^{22}\text{Ne}$  isotope ratio in air and mantle and the deficiency of mantle Ne together offer strong evidence for extraterrestrial source of Ne due to impact degassing in early Earth history and continuously after Earth formation.

#### 6.2.4.3.2 Cometary injection

Cometary injection of volatiles is a special category of impact (or accretion) degassing. Unlike asteroids, comets are mostly made of volatiles, especially H<sub>2</sub>O. Because the isotopic compositions of some comets have been determined recently, the data have played a main role in discussing possible contributions by comets. Lunar impact records indicate heavy bombardment of lunar surface between 4.5 and 3.8 Ga (Chapman et al., 2007; Le Feuvre and Wieczorek, 2011; Tera et al., 1974). Chyba (1987) used a mass-scaling law to scale the lunar impact records to estimate impact bombardment of the early Earth and concluded that all ocean water could be delivered during such bombardments if comets accounted for about 10% or greater of the impact mass. This argument is a possibility argument, without direct evidence (on the other hand, mantle degassing can be observed). Nonetheless, for some time, there was no direct argument against the claim either, until Balsiger et al. (1995) and Meier et al. (1998) reported  $^2\text{H}/^1\text{H}$  ratios in comets to be about two times the ratio in ocean water, which allowed preliminary evaluation of the cometary injection hypothesis. If ocean water is treated as a mixture of mantle H<sub>2</sub>O (since mantle degassing is ubiquitous) and cometary H<sub>2</sub>O, assuming no  $^2\text{H}/^1\text{H}$  isotopic fractionation during mantle degassing, cometary contribution to ocean water would be about 7% (Dauphas et al., 2000; Zhang, 2002). If  $^2\text{H}/^1\text{H}$  fractionation factor between water vapor and magma is

assumed to be 1.03 (Dobson et al., 1989), cometary contribution would be 4–5%. Marty and Meibom (2007) placed an even more stringent limit of <1% on cometary contribution to ocean water. Hutsemekers et al. (2009) used nitrogen isotope ratios to conclude that no more than a few percent of Earth's water can be attributed to comets. However, recently, Hartogh et al. (2011) discovered that a Jupiter-family comet has ocean-like  $^2\text{H}/^1\text{H}$  ratio, reviving the possibility that Jupiter-family comets can be major contributors of ocean water.

Possible cometary contribution to N<sub>2</sub> in air has also been discussed (Hutsemekers et al., 2009).  $^{15}\text{N}/^{14}\text{N}$  ratio in air N<sub>2</sub> is 0.003676, similar to 0.00364 in mantle N<sub>2</sub> as reported by Marty and Humbert (1997), and similar to the chondritic ratio (e.g.,  $^{15}\text{N}/^{14}\text{N}$  in enstatite chondrite is 0.00355, only 3.5% lower than that in air; Pepin, 1991). On the other hand,  $^{15}\text{N}/^{14}\text{N}$  ratio in comets is 0.00677 (Hutsemekers et al., 2009), about two times that in air N<sub>2</sub>, and that in Jupiter is 0.0023 (Meibom et al., 2007; Owen et al., 2001). Hence, contribution by comets to air N<sub>2</sub> is negligible. Furthermore, mass balance calculations based on N<sub>2</sub> content in UPM, DMM, and atmosphere show that all atmospheric N<sub>2</sub> can be well accounted for in the context of closed-system degassing, needing little if any extraterrestrial N<sub>2</sub>.

Holland et al. (2009) speculated that cometary injection might have supplied a significant fraction of Kr and Xe in air. It is difficult to evaluate the claim at the present time.

## 6.2.5 Discussion

### 6.2.5.1 Where Is the Primitive Undegassed Mantle?

K-Ar systematics shows that  $(49 \pm 12)\%$  of the whole mantle is not degassed, at least in terms of  $^{40}\text{Ar}$ . The estimate is based on K concentration in BSE and  $^{40}\text{Ar}$  in AOC, all of which are well constrained. The estimate is used to construct mass balance argument to infer volatile budget of various reservoirs. However, the truly primitive undegassed mantle does not seem to be sampled by any erupted basalt. OIB, including those with low  $^4\text{He}/^3\text{He}$  and  $^{21}\text{Ne}/^{22}\text{Ne}$  ratios, has DMM signatures in terms of  $^{143}\text{Nd}/^{144}\text{Nd}$  and  $^{87}\text{Sr}/^{86}\text{Sr}$  ratios. Is it reasonable to assume decoupling between degassing and depletion and use the least-radiogenic OIB in terms of  $^4\text{He}/^3\text{He}$ ,  $^{21}\text{Ne}/^{22}\text{Ne}$ ,  $^{40}\text{Ar}/^{36}\text{Ar}$ , and  $^{129}\text{Xe}/^{130}\text{Xe}$  ratios to represent the primitive undegassed mantle regardless of the Sr-Nd isotope ratios? The fact that there is also a MORB–Azores–Reunion–Kerguelen trend toward UPM suggests that the lowest  $^4\text{He}/^3\text{He}$  OIB sources are still possible candidate for UPM.

Because the lower mantle has never been sampled, it is certainly possible that UPM physically lies somewhere but hidden in the lower mantle. However, mantle convection models do not support the presence of about half of the mantle being primitive (van Keken and Ballentine, 1999; van Keken et al., 2002). Furthermore, UPM is a hypothetical construct and does not have to be physically present as a single continuous reservoir. As discussed earlier, it might be that every part of the mantle is degassed to some degree. Hence, every part of the mantle may be regarded to be a mixture of the DMM end-member and UPM end-member (e.g., Figure 6), although a large part of the mantle is almost pure DMM. In this way, it is

possible that UPM is present as a fraction of many parts of the mantle, but not as a pure physical entity. That is, there does not have to be a large and pure UPM. If so, the mass fraction of UPM does not have to be the same 49% for gases other than  $^{40}\text{Ar}$ . In this scenario, the undegassed mantle and undepleted mantle do not have to be the same. On the other hand, the estimated mass fraction of degassed mantle (51%) is similar to that of depleted mantle (50%) by Hofmann (see Chapter 3.3), supporting that DMM and UPM are a real physical entity.

#### 6.2.5.2 Paradigm Shift from the Assumption of Closed-System Degassing to Open-System Degassing

Degassing models or atmosphere evolution models before 1980 are mostly rudimentary due to lack of data. In the 1980s and 1990s, various highly quantitative degassing models were developed, mostly assuming closed-system degassing (see section on degassing models), meaning that mantle degassing and atmosphere formation were essentially equivalent. Degassing models adopting the closed-system degassing assumption can use constraints from atmospheric inventory and isotopic ratios as major constraints so that the models are fairly well constrained, making such models highly sophisticated. However, some authors argued for the importance of impact degassing (e.g., Lange and Ahrens, 1982; Lange et al., 1985), but it did not deter the closed-system degassing models, especially because giant impacts can also erode atmospheres (e.g., review by Ahrens, 1993) to set the initial point for closed-system mantle degassing. Furthermore, based on Ne isotopes in air and in mantle-derived rocks, Marty (1989) suggested that in addition to mantle degassing, an extraterrestrial source is also important for atmosphere formation. However, Ne isotope data may also be explained by the escape of air Ne (such as impact erosion or hydrodynamic escape). Some authors (e.g., Chyba, 1987) hypothesized that cometary injection is a major source for ocean water. Because that was a possibility argument without actual geochemical data to support it, the hypothesis did not gain a lot of support among solid earth geochemists, and it quickly faded away when  $^2\text{H}/^1\text{H}$  ratio in comets was found to be too high for ocean water (e.g., Balsiger et al., 1995; Meier et al., 1998).

Now, with many new data available, the case for open-system degassing is strong, and it is time for a paradigm shift from closed-system degassing to open-system degassing (in addition to hydrodynamic or gradual escape from air), at least for some gas species. The evidence for open-system degassing includes the following:

1. The amount of  $^{20}\text{Ne}$ ,  $^{21}\text{Ne}$ , and  $^{22}\text{Ne}$  in the primordial mantle is not enough to supply Ne in air. Furthermore, nonradiogenic Ne isotope ratio ( $^{20}\text{Ne}/^{22}\text{Ne}$ ) in mantle-derived rocks is different from that in air. Explaining the difference by hydrodynamic escape encounters the difficulty that there is not enough Ne in the primordial mantle to supply air Ne.
2. The amount of  $^{36}\text{Ar}$  in the primordial mantle does not seem to be enough to supply  $^{36}\text{Ar}$  in air. On the other hand, there is still other possibility to explain this (e.g., some OIBs have low  $^{40}\text{Ar}/^{36}\text{Ar}$  even after correction of atmospheric contamination).

3. Nonradiogenic Xe and Kr isotopes in well gases are different from those in air, indicating either hydrodynamic escape or an extraterrestrial source.
4.  $\text{H}_2\text{O}$  concentration in the primordial mantle (estimated from  $\text{H}_2\text{O}/\text{Ce}$  ratio) is not enough to provide all ocean water.

The earlier mentioned lines of evidence, taken together, are strong and indicate that it is time for a paradigm shift from closed-system degassing to open-system degassing in modeling atmosphere evolution and mantle degassing. With such a paradigm shift, atmosphere inventory and isotopes cannot be used to constrain mantle degassing models. One must use only inventories and isotopes of DMM and UPM to constrain such models. In the closed-system degassing models, Xe, Ar, and He systems provided the most constraints. However, for future modeling using open-system degassing, it appears that He and Ne would provide the best and internally consistent constraints.

#### 6.2.5.3 Recycling from Surface to the Mantle and Volatile Fluxes from the Core

When choosing noble gas isotope ratios in DMM, effort was made to remove the effect of recent and ancient atmospheric contamination, which means that if there were recycled noble gases in DMM, its effect has been removed. For example, recycling might have brought surface Ne (with low  $^{20}\text{Ne}/^{22}\text{Ne}$  ratio) back into DMM, which would have lowered the  $^{20}\text{Ne}/^{22}\text{Ne}$  ratio in DMM. However, when data are interpreted, the  $^{20}\text{Ne}/^{22}\text{Ne}$  ratio is assumed to be the extreme value, such as 13.0 or 13.8. The  $^{21}\text{Ne}/^{22}\text{Ne}$  ratio in the mantle can be corrected fairly reliably to  $^{20}\text{Ne}/^{22}\text{Ne}=13.0$ . The  $^{40}\text{Ar}/^{36}\text{Ar}$ ,  $^{129}\text{Xe}/^{130}\text{Xe}$ , and  $^{136}\text{Xe}/^{130}\text{Xe}$  ratios are also roughly estimated at  $^{20}\text{Ne}/^{22}\text{Ne}=13.0$  from mixing trends. Therefore, any recycled component has been corrected by this procedure (albeit imperfectly for Ar and Xe isotopes), and models using these isotope ratios cannot separately treat recycling. The correction procedure does show that contamination either in the lab or by air during the eruption process or by recycled materials into the mantle can easily account for  $\geq 50\%$  of nonradioactive gases measured in mantle rocks. For example, assuming true mantle  $^{20}\text{Ne}/^{22}\text{Ne}$  is 13.0, any mantle rock with  $^{20}\text{Ne}/^{22}\text{Ne} \leq 11.4$  means more than 50% contamination in terms of  $^{22}\text{Ne}$  (either recently or by recycled materials). If the ratio is  $\leq 10.1$ , then more than 90% of  $^{22}\text{Ne}$  is due to contamination. For Ar, if  $^{40}\text{Ar}/^{36}\text{Ar}$  in DMM is taken to be 35 000, any MORB with  $^{40}\text{Ar}/^{36}\text{Ar} \leq 645$  means that more than 99% of  $^{36}\text{Ar}$  is from air contamination.

On the other hand, for the major gases,  $\text{CO}_2$ ,  $\text{N}_2$ , and  $\text{H}_2\text{O}$ , no correction against surface contamination can be readily made, and the recycling effect must be considered in interpretation and modeling. Zhang and Zindler (1993) discussed the importance of recycling for the major gases and explicitly included the effect of recycling in modeling  $\text{CO}_2$  and  $\text{N}_2$  degassing. If recycling of the major volatiles is accompanied by recycling of Ne, it may be useful to infer relevant ratios such as the  $\text{CO}_2/\text{He}$  ratio at  $^{20}\text{Ne}/^{22}\text{Ne}=13.0$  so as to remove the effect of recycling on carbon to assess the true mantle ratio of  $\text{CO}_2/\text{He}$ . Knowing the true mantle ratios versus the uncorrected ratios, the effect of recycling can be assessed independently. This would improve one's understanding of the evolution of the major volatiles.

Hirschmann (2006) and Dasgupta and Hirschmann (2010) further discussed H<sub>2</sub>O and CO<sub>2</sub> global cycles between the surface and deep Earth. Hayden and Watson (2008) proposed that carbon from the core might have ‘buffered’ carbon concentration in the mantle. This core flux has not been modeled quantitatively because the characteristics (e.g., isotope ratios) of the components from the core are not known. The extremely high concentration of CO<sub>2</sub> in UPM obtained in Section 6.2.3.8 is unexpected and deserves further investigation.

#### 6.2.5.4 Updating Models on Mantle Degassing, Recycling, and Atmosphere Evolution

No existing degassing and atmosphere evolution models are consistent with all data currently available (Section 6.2.3). Hence, there is a great need to develop new mantle degassing and atmosphere evolution models. In future models, the possibility that the atmosphere contains initial gases (accretion degassing or after impact erosion) or an extraterrestrial source is one issue to address. To model CO<sub>2</sub> degassing and evolution, contribution from the outer core needs to be estimated. In developing mantle degassing models, it is necessary to evaluate carefully the various input data, use only constraints obtained from the mantle, and avoid using constraints based on atmosphere budget assuming closed system (but <sup>40</sup>Ar in air can still be used as a constraint). The important constraints include isotope ratios in different mantle reservoirs and the present-day degassing rates from the mantle.

### 6.2.6 Conclusions and Outlook

#### 6.2.6.1 What Are Known About Earth Degassing?

1. The degassing of Earth’s mantle has contributed significantly to the atmosphere and has extensively depleted volatile contents in the degassed mantle.
2. MORB mantle is relatively uniform and is highly degassed. Mantle sources sampled by OIBs are less degassed. <sup>4</sup>He/<sup>3</sup>He and contamination-corrected <sup>21</sup>Ne/<sup>22</sup>Ne ratios from mantle-derived samples form a well-correlated ‘mantle array,’ similar to the mantle array of Sr–Nd isotopes. The OIB mantle sources seem to have been degassed to various degrees or can be viewed as mixtures of a highly degassed mantle and primitive undegassed mantle, as indicated by the large range of <sup>4</sup>He/<sup>3</sup>He and contamination-corrected <sup>21</sup>Ne/<sup>22</sup>Ne ratios. There is self-consistency in the behavior of noble gas isotopes (e.g., more radiogenic in MORB and less radiogenic in many OIBs). HIG samples are the least radiogenic in terms of <sup>4</sup>He/<sup>3</sup>He, <sup>21</sup>Ne/<sup>22</sup>Ne, and Ar and Xe isotopes after correcting for atmosphere contamination.
3. If the variably degassed mantle reservoirs are ‘decomposed’ into degassed and undegassed end-members (the undegassed end-member may not be a physically continuous entity), the mass of the degassed mantle (DMM) is (51 ± 12)% of the whole mantle and that of the primitive undegassed mantle (UPM) accounts for (49 ± 12)% of the whole mantle in terms of <sup>40</sup>Ar. It is likely that the same mass fractions apply to <sup>36</sup>Ar and other noble gases.
4. The degassed mantle end-member (DMM) has been degassed to very high degree using data corrected for contamination and recycling. For the nonradiogenic noble

gases, the degrees of degassing are >99%. For the radiogenic noble gases, the degrees of degassing depend on the half-lives of the parents and are typically >90%.

5. Based on Xe isotopes, mantle degassing must be very effective during early Earth evolution. MORB mantle and OIB mantle have not mixed well since about 4.4 Ga. Based on He isotopes, mantle degassing is still continuing.
6. Mantle degassing is best described to be solubility-controlled.
7. Some gases in the atmosphere are not entirely from mantle degassing. The lower <sup>20</sup>Ne/<sup>22</sup>Ne ratio in air than in the mantle and the high amount of Ne in air demand nonmantle contributions for Ne. For <sup>36</sup>Ar, the lower <sup>40</sup>Ar/<sup>36</sup>Ar ratio inferred for AOC+DMM using mass balance than the least-radiogenic OIB samples after using <sup>20</sup>Ne/<sup>22</sup>Ne to remove air contamination can be explained by nonmantle <sup>36</sup>Ar in air. Kr and Xe isotopic measurements in well gases also support that Kr and Xe in air are not entirely from mantle degassing. Hence, atmospheric evolution is more than the simple complementary of mantle degassing.

#### 6.2.6.2 Uncertainties and Paradoxes

1. Even with a huge database on various volatile components, especially noble gas isotopes, a comprehensive understanding of Earth’s degassing history is still elusive. In fact, no single proposed degassing model in the literature is consistent with all observations. For example, to explain the different <sup>20</sup>Ne/<sup>22</sup>Ne ratios between air and mantle, one must consider both (1) degassing and (2) extraterrestrial or initial Ne in air.
2. Least-radiogenic noble gas isotope ratios in OIB mantle are associated with depleted Sr–Nd–Hf–Os–Pb isotope ratios. That is, there does not seem to be consistency between mantle degassing and mantle depletion.
3. There are numerous old and new paradoxes in noble gas budgets and isotopes, as well as in H<sub>2</sub>O and CO<sub>2</sub>. The newly identified paradoxes in this chapter include insufficient Ne, <sup>36</sup>Ar, and H<sub>2</sub>O in the mantle to supply these volatiles in the atmosphere and extremely high CO<sub>2</sub> concentration in UPM compared to AOC+DMM. The former may be resolved by allowing nonmantle sources to the atmosphere, and the latter may be explained by carbon flux from the outer core to the mantle.

#### 6.2.6.3 Key Measurements That Are Needed

1. Simultaneous measurement of Ne isotope ratios and all other noble gas isotope ratios (and Sr–Nd isotope ratios) in rocks with very low <sup>4</sup>He/<sup>3</sup>He (as low as 14 300) in early Tertiary Iceland plume rocks and other low <sup>4</sup>He/<sup>3</sup>He rocks will be key to pin down the isotopic signature of the least-radiogenic OIB mantle.
2. There are samples with very low <sup>40</sup>Ar/<sup>36</sup>Ar ratios at high <sup>20</sup>Ne/<sup>22</sup>Ne (e.g., there is one point with <sup>20</sup>Ne/<sup>22</sup>Ne = 12.1 and <sup>40</sup>Ar/<sup>36</sup>Ar = 425; Valbracht et al., 1997). These samples need to be investigated systematically to test whether they are unusual measurements or whether they represent the

- true UPM end-member. For example, if they represent the UPM end-member, Ar paradox would disappear.
3. Even though Ne isotope data in mantle-derived rocks are abundant and have been instrumental in pinning down the true (uncontaminated) isotope ratios of other gases, it is still necessary to resolve the uncertainty on whether the primordial  $^{20}\text{Ne}/^{22}\text{Ne}$  ratio is 13.8 or 13.0. There does not seem to be an easy way to resolve this except by high-quality measurements of many more basalt samples.
  4. Caffee et al. (1999) showed that nonradiogenic Xe isotope ratios in well gases are different from those in air, and Holland et al. (2009) showed the same for nonradiogenic Kr isotopes. It will be critical to accurately determine these isotopes in mantle-derived rocks to a similar precision as in well gases. If the nonradiogenic Xe isotopes in mantle-derived rocks can be resolved to be different from air Xe, the true radiogenic Xe isotope ratios may be estimated using the same approach as the Ne isotopic system (e.g., Figure 5). On the other hand, if nonradiogenic Xe isotopes in mantle-derived rocks are the same as air Xe, that would also significantly constrain mantle degassing and atmosphere evolution models.
  5. In order to address the importance of recycling of carbon to the mantle, the measurement of  $\text{CO}_2/^{3}\text{He}$  and  $\text{CO}_2/^{4}\text{He}$  ratios in mantle-derived rocks simultaneously with the  $^{20}\text{Ne}/^{22}\text{Ne}$  ratio would allow constraining the uncontaminated  $\text{CO}_2/\text{He}$  ratio in different mantle reservoirs.
  6. Best constraints will come from simultaneous and high-quality measurements of all noble gas isotope ratios and concentrations, all major volatile concentrations and isotope ratios, and Sr-Nd isotope ratios in well-chosen suites of rocks, such as previously done on the popping rocks. Candidates are submarine HIG basalts, as well as suites in the MORB-Azores-Reunion-Kerguelen trend in Figure 4.

## Acknowledgment

The author thanks Bernard Marty and an anonymous reviewer for constructive reviews and David Graham and Jie Li for discussion. This research is partially supported by NASA grant NNX10AH74G and NSF grants EAR-0838127 and EAR-1019440.

## References

- Ahrens TJ (1993) Impact erosion of terrestrial planetary atmospheres. *Annual Review of Earth and Planetary Sciences* 21: 525–555.
- Ahrens TJ, Shen AH, and Ni S (2004) Giant impact induced atmospheric blow-off. In: *Shock Compression of Condensed Matter, Proceedings*, pp.1419–1422.
- Albarede F (1998) Time-dependent models of U–Th–He and K–Ar evolution and the layering of mantle convection. *Chemical Geology* 145: 413–429.
- Albarede F (2008) Rogue mantle helium and neon. *Science* 319: 943–945.
- Allegre CJ, Manhes G, and Gopel C (1995a) The age of the Earth. *Geochimica et Cosmochimica Acta* 59: 1445–1456.
- Allegre CJ, Manhes G, and Gopel C (2008) The major differentiation of the Earth at 4.45 Ga. *Earth and Planetary Science Letters* 267: 386–398.
- Allegre CJ, Poirier J-P, Humler E, and Hofmann AW (1995b) The chemical composition of the earth. *Earth and Planetary Science Letters* 134: 515–526.
- Allegre CJ, Staudacher T, and Sarda P (1986/87) Rare gas systematics: Formation of the atmosphere, evolution and structure of the Earth's mantle. *Earth and Planetary Science Letters* 81: 127–150.
- Allegre CJ, Staudacher T, Sarda P, and Kurz M (1983) Constraints on evolution of Earth's mantle from rare gas systematics. *Nature* 303: 762–766.
- Anders E and Grevesse N (1989) Abundances of the elements: Meteoritic and solar. *Geochimica et Cosmochimica Acta* 197–214.
- Anderson DL (1998a) The helium paradoxes. *Proceedings of the National Academy of Sciences* 95: 4822–4827.
- Anderson DL (1998b) A model to explain the various paradoxes associated with mantle noble gas geochemistry. *Proceedings of the National Academy of Sciences* 95: 9087–9092.
- Arevalo R, McDonough WF, and Luong M (2009) The K/U ratio of the silicate Earth: Insights into mantle composition, structure and thermal evolution. *Earth and Planetary Science Letters* 278: 361–369.
- Ballentine CJ, Marty B, Lollar BS, and Cassidy M (2005) Neon isotopes constrain convection and volatile origin in the Earth's mantle. *Nature* 433: 33–38.
- Balsiger H, Altwein K, and Geiss J (1995) D/H and  $^{18}\text{O}/^{16}\text{O}$  ratio in the hydronium ion and in neutral water from in situ ion measurements in comet Halley. *Journal of Geophysical Research* 100: 5827–5834.
- Baxter EF, Asimow PD, and Farley KA (2007) Grain boundary partitioning of Ar and He. *Geochimica et Cosmochimica Acta* 71: 434–451.
- Behrens H (2010) Noble gas diffusion in silicate glasses and melts. *Reviews in Mineralogy and Geochemistry* 72: 227–267.
- Bender ML, Barnett B, Dreyfus G, Jouzel J, and Porcelli D (2008) The contemporary degassing rate of  $^{40}\text{Ar}$  from the solid Earth. *Proceedings of the National Academy of Sciences* 105: 8232–8237.
- Bianchi D, Sarmiento JL, Gnanesikan A, Key RM, Schlosser P, and Newton R (2010) Low helium flux from the mantle inferred from simulations of oceanic helium isotope data. *Earth and Planetary Science Letters* 297: 379–386.
- Bieri R, Koide M, and Goldberg ED (1964) Noble gases in sea water. *Science* 146: 1035–1037.
- Black DC and Pepin RO (1969) Trapped neon in meteorites – II. *Earth and Planetary Science Letters* 6: 395–405.
- Blank JG, Stolper EM, and Carroll MR (1993) Solubilities of carbon dioxide and water in rhyolitic melt at 850 °C and 750 bars. *Earth and Planetary Science Letters* 119: 27–36.
- Boslough MB, Ahrens TJ, Vizgirda J, Becker RH, and Epstein S (1982) Shock-induced devolatilization of calcite. *Earth and Planetary Science Letters* 61: 166–170.
- Boyet M and Carlson RW (2005)  $^{142}\text{Nd}$  evidence for early (>4.53 Ga) global differentiation of the silicate Earth. *Science* 309: 576–581.
- Boyet M and Carlson RW (2006) A new geochemical model for the Earth's mantle inferred from  $^{146}\text{Sm}–^{142}\text{Nd}$  systematics. *Earth and Planetary Science Letters* 250: 254–268.
- Brandon AD, Graham DW, Waught T, and Gautason B (2007)  $^{186}\text{Os}$  and  $^{187}\text{Os}$  enrichments and high- $^{3}\text{He}/^{4}\text{He}$  sources in the Earth's mantle: Evidence from Icelandic picrites. *Geochimica et Cosmochimica Acta* 71: 4570–4591.
- Brandon AD, Norman MD, Walker RJ, and Morgan JW (1999)  $^{186}\text{Os}–^{187}\text{Os}$  systematics of Hawaiian picrites. *Earth and Planetary Science Letters* 174: 25–42.
- Brandon AD, Walker RJ, Morgan JW, Norman MD, and Prihard HM (1998) Coupled  $^{186}\text{Os}$  and  $^{187}\text{Os}$  evidence for core–mantle interaction. *Science* 280: 1570–1573.
- Broecker WS and Peng T (1982) *Tracers in the Sea*. Palisades, NY: Lamont-Doherty Geological Observatory.
- Brooker RA, Du Z, Blundy JD, et al. (2003) The 'zero charge' partitioning behavior of noble gases during mantle melting. *Nature* 423: 738–741.
- Brown H (1952) Rare gases and formation of the earth's atmosphere. In: Kuiper GP (ed.) *The Atmospheres of the Earth and Planets*, pp. 258–266. Chicago: University of Chicago Press.
- Burnard P, Graham D, and Turner G (1997) Vesicle-specific noble gas analyses of 'popping rock': Implications for primordial noble gases in Earth. *Science* 276: 568–571.
- Caffee MW, Hudson GB, Veloski C, Huss GR, Alexander EC, and Chivas AR (1999) Primordial noble gases from Earth's mantle: Identification of a primitive volatile component. *Science* 285: 2115–2118.
- Cardogan PH (1977) Palaeoatmospheric argon in Rhynie chert. *Nature* 268: 38–41.
- Cartigny P, Pineau F, Aubaud C, and Javoy M (2008) Towards a consistent mantle carbon flux estimate: Insight from volatile systematics ( $\text{H}_2\text{O/Ce}$ ,  $\delta\text{D}$ ,  $\text{CO}_2/\text{Nb}$ ) in the North Atlantic mantle (14°N and 34°N). *Earth and Planetary Science Letters* 265: 672–685.
- Chapman CR, Cohen BA, and Grinspoon DH (2007) What are the real constraints on the existence and magnitude of the late heavy bombardment? *Icarus* 189: 233–245.
- Chen Y, Zhang Y, Graham D, Su SG, and Deng JF (2007) Geochemistry of Cenozoic basalts and mantle xenoliths in Northeast China. *Lithos* 96: 108–126.

- Chyba CF (1987) The cometary contribution to the oceans of primitive Earth. *Nature* 330: 632–635.
- Clarke WB, Beg MA, and Craig H (1969) Excess  $^3\text{He}$  in the sea: Evidence for terrestrial primordial helium. *Earth and Planetary Science Letters* 6: 213–220.
- Clayton RN (1981) Isotopic variations in primitive meteorites. *Philosophical Transactions of the Royal Society of London A* 303: 339–349.
- Corgne A, Keshav S, Fei Y, and McDonough WF (2007) How much potassium is in the Earth's core? New insights from partitioning experiments. *Earth and Planetary Science Letters* 256: 567–576.
- Craig H, Clarke WB, and Beg MA (1975) Excess  $^3\text{He}$  in deep water on the East Pacific Rise. *Earth and Planetary Science Letters* 26: 125–132.
- Craig H and Lupton JE (1976) Primordial neon, helium and hydrogen in oceanic basalts. *Earth and Planetary Science Letters* 31: 369–385.
- Crisp JA (1984) Rates of magma emplacement and volcanic output. *Journal of Volcanology and Geothermal Research* 20: 177–211.
- Dasgupta R and Hirschmann MM (2010) The deep carbon cycle and melting in Earth's interior. *Earth and Planetary Science Letters* 298: 1–13.
- Dasgupta R and Walker D (2008) Carbon solubility in core melts in a shallow magma ocean environment and distribution of carbon between the Earth's core and the mantle. *Geochimica et Cosmochimica Acta* 72: 4627–4641.
- Dauphas N (2003) The dual origin of the terrestrial atmosphere. *Icarus* 165: 326–339.
- Dauphas N, Robert F, and Marty B (2000) The late asteroidal and cometary bombardment of Earth as recorded in water deuterium to protium ratio. *Icarus* 148: 508–512.
- Deruelle B, Dreibus G, and Jambon A (1992) Iodine abundances in oceanic basalts: Implications for Earth dynamics. *Earth and Planetary Science Letters* 108: 217–227.
- Dixon JE (1997) Degassing of alkalic basalts. *American Mineralogist* 82: 368–378.
- Dixon JE, Honda M, McDougall I, Campbell IH, and Sigurdsson I (2000) Preservation of near-solar neon isotopic ratios in Icelandic basalts. *Earth and Planetary Science Letters* 180: 309–324.
- Dixon JE, Stolper EM, and Delaney JR (1988) Infrared spectroscopic measurements of  $\text{CO}_2$  and  $\text{H}_2\text{O}$  in Juan de Fuca Ridge basaltic glasses. *Earth and Planetary Science Letters* 90: 87–104.
- Dixon JE, Stolper EM, and Holloway JR (1995) An experimental study of water and carbon dioxide solubilities in mid-ocean ridge basaltic liquids. Part I: Calibration and solubility models. *Journal of Petrology* 36: 1607–1631.
- Dobson PF, Epstein S, and Stolper EM (1989) Hydrogen isotope fractionation between coexisting vapor and silicate glasses and melts at low pressure. *Geochimica et Cosmochimica Acta* 53: 2723–2730.
- Drever JI (1997) *The Geochemistry of Natural Waters*. New Jersey: Prentice Hall.
- Ellam RM and Stuart FM (2004) Coherent He–Nd–Sr isotopic trends in high  $^3\text{He}/^4\text{He}$  basalts: Implications for a common reservoir, mantle heterogeneity and convection. *Earth and Planetary Science Letters* 228: 511–523.
- Farley KA (1995) Cenozoic variations in the flux of interplanetary dust recorded by  $^3\text{He}$  in a deep-sea sediment. *Nature* 376: 153–156.
- Fields PR, Friedman AM, Milsted J, Lerner J, Stevens CM, and Metta D (1969) Decay properties of plutonium-244, and comments on its existence in nature. *Nature* 212: 131–134.
- Foulger GR (2005) Mantle plumes: Why the current skepticism? *Chinese Science Bulletin* 50: 1555–1560.
- Frost DJ and McCammon CA (2008) The redox state of Earth's mantle. *Annual Review of Earth and Planetary Science* 36: 389–420.
- Furi E, Hilton DR, Halldorsson SA, et al. (2010) Apparent decoupling of He and Ne isotope systematics of the Icelandic mantle: The role of He depletion, melt mixing, degassing fractionation and air interaction. *Geochimica et Cosmochimica Acta* 74: 3307–3332.
- Gazis C and Ahrens TJ (1991) Solution and shock-induced exsolution of argon in vitreous carbon. *Earth and Planetary Science Letters* 104: 337–349.
- Gonnermann HM and Mukhopadhyay S (2007) Non-equilibrium degassing and a primordial source for helium in ocean-island volcanism. *Nature* 449: 1037–1040.
- Gonnermann HM and Mukhopadhyay S (2009) Preserving noble gases in a convecting mantle. *Nature* 459: 560–564.
- Grady MM, Wright IP, Carr LP, and Pillinger CT (1986) Compositional differences in enstatite chondrites based on carbon and nitrogen stable isotope measurements. *Geochimica et Cosmochimica Acta* 50: 2799–2813.
- Graham DW (2002) Noble gas isotope geochemistry of mid-ocean ridge and ocean island basalts: Characterization of mantle source reservoirs. *Reviews in Mineralogy and Geochemistry* 47: 247–317.
- Graham DW, Larsen LM, Hanan BB, Storey M, Pedersen AK, and Lupton JE (1998) Helium isotope composition of the early Iceland mantle plume inferred from the Tertiary picrites of West Greenland. *Earth and Planetary Science Letters* 160: 241–255.
- Hanyu T, Dunai TJ, Davis GR, Kaneoka I, Nohda S, and Uto K (2001) Noble gas study of the Reunion hotspot: Evidence for distinct less-degassed mantle sources. *Earth and Planetary Science Letters* 193: 83–98.
- Hanyu T, Johnson KTM, Hirano N, and Ren ZY (2007) Noble gas and geochronology study of the Hana Ridge, Haleakala volcano, Hawaii; implications to the temporal change of magma source and the structural evolution of the submarine ridge. *Chemical Geology* 238: 1–18.
- Hart R, Hogan L, and Dymond J (1985) The closed-system approximation for evolution of argon and helium in the mantle, crust and atmosphere. *Chemical Geology* 52: 45–73.
- Hart SR and Zindler A (1989) Isotope fractionation laws: A test using calcium. *International Journal of Mass Spectrometry and Ion Processes* 89: 287–301.
- Hartogh P, Lis DC, Bockelee-Morvan D, et al. (2011) Ocean-like water in the Jupiter-family comet 103P/Hartley 2. *Nature* 478: 218–220.
- Hawkesworth CJ, Dhuime B, Peitranik AB, Cawood PA, Kemp AIS, and Storey CD (2010) The generation and evolution of the continental crust. *Journal of the Geological Society of London* 167: 229–248.
- Hayden LA and Watson EB (2008) Grain boundary mobility of carbon in Earth's mantle: A possible carbon flux from the core. *Proceedings of the National Academy of Sciences* 105: 8537–8541.
- Heber VS, Brooker RA, Kelley SP, and Wood BJ (2007) Crystal-melt partitioning of noble gases (helium, neon, argon, krypton, and xenon) for olivine and clinopyroxene. *Geochimica et Cosmochimica Acta* 71: 1041–1061.
- Hekinian R, Chaigneau M, and Cheminee JL (1973) Popping rocks and lava tubes from the Mid-Atlantic Rift Valley at 36°N. *Nature* 245: 371–373.
- Helo C, Longpre MA, Shimizu N, Clague DA, and Stix J (2011) Explosive eruptions at mid-ocean ridges driven by  $\text{CO}_2$ -rich magmas. *Nature Geoscience* 4: 260–263.
- Hiess J, Condon DJ, McLean N, and Noble SR (2012)  $^{238}\text{U}/^{235}\text{U}$  systematics in terrestrial uranium-bearing minerals. *Science* 335: 1610–1614.
- Hilton DR, Gronvold K, Macpherson CG, and Castillo PR (1999) Extreme  $^3\text{He}/^4\text{He}$  ratios in Northwest Iceland: Constraining the common component in mantle plumes. *Earth and Planetary Science Letters* 173: 53–60.
- Hilton DR, Thirlwall MF, Taylor RN, Murton BJ, and Nichols A (2000) Controls on magmatic degassing along the Reykjanes Ridge with implications for the helium paradox. *Earth and Planetary Science Letters* 183: 43–50.
- Hiraga T, Anderson IM, and Kohlstedt DL (2004) Grain boundaries as reservoirs of incompatible elements in the Earth's mantle. *Nature* 427: 699–703.
- Hirschmann MM (2006) Water, melting and the deep Earth  $\text{H}_2\text{O}$  cycle. *Annual Review of Earth and Planetary Science* 34: 629–653.
- Hiyagon H, Ozima M, Marty B, Zashu S, and Sakai H (1992) Noble gases in submarine glasses from mid-oceanic ridges and Loihi seamount: Constraints on the early history of the Earth. *Geochimica et Cosmochimica Acta* 56: 1301–1316.
- Holland HD (1978) *The Chemistry of the Atmosphere and Oceans*. New York: Wiley.
- Holland G, Cassidy M, and Ballentine CJ (2009) Meteorite Kr in Earth's mantle suggests a late accretionary source for the atmosphere. *Science* 326: 1522–1525.
- Honda M and McDougall I (1998) Primordial helium and neon in the Earth – A speculation on early degassing. *Geophysical Research Letters* 25: 1951–1954.
- Honda M, McDougall I, Patterson DB, Doulgeris A, and Clague DA (1991) Possible solar noble-gas component in Hawaiian basalts. *Nature* 349: 149–151.
- Honda M, McDougall I, Patterson DB, Doulgeris A, and Clague DA (1993) Noble gases in submarine pillow glasses from Loihi and Kilauea, Hawaii: A solar component in the Earth. *Geochimica et Cosmochimica Acta* 57: 859–874.
- Honda M, Phillips D, Harris JW, and Matsumoto T (2011) He, Ne and Ar in peridotitic and eclogitic paragenesis diamonds from the Jwaneng kimberlite, Botswana – Implications for mantle evolution and diamond formation ages. *Earth and Planetary Science Letters* 301: 43–51.
- Hopp J and Trieloff M (2008) Helium deficit in high- $^3\text{He}/^4\text{He}$  parent magmas: Predegassing fractionation, not a 'helium paradox'. *Geochemistry, Geophysics, Geosystems* 9: Q03009. <http://dx.doi.org/10.1029/2007GC001833>.
- Hudson GB, Kennedy BM, Podosek FA, and Hohenberg CM (1989) The early solar system abundance of  $^{244}\text{Pu}$  as inferred from the St. Severin chondrite. In: *Proceedings of the 19th Lunar and Planetary Science Conference*, pp. 547–557.
- Hunt JM (1972) Distribution of carbon in crust of earth. *Bulletin of the American Association of Petroleum Geologists* 56: 2273–2277.
- Hunten DM, Pepin RO, and Walker JCG (1987) Mass fractionation in hydrodynamic escape. *Icarus* 69: 532–549.
- Huss GR, Lewis RS, and Hemkin S (1996) The 'normal planetary' noble gas component in primitive chondrites: Compositions, carrier, and metamorphic history. *Geochimica et Cosmochimica Acta* 60: 3311–3340.
- Hutsemekers D, Manfroid J, Jehin E, and Arpigny C (2009) New constraints on the delivery of cometary water and nitrogen to Earth from the  $^{15}\text{N}/^{14}\text{N}$  isotopic ratio. *Icarus* 204: 346–348.

- Iacono-Marziano G, Paonita A, Rizzo A, Scaillet B, and Gaillard F (2010) Noble gas solubilities in silicate melts: New experimental results and a comprehensive model of the effects of liquid composition, temperature and pressure. *Chemical Geology* 279: 145–157.
- Jackson MG, Carlson RW, Kurz MD, Kempton PD, Francis D, and Bluszta J (2010) Evidence for the survival of the oldest terrestrial mantle reservoir. *Nature* 466: 853–858.
- Jackson MG, Kurz MD, and Hart SR (2009) Helium and neon isotopes in phenocrysts from Samoan lavas: Evidence for heterogeneity in the terrestrial high  $^3\text{He}/^4\text{He}$  mantle. *Earth and Planetary Science Letters* 287: 519–528.
- Jackson MG, Kurz MD, Hart SR, and Workman RK (2007) New Samoan lavas from Ofu Island reveal a hemispherically heterogeneous high  $^3\text{He}/^4\text{He}$  mantle. *Earth and Planetary Science Letters* 264: 360–374.
- Jambon A, Weber H, and Braun O (1986) Solubility of He, Ne, Ar, Kr, and Xe in a basalt melt in the range of 1250–1600°C: Geochemical implications. *Geochimica et Cosmochimica Acta* 50: 401–408.
- Javoy M and Pineau F (1991) The volatile record of a 'popping' rock from the Mid-Atlantic Ridge at 14°N: Chemical and isotopic composition of gas trapped in the vesicles. *Earth and Planetary Science Letters* 107: 598–611.
- Javoy M, Pineau F, and Delorme H (1986) Carbon and nitrogen isotopes in the mantle. *Chemical Geology* 57: 41–62.
- Jean-Baptiste P (1992) Helium-3 distribution in the deep world ocean. In: Rozanski K (ed.) *Isotopes of Noble Gases as Tracers in Environmental Studies*, pp. 219–240. Vienna: International Atomic Energy Agency.
- Jochum KP, Hofmann AW, Ito E, Seufert HM, and White WM (1983) K, U, and Th in mid-ocean ridge basalt glasses and heat production, K/U and K/Pb in the mantle. *Nature* 306: 431–436.
- Kerridge JF (1985) Carbon, hydrogen and nitrogen in carbonaceous chondrites: Abundances and isotopic compositions in bulk samples. *Geochimica et Cosmochimica Acta* 49: 1707–1714.
- Kingsley RH, Schilling JG, Dixon JE, Swart P, Poreda RJ, and Simons K (2002) D/H ratios in basalt glasses from the Salas y Gomez mantle plume interacting with the East Pacific Rise: Water from old D-rich recycled crust or primordial water from the lower mantle? *Geochemistry, Geophysics, Geosystems* 3. <http://dx.doi.org/10.1029/2001GC000199>.
- Klein EM and Langmuir CH (1987) Global correlations of ocean ridge basalt chemistry with axial depth and crustal thickness. *Journal of Geophysical Research* 92: 8089–8115.
- Kohn SC and Grant KJ (2006) The partitioning of water between nominally anhydrous minerals and silicate melts. *Reviews in Mineralogy and Geochemistry* 62: 231–241.
- Kunz J, Staudacher T, and Allegre CJ (1998) Plutonium-fission xenon found in Earth's mantle. *Science* 280: 877–880.
- Kurz MD, Curtice J, Fornari D, Geist D, and Moreira M (2009) Primitive neon from the center of the Galapagos hotspot. *Earth and Planetary Science Letters* 286: 23–34.
- Kyser TK and O'Neil JR (1984) Hydrogen isotope systematics of submarine basalts. *Geochimica et Cosmochimica Acta* 48: 2123–2133.
- Lange MA and Ahrens TJ (1982) The evolution of an impact-generated atmosphere. *Icarus* 51: 96–120.
- Lange MA and Ahrens TJ (1986) Shock-induced CO<sub>2</sub> loss from CaCO<sub>3</sub>: Implications for early planetary atmospheres. *Earth and Planetary Science Letters* 77: 409–418.
- Lange MA, Lambert P, and Ahrens TJ (1985) Shock effects on hydrous minerals and implications for carbonaceous meteorites. *Geochimica et Cosmochimica Acta* 49: 1715–1726.
- Le Feuvre M and Wieczorek MA (2011) Nonuniform cratering of the Moon and a revised crater chronology of the inner Solar System. *Icarus* 214: 1–20.
- Lee CTA, Luffi P, Hoink T, Li J, Dasgupta R, and Hernlund J (2010) Upside-down differentiation and generation of a 'primordial' lower mantle. *Nature* 463: 930–935.
- Lee JY, Marti K, Severinghaus JP, et al. (2006) A redetermination of the isotopic abundances of atmospheric Ar. *Geochimica et Cosmochimica Acta* 70: 4507–4512.
- Lesne P, Scaillet B, Pichavant M, and Beny JM (2011a) The carbon dioxide solubility in alkali basalts: An experimental study. *Contributions to Mineralogy and Petrology* 162: 153–168.
- Lesne P, Scaillet B, Pichavant M, Iacono-Marziano G, and Beny JM (2011b) The H<sub>2</sub>O solubility of alkali basaltic melts: An experimental study. *Contributions to Mineralogy and Petrology* 162: 133–151.
- Leya I and Wieler R (1999) Nucleogenic production of Ne isotopes in Earth's crust and upper mantle induced by alpha particles from the decay of U and Th. *Journal of Geophysical Research* 104: 15439–15450.
- Libourel G, Marty B, and Humbert F (2003) Nitrogen solubility in basaltic melt. Part I. Effect of oxygen fugacity. *Geochimica et Cosmochimica Acta* 67: 4123–4135.
- Liu Y, Zhang Y, and Behrens H (2005) Solubility of H<sub>2</sub>O in rhyolitic melts at low pressures and a new empirical model for mixed H<sub>2</sub>O–CO<sub>2</sub> solubility in rhyolitic melts. *Journal of Volcanology and Geothermal Research* 143: 219–235.
- Lupton JE (1983) Terrestrial inert gases: Isotope tracer studies and clues to primordial components in the mantle. *Annual Review of Earth and Planetary Sciences* 11: 371–414.
- Mahaffy PR, Donahue TM, Atreya SK, Owen TC, and Niemann HB (1998) Galileo probe measurements of D/H and  $^3\text{He}/^4\text{He}$  in Jupiter's atmosphere. *Space Science Reviews* 84: 251–263.
- Manfroid J, Jehin E, Hutsemekers D, et al. (2009) The CN isotopic ratios in comets. *Astronomy and Astrophysics* 503: 613–624.
- Marty B (1989) Neon and xenon isotopes in MORB: Implications for the earth-atmosphere evolution. *Earth and Planetary Science Letters* 94: 45–56.
- Marty B (1995) Nitrogen content of the mantle inferred from N<sub>2</sub>–Ar correlation in oceanic basalts. *Nature* 377: 326–329.
- Marty B (2012) The origins and concentrations of water, carbon, nitrogen, and noble gases on Earth. *Earth and Planetary Science Letters* 313–314: 56–66.
- Marty B, Chaussidon M, Wiens RC, Jurewicz AJG, and Burnett DS (2011) A 15N-poor isotopic composition for the solar system as shown by genesis solar wind samples. *Science* 332: 1533–1536.
- Marty B and Dauphas N (2003) The nitrogen record of crust-mantle interaction and mantle convection from Archean to Present. *Earth and Planetary Science Letters* 206: 397–410.
- Marty B and Humbert F (1997) Nitrogen and argon isotopes in oceanic basalts. *Earth and Planetary Science Letters* 152: 101–112.
- Marty B and Meibom A (2007) Noble gas signature of the Late Heavy Bombardment in the Earth's atmosphere. *eEarth* 2: 43–49.
- Marty B and Tolstikhin IN (1998) CO<sub>2</sub> fluxes from mid-ocean ridges, arcs and plumes. *Chemical Geology* 145: 233–248.
- Marty B, Tolstikhin IN, Nivin VA, Balaganskaya EG, and Zimmermann JL (1998a) Plume-derived rare gases in 380 Ma carbonatites from the Kola region (Russia) and the argon isotopic composition in the deep mantle. *Earth and Planetary Science Letters* 164: 179–192.
- Marty B, Upton BGJ, and Ellam RM (1998b) Helium isotopes in early Tertiary basalts northeast Greenland: Evidence for 58 Ma plume activity in the North Atlantic–Iceland volcanic province. *Geology* 26: 407–410.
- Mazor E, Heymann D, and Anders E (1970) Noble gases in carbonaceous chondrites. *Geochimica et Cosmochimica Acta* 34: 781–824.
- McDonough WF and Sun S-S (1995) The composition of the Earth. *Chemical Geology* 120: 223–253.
- Meibom A, Krot AN, Robert F, et al. (2007) Nitrogen and carbon isotopic composition of the Sun inferred from a high-temperature solar nebular condensate. *The Astrophysical Journal* 656: L33–L36.
- Meier R, Owen TC, Matthews HE, et al. (1998) A determination of the HDO/H<sub>2</sub>O ratio in Comet C/1995 O1 (Hale-Bopp). *Science* 279: 842–844.
- Michael PJ (1988) The concentration, behavior and storage of H<sub>2</sub>O in the suboceanic upper mantle: Implications for mantle metasomatism. *Geochimica et Cosmochimica Acta* 52: 555–566.
- Michael PJ (1995) Regionally distinctive sources of depleted MORB: Evidence from trace elements and H<sub>2</sub>O. *Earth and Planetary Science Letters* 131: 301–320.
- Ming T and Anders E (1988) Isotopic anomalies of Ne, Xe, and C in meteorites. II. Interstellar diamond and SiC: Carriers of exotic noble gases. *Geochimica et Cosmochimica Acta* 52: 1235–1244.
- Miyazaki A, Hiroyama H, Sugiyama N, Hirose K, and Takahashi E (2004) Solubilities of nitrogen and noble gases in silicate melts under various oxygen fugacities: Implications for the origin and degassing history of nitrogen and noble gases in the Earth. *Geochimica et Cosmochimica Acta* 68: 387–401.
- Morbidelli A, Chambers J, Lunine JI, et al. (2000) Source regions and timescales for the delivery of water to Earth. *Meteoritics and Planetary Science* 35: 1309–1320.
- Moreira M and Allegre CJ (1998) Helium–neon systematics and the structure of the mantle. *Chemical Geology* 147: 53–59.
- Moreira M and Allegre CJ (2002) Rare gas systematics on Mid Atlantic Ridge (37–40°N). *Earth and Planetary Science Letters* 198: 401–416.
- Moreira M, Breddam K, Curtice J, and Kurz MD (2001) Solar neon in the Icelandic mantle: New evidence for an undegassed lower mantle. *Earth and Planetary Science Letters* 185: 15–23.
- Moreira M, Kunz J, and Allegre CJ (1998) Rare gas systematics in popping rock: Isotopic and elemental compositions in the upper mantle. *Science* 278: 1178–1181.
- Moreira M and Raquin A (2007) The origin of rare gases on Earth: The noble gas 'subduction barrier' revisited.. *C.R. Geoscience* 339: 937–945.
- Moreira M and Sarda P (2000) Noble gas constraints on degassing processes. *Earth and Planetary Science Letters* 176: 375–386.

- Moreira M, Staudacher T, Sarda P, Schilling JG, and Allegre CJ (1995) A primitive plume neon component in MORB: The Shona ridge-anomaly, South Atlantic (51–52°S). *Earth and Planetary Science Letters* 133: 367–377.
- Moreira M, Valbracht PJ, Staudacher T, and Allegre CJ (1996) Rare gas systematics in Red Sea ridge basalts. *Geophysical Research Letters* 23: 2453–2456.
- Mukhopadhyay S (2012) Early differentiation and volatile accretion recorded in deep-mantle neon and xenon. *Nature* 486: 101–104.
- Nakajima Y, Takahashi E, Suzuki T, and Funakoshi KI (2009) Carbon in the core revisited. *Physics of the Earth and Planetary Interiors* 174: 202–211.
- Niedermann S and Bach W (1998) Anomalously nucleogenic neon in North Chile Ridge basalt glasses suggesting a previously degassed mantle source. *Earth and Planetary Science Letters* 160: 447–462.
- Niu Y (1997) Mantle melting and melt extraction processes beneath ocean ridges: Evidence from abyssal peridotites. *Journal of Petrology* 38: 1047–1074.
- O'Neill HSC and Palme H (1998) Composition of the silicate earth: Implications for accretion and core formation. In: Jackson I (ed.) *The Earth's Mantle: Structure, Composition, and Evolution*, pp. 3–126. Cambridge: Cambridge University Press.
- Owen T, Mahaffy PR, Niemann HB, Atreya SK, and Wong M (2001) Protosolar nitrogen. *The Astrophysical Journal Letters* 553: L77–L79.
- Ozima M (1975) Ar isotopes and Earth–atmosphere evolution models. *Geochimica et Cosmochimica Acta* 39: 1127–1134.
- Ozima M and Podosek FA (1983) *Noble Gas Geochemistry*. Cambridge: Cambridge University Press.
- Ozima M and Podosek FA (2002) *Noble Gas Geochemistry*. Cambridge: Cambridge University Press.
- Paonita A (2005) Noble gas solubility in silicate melts: A review of experimentation and theory, and implications regarding magma degassing processes. *Annals of Geophysics* 48: 647–669.
- Parai R, Mukhopadhyay S, and Lassiter JC (2009) New constraints on the HIMU mantle from neon and helium isotopic compositions of basalts from the Cook–Austral Islands. *Earth and Planetary Science Letters* 277: 253–261.
- Patterson DB, Honda M, and McDougall I (1990) Atmospheric contamination: A possible source for heavy noble gases in basalts from Loihi Seamount, Hawaii. *Geophysical Research Letters* 17: 705–708.
- Peate DW, Baker DR, Blachert-Toft J, et al. (2003) The prinsen af Wales Bjerge Formation lavas, East Greenland: The transition from tholeiitic to alkalic magmatism during Palaeogene continental break-up. *Journal of Petrology* 44: 279–304.
- Pepin RO (1991) On the origin and early evolution of terrestrial planet atmospheres and meteoritic volatiles. *Icarus* 92: 2–79.
- Pepin RO and Phinney D (1978) Components of xenon in the solar system. Unpublished preprints.
- Pepin RO and Porcelli D (2002) Origin of noble gases in the terrestrial planets. *Reviews in Mineralogy and Geochemistry* 47: 191–246.
- Pepin RO and Porcelli D (2006) Xenon isotope systematics, giant impacts, and mantle degassing on the early Earth. *Earth and Planetary Science Letters* 250: 470–485.
- Peterson BT and DePaolo DJ (2007) Mass and composition of the continental crust estimated using the CRUST2.0 model. *Eos* 88: V33A–V1161A.
- Phinney D, Tennyson J, and Frick U (1978) Xenon in CO<sub>2</sub> well gas revisited. *Journal of Geophysical Research* 83: 2313–2319.
- Porcelli D, Ballentine CJ, and Wieller R (eds.) (2002) *Reviews in Mineralogy and Geochemistry, Vol. 47: Noble Gases in Geochemistry and Cosmochemistry*, p. 844. Washington, DC: Mineralogical Society of America.
- Porcelli D and Halliday AN (2001) The core as a possible source of mantle helium. *Earth and Planetary Science Letters* 192: 45–56.
- Porcelli D and Wasserburg GJ (1995a) Mass transfer of xenon through a steady-state upper mantle. *Geochimica et Cosmochimica Acta* 59: 1991–2007.
- Porcelli D and Wasserburg GJ (1995b) Mass transfer of helium, neon, argon, and xenon through a steady-state upper mantle. *Geochimica et Cosmochimica Acta* 59: 4921–4937.
- Poreda RJ and Farley KA (1992) Rare gases in Samoan xenoliths. *Earth and Planetary Science Letters* 113: 129–144.
- Pujol M, Marty B, and Burgess R (2011) Chondritic-like xenon trapped in Archean rocks: A possible signature of the ancient atmosphere. *Earth and Planetary Science Letters* 308: 298–306.
- Raquin A and Moreira M (2009) Atmospheric <sup>38</sup>Ar/<sup>36</sup>Ar in the mantle: Implications for the nature of the terrestrial parent bodies. *Earth and Planetary Science Letters* 287: 551–558.
- Raquin A, Moreira M, and Guillou F (2008) He, Ne and Ar systematics in single vesicles: Mantle isotopic ratios and origin of the air component in basaltic glasses. *Earth and Planetary Science Letters* 274: 142–150.
- Richard D, Marty B, Chaussidon M, and Arndt N (1996) Helium isotopic evidence for a lower mantle component in depleted Archean komatiite. *Science* 273: 93–95.
- Robert F (2003) The D/H ratio in chondrites. *Space Science Reviews* 106: 87–101.
- Rubey WW (1951) Geological history of sea water: An attempt to state the problem. *GSA Bulletin* 62: 1111–1148.
- Rubey WW (1955) Development of the hydrosphere and atmosphere, with special reference to probable composition of the early atmosphere. *GSA Special Paper* 62: 631–650.
- Saal AE, Hauri EH, Langmuir CH, and Perfit MR (2002) Vapor undersaturation in primitive mid-ocean-ridge basalt and the volatile content of Earth's upper mantle. *Nature* 419: 451–455.
- Salters VJ and Stracke A (2004) Composition of the depleted mantle. *Geochemistry, Geophysics, Geosystems* 5: Q05004.
- Sarda P and Graham D (1990) Mid-ocean ridge popping rocks: Implications for degassing at ridge crests. *Earth and Planetary Science Letters* 97: 268–289.
- Sarda P, Moreira M, and Staudacher T (1999) Argon–lead isotopic correlation in Mid-Atlantic Ridge basalts. *Science* 283: 666–668.
- Sarda P, Moreira M, Staudacher T, Schilling JG, and Allegre CJ (2000) Rare gas systematics on the southernmost Mid-Atlantic Ridge: Constraints on the lower mantle and the Dupal source. *Journal of Geophysical Research* 105: 5973–5996.
- Sarda P and Staudacher T (1991) Terrestrial primordial neon. *Nature* 352: 388.
- Sarda P, Staudacher T, and Allegre CJ (1985) <sup>40</sup>Ar/<sup>36</sup>Ar in MORB glasses: Constraints on atmosphere and mantle evolution. *Earth and Planetary Science Letters* 72: 357–375.
- Sarda P, Staudacher T, and Allegre CJ (1988) Neon isotopes in submarine basalts. *Earth and Planetary Science Letters* 91: 73–88.
- Schwartzman DW (1973) Ar degassing and the origin of the sialic crust. *Geochimica et Cosmochimica Acta* 37: 2479–2495.
- Shannon RD (1976) Revised effective ionic radii and systematic studies of interatomic distances in halides and chalcogenides. *Acta Crystallographica A32*: 751–767.
- Shaw AM, Hilton DR, Macpherson CG, and Sinton JM (2001) Nucleogenic neon in high <sup>3</sup>He/<sup>4</sup>He lavas from the Manus back-arc basin: A new perspective on He–Ne decoupling. *Earth and Planetary Science Letters* 194: 53–66.
- Soule SA, Nakata DS, Fornari DJ, Fundis AT, Perfit MR, and Kurz MD (2012) CO<sub>2</sub> variability in mid-ocean ridge basalts from syn-emplacement degassing: Constraints on eruption dynamics. *Earth and Planetary Science Letters* 327–328: 39–49.
- Starkey NA, Stuart FM, Ellam RM, Fitton JG, Basu S, and Larsen LM (2009) Helium isotopes in early Iceland plume picrites: Constraints on the composition of high <sup>3</sup>He/<sup>4</sup>He mantle. *Earth and Planetary Science Letters* 277: 91–100.
- Staudacher T (1987) Upper mantle origin for Harding County well gases. *Nature* 325: 605–607.
- Staudacher T and Allegre CJ (1982) Terrestrial xenology. *Earth and Planetary Science Letters* 60: 389–406.
- Staudacher T and Allegre CJ (1989) Noble gases in glass samples from Tahiti: Teahitia, Rocard and Mehetia. *Earth and Planetary Science Letters* 93: 210–222.
- Staudacher T, Kurz MD, and Allegre CJ (1986) New noble-gas data on glass samples from Loihi Seamount and Hualalai and on dunite samples from Loihi and Reunion Island. *Chemical Geology* 56: 193–205.
- Staudacher T, Sarda P, and Allegre CJ (1990) Noble gas systematics of Reunion Island, Indian Ocean. *Chemical Geology* 89: 1–17.
- Staudacher T, Sarda P, Richardson SH, Allegre CJ, Sagna I, and Dmitriev LV (1989) Noble gases in basalts from a Mid-Atlantic Ridge topographic high at 14°N: Geodynamic consequences. *Earth and Planetary Science Letters* 96: 119–133.
- Stolper EM (1982) The speciation of water in silicate melts. *Geochimica et Cosmochimica Acta* 46: 2609–2620.
- Stronck NA, Niedermann S, and Haase KM (2007) Neon and helium isotopes as tracers of mantle reservoirs and mantle dynamics. *Earth and Planetary Science Letters* 258: 334–344.
- Stuart FM, Lass-Evans S, Fitton JG, and Ellam RM (2003) High <sup>3</sup>He/<sup>4</sup>He ratios in picritic basalts from Baffin Island and the role of a mixed reservoir in mantle plumes. *Nature* 424: 57–59.
- Swindle TD and Podosek FA (1988) Iodine–xenon dating. In: Kerridge JF and Matthews MS (eds.) *Meteorites and the Early Solar System*, pp. 1127–1146. Tucson, AZ: University of Arizona Press.
- Tera F, Papanastassiou DA, and Wasserburg GJ (1974) Isotopic evidence for a terminal lunar cataclysm. *Earth and Planetary Science Letters* 22: 1–21.
- Tolstikhin IN, Kamensky IL, Marty B, et al. (2002) Rare gas isotopes and parent trace elements in ultrabasic–alkaline–carbonatite complexes, Kola Peninsula: Identification of lower mantle plume component. *Geochimica et Cosmochimica Acta* 66: 881–901.
- Tolstikhin IN and Marty B (1998) The evolution of terrestrial volatiles: A view from helium, neon, argon and nitrogen isotope modeling. *Chemical Geology* 147: 27–52.

- Tolstikhin IN and O'Nions RK (1994) The Earth's missing xenon: A combination of early degassing and of rare gas loss from the atmosphere. *Chemical Geology* 115: 1–6.
- Trieloff M, Jessberger EK, Herrwerth I, et al. (2003) Structure and thermal history of the H-chondrite parent asteroid revealed by thermochronometry. *Nature* 422: 502–506.
- Trieloff M and Kunz J (2005) Isotope systematics of noble gases in the Earth's mantle: Possible sources of primordial isotopes and implications for mantle structure. *Physics of the Earth and Planetary Interiors* 148: 13–38.
- Trieloff M, Kunz J, and Allegre CJ (2002) Noble gas systematics of the Reunion mantle plume source and the origin of primordial noble gases in Earth's mantle. *Earth and Planetary Science Letters* 200: 297–313.
- Trieloff M, Kunz J, Clague DA, Harrison D, and Allegre CJ (2000) The nature of pristine noble gases in mantle plumes. *Science* 288: 1036–1038.
- Turekian KK (1959) The terrestrial economy of helium and argon. *Geochimica et Cosmochimica Acta* 17: 37–43.
- Turner G, Harrison TM, Holland G, Mojzsis SJ, and Gilmour J (2004) Extinct  $^{244}\text{Pu}$  in ancient zircons. *Science* 306: 89–91.
- Valbracht PJ, Honda M, Matsumoto T, et al. (1996) Helium, neon and argon isotope systematics in Kerguelen ultramafic xenoliths: Implications for mantle source signatures. *Earth and Planetary Science Letters* 138: 29–38.
- Valbracht PJ, Staudacher T, Malahoff A, and Allegre CJ (1997) Noble gas systematics of deep rift zone glasses from Loihi Seamount, Hawaii. *Earth and Planetary Science Letters* 150: 399–411.
- van Keeken PE and Ballentine CJ (1999) Dynamical models of mantle volatile evolution and the role of phase transitions and temperature-dependent rheology. *Journal of Geophysical Research* 104: 7137–7151.
- van Keeken PE, Hauri EH, and Ballentine CJ (2002) Mantle mixing: The generation, preservation, and destruction of chemical heterogeneity. *Annual Review of Earth and Planetary Sciences* 30: 493–525.
- Walker JCG (1986) Impact erosion of planetary atmospheres. *Icarus* 68: 87–98.
- Wetherill GW (1953) Spontaneous fission yields from uranium and thorium. *Physical Review* 92: 907–912.
- Wetherill GW (1975) Radiometric chronology of the early solar system. *Annual Review of Nuclear Science* 25: 283–328.
- Wheeler KT, Walker D, Fei Y, Minarik WG, and McDonough WF (2006) Experimental partitioning of uranium between liquid iron sulfide and liquid silicate: Implications for radioactivity in the Earth's core. *Geochimica et Cosmochimica Acta* 70: 1537–1547.
- Yamamoto J, Hirano N, Abe N, and Hanyu T (2009) Noble gas isotopic compositions of mantle xenoliths from northwestern Pacific lithosphere. *Chemical Geology* 268: 313–323.
- Yatsevich I and Honda M (1997) Production of nucleogenic neon in the Earth from natural radioactive decay. *Journal of Geophysical Research* 102: 10291–10298.
- Yokochi R and Marty B (2004) A determination of the neon isotopic composition of the deep mantle. *Earth and Planetary Science Letters* 225: 77–88.
- Yokochi R and Marty B (2005) Geochemical constraints on mantle dynamics in the Hadean. *Earth and Planetary Science Letters* 238: 17–30.
- Yokochi R, Marty B, Pik R, and Burnard P (2005) High  $^3\text{He}/^4\text{He}$  ratios in peridotite xenoliths from SW Japan revisited: Evidence for cosmogenic  $^3\text{He}$  released by vacuum crushing. *Geochemistry, Geophysics, Geosystems* 6. <http://dx.doi.org/10.1029/2004GC000836>.
- York D (1969) Least-squares fitting of a straight line with correlated errors. *Earth and Planetary Science Letters* 5: 320–324.
- Zhang Y (1997) Mantle degassing and origin of the atmosphere. In: *30th Geological Congress Proceedings*, Beijing, vol. 1, pp. 61–78.
- Zhang Y (1998) The young age of Earth. *Geochimica et Cosmochimica Acta* 62: 3185–3189.
- Zhang Y (1999)  $\text{H}_2\text{O}$  in rhyolitic glasses and melts: Measurement, speciation, solubility, and diffusion. *Reviews in Geophysics* 37: 493–516.
- Zhang Y (2002) The age and accretion of the earth. *Earth-Science Reviews* 59: 235–263.
- Zhang Y (2008) *Geochemical Kinetics*. Princeton, NJ: Princeton University Press.
- Zhang Y and Ni H (2010) Diffusion of H, C, and O components in silicate melts. *Reviews in Mineralogy and Geochemistry* 72: 171–225.
- Zhang Y, Ni H, and Chen Y (2010) Diffusion data in silicate melts. *Reviews in Mineralogy and Geochemistry* 72: 311–408.
- Zhang Y and Xu Z (1995) Atomic radii of noble gas elements in condensed phases. *American Mineralogist* 80: 670–675.
- Zhang Y, Xu Z, Zhu M, and Wang H (2007) Silicate melt properties and volcanic eruptions. *Reviews in Geophysics* 45: RG4004. <http://dx.doi.org/10.1029/2006RG000216>.
- Zhang Y and Zindler A (1989) Noble gas constraints on the evolution of Earth's atmosphere. *Journal of Geophysical Research* 94: 13719–13737.
- Zhang Y and Zindler A (1993) Distribution and evolution of carbon and nitrogen in Earth. *Earth and Planetary Science Letters* 117: 331–345.
- Zindler A and Hart S (1986) Chemical geodynamics. *Annual Review of Earth and Planetary Sciences* 14: 493–571.
- Zou H (2007) *Quantitative Geochemistry*. London: Imperial College Press.